EnMAP Science Plan

Environmental Mapping and Analysis Program (EnMAP)

L. Guanter, H. Kaufmann, S. Foerster, A. Brosinsky, H. Wulf, M. Bochow, N. Boesche, M. Brell, H. Buddenbaum, S. Chabrillat, T. Hank, U. Heiden, B. Heim, W. Heldens, J. Hill, A. Hollstein, P. Hostert, H. Krasemann, P. J. Leitão, S. van der Linden, W. Mauser, C. Mielke, A. Müller, N. Oppelt, S. Roessner, R. Röttgers, T. Schneiderhan, K. Staenz, K. Segl

Recommended citation:

Guanter, L.; Kaufmann, H.; Foerster, S.; Brosinsky, A.; Wulf, H.; Bochow, M.; Boesche, N.; Brell, M.; Buddenbaum, H.; Chabrillat, S.; Hank, T.; Heiden, U.; Heim, B.; Heldens, W.; Hill, J.; Hollstein, A.; Hostert, P.; Krasemann, H.; Leitão, P. J.; van der Linden, S.; Mauser, W.; Mielke, C.; Müller, A.; Oppelt, N.; Roessner, S.; Röttgers, R.; Schneiderhan, T.; Staenz, K.; Segl, K. (2016) EnMAP Science Plan. EnMAP Technical Report, GFZ Data Services.

DOI: http://doi.org/10.2312/enmap.2016.006

Imprint

EnMAP Consortium

GFZ Data Services

Telegrafenberg
D-14473 Potsdam

Published in Potsdam, Germany
July 2016

http://doi.org/10.2312/enmap.2016.006

Scientific Principal Investigator

Luis Guanter (Helmholtz Centre Potsdam GFZ German Research Centre for Geosciences) supported by the EnMAP Science Advisory Group (EnSAG)

Funding

The project is funded under the DLR Space Administration with resources from the German Federal Ministry for Economic Affairs and Energy and contributions from OHB System AG, GFZ and DLR.

Supported by:

Federal Ministry
for Economic Affairs
and Energy

on the basis of a decision
by the German Bundestag

www.enmap.org

Science Plan authors

L. Guanter (1), H. Kaufmann (1), S. Foerster (1), A. Brosinsky (1), H. Wulf (1), M. Bochow (1), N. Boesche (1), M. Brell (1), H. Buddenbaum (2), S. Chabrillat (1), T. Hank (3), U. Heiden (4), B. Heim (5), W. Heldens (4), J. Hill (2), A. Hollstein (1), P. Hostert (6), H. Krasemann (7), P.J. Leitão (6), S. van der Linden (6), W. Mauser (3), C. Mielke (1), A. Müller (4), N. Oppelt (8), S. Roessner (1), R. Röttgers (7), T. Schneiderhan (4), K. Staenz (9), K. Segl (1)

(1) Helmholtz Centre Potsdam GFZ German Research Centre for Geosciences (GFZ)
(2) Trier University
(3) Ludwig-Maximilian-Universität München (LMU)
(4) German Aerospace Centre (DLR)
(5) Alfred Wegener Institute for Polar and Marine Research - Research Unit Potsdam (AWI)
(6) Humboldt-Universität zu Berlin
(7) Helmholtz-Centre Geesthacht, Centre for Materials and Coastal Research (HZG)
(8) Kiel University
(9) University of Lethbridge

Contents

Preface

The scope of the Science Plan is to describe the scientific background, applications, and activities related to the Environmental Mapping and Analysis Program (EnMAP) mission. Primarily, the document addresses scientists and funding institutions, but it may also be of interest for environmental stakeholders and governmental bodies. It is conceived to be a living document that will be updated throughout the entire mission.

Chapter 1 provides a brief overview of the principles and current state of imaging spectroscopy. This is followed by an introduction to the EnMAP mission, including its objectives and potential impact on international programs as well as major environmental and societal challenges to their understanding and management EnMAP can contribute. Chapter 2 describes the EnMAP system together with data products and access, calibration/validation issues, and synergies with other missions. Chapter 3 gives an overview of the relevance, current lines of research, and potential contributions of EnMAP for major fields of application, such as vegetation, geology and soils, coastal and inland waters, cryosphere, urban areas, atmosphere and hazards to address the environmental and societal challenges presented in Chapter 1. Finally, Chapter 4 outlines the scientific exploitation strategy, which includes the strategy for community building and training, preparatory flight campaigns and software developments.

A list of abbreviations is provided in the annex to this document, while an extended glossary of terms and abbreviations is available at the EnMAP website.

1 Introduction

1.1 Principles of imaging spectroscopy

Surface materials, such as vegetation, soil, and rock, can be discriminated and characterized based on their so-called spectral signatures, i.e., diagnostic absorption and reflection characteristics over the electromagnetic spectrum. Because every material is formed by chemical bonds, their harmonics and overtones of vibrational electronic transitions result in characteristic spectral absorption features that can be detected in narrow wavelength intervals. Some of the most significant absorption features occur between wavelengths of 400 nm to 2500 nm, where reflected solar radiation dominates the natural electromagnetic spectrum (Figure 1). These absorption characteristics can vary in their spectral depth, width, and location and, therefore, serve as diagnostic indicators, which enable to characterize vegetation conditions (e.g., Knipling, 1970) to detect water constituents (Lee et al., 1999) or to identify mineral assemblages (e.g., Hunt and Salisbury, 1970).

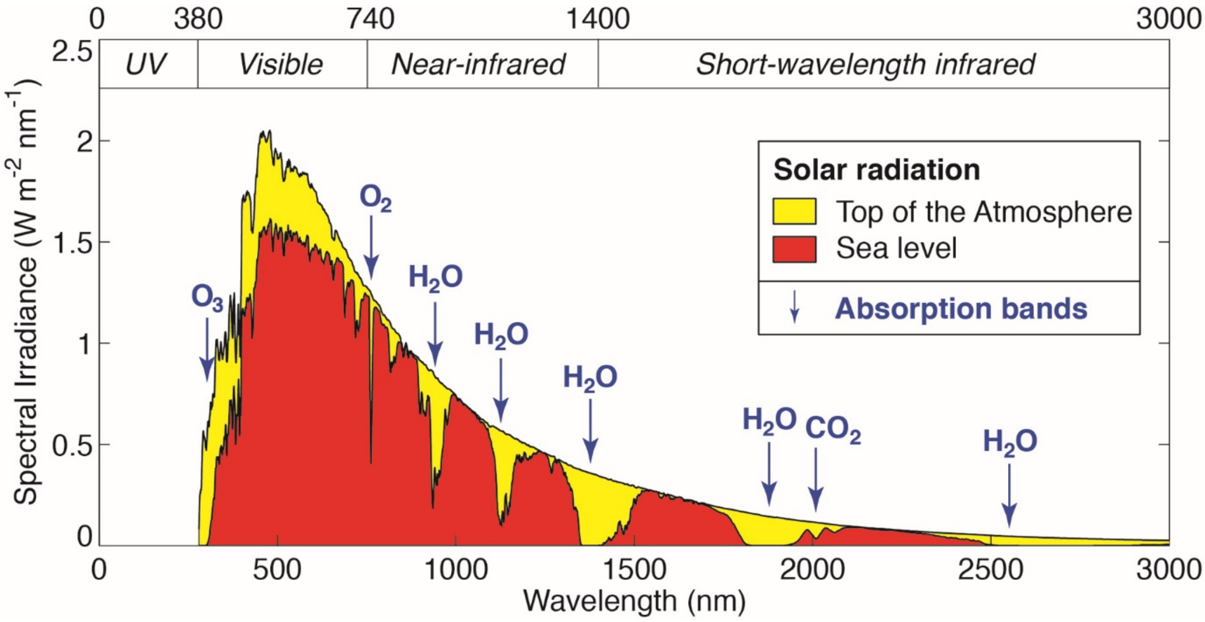

Fig. 1: Solar radiation spectrum of extra-terrestrial radiation (Top of Atmosphere) and global radiation (Sea level, composed of incoming, diffuse, and reflected radiation) with major atmospheric absorption bands. Irradiance data are derived from the American Society for Testing and Materials' (ASTM's) Terrestrial Reference Spectra (http://rredc.nrel.gov/solar/spectra/am1.5/).

Imaging spectroscopy, also known as hyperspectral imaging, is defined as a passive remote sensing technology that acquires simultaneous images in many spectrally contiguous, narrow bands such that for each pixel a reflectance spectrum can be derived (Goetz et al., 1985; Schaepman, 2007). As described hereinafter, application areas of hyperspectral sensing include ecosystem processes, surface mineralogy, water quality, soil type and erosion, vegetation type and condition, canopy chemistry, snow and ice properties, but it is also widely used in other areas, such as in medicine or manufacturing industries.

In ecosystem studies, the spectroscopic focus is on the detection and identification of plant succession, phenology, plant health, and invasive species to provide information about ecosystem conditions in general and the locations and types of environmental stresses in particular (Asner et al., 2008; Schmidtlein and Sassin, 2004; Ustin et al., 2004). In the past, most research has been focused on the spectral properties of leaves and canopies, providing estimates of (forest) species, foliar chemistry, biomass and carbon (Goodenough et al., 2012). In general, the spectral characteristics of vegetation exhibit strong pigment absorptions in the visible (VIS: 400 nm to 700 nm) portion of the spectrum (Figure 2). The near infrared (NIR: 700 nm to 1400 nm) is marked by a steep increase of reflectance that can be related to biomass, state and type of cellular arrangement, density, geometry and water content of a vegetation canopy. A shift of the "red edge" at 680 nm to 780 nm to shorter wavelengths is related to chlorophyll decrease, which can in turn be an indication of heavy metal, water or nutrient stress. Also senescent leaves are characterised by a decrease in chlorophyll, followed by losses of other pigments and leaf water content (Ustin et al., 2004). The biochemical content of leaves and canopies, including nitrogen-containing compounds and lignin, absorbs radiation at fundamental stretching frequencies, generally in the NIR and shortwave-infrared (SWIR: 1400 nm to 2500 nm) regions. In general, stress and aging increase the VIS and SWIR reflectance while decreasing it in the NIR (Ustin et al., 2004). Consequently, imaging spectroscopy is highly suitable to quantify vegetation state and to distinguish between various vegetation species.

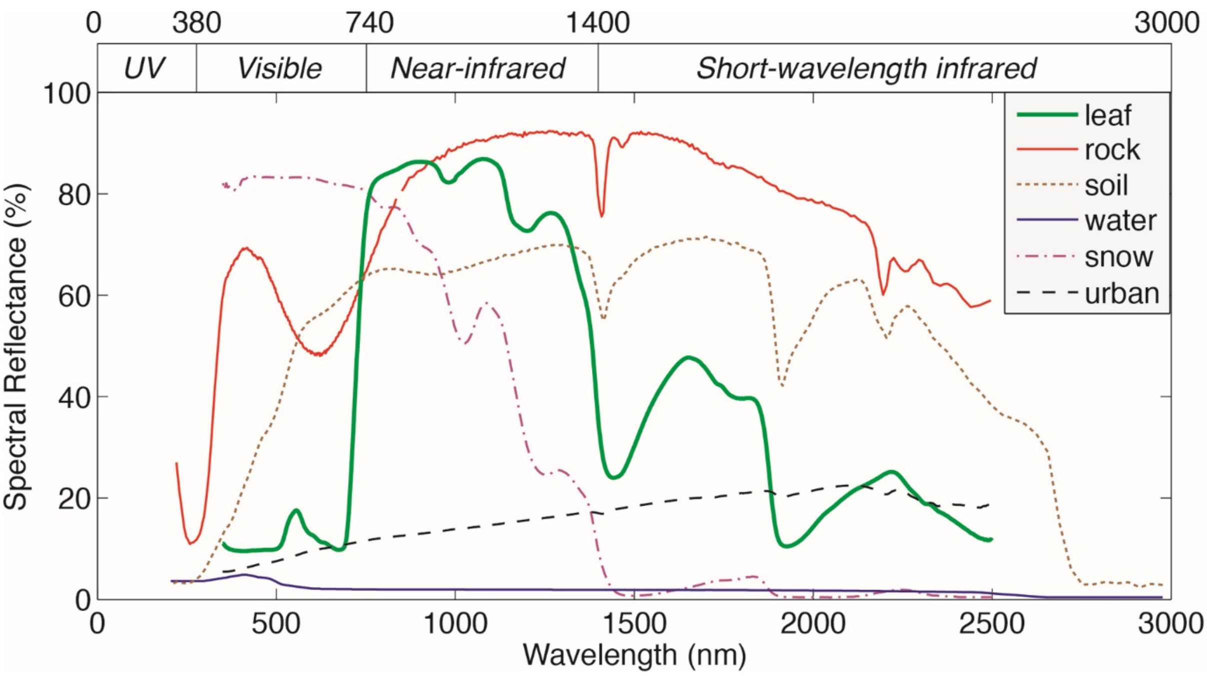

Fig. 2: Reflectance spectra of selected Earth's surface components. Reflectance data are derived from the USGS Digital Spectral Library (http://speclab.cr.usgs.gov/spectral.lib06/). The laboratory measurements represent samples of an oak leaf from Colorado (leaf), Aventurine quartz from India (rock), montmorillonite and illite from Virginia (soil), seawater from the Pacific Ocean (water), fresh snow from Colorado (snow), and black road asphalt from Colorado (urban).

For geologic applications, imaging spectroscopy is used to map the Earth's surface composition (in terms of mineralogy or lithology) and quantify rock and soil chemistry, which is based on spectral absorption features. Reflectance spectra of minerals are dominated in the visible near-infrared (VNIR) wavelength range (400 nm to 1400 nm) by the presence or absence of transition metal ions (e.g., Fe, Cr, Co, Ni) resulting in absorption features due to electronic processes. The presence or absence of water and hydroxyl, carbonate and sulphate determine absorption features in the SWIR region due to vibrational processes. These phyllosilicates, sorosilicates, hydroxides, sulphates, amphiboles and carbonates are widespread components of the Earth's surface. The absorption band depth is related to grain or particle size, as the amount of light scattered and absorbed by a grain is dependent on grain size (van der Meer et al., 2012). In general, absorption band depth is correlated with the (relative) amount of material present. Based on the relative absorption depth, for example, it has been shown that kaolinite and organic carbon content can be derived with an accuracy of about 2 % by weight (Krueger et al., 1998).

Soils are dynamic environmental components of extremely variable physical and chemical composition (Ben-Dor et al., 1999) and essential for ecosystem functions. They comprise a major sink for biospheric carbon and organic matter in the topsoil, whereas the proportion of these components provides a good indication of soil quality, erosion, and dominant physical processes (Ustin et al., 2004). Since the major constituents of soil minerals do not exhibit absorption features in the VNIR and SWIR range (Hunt, 1977), their spectral reflectance characteristics are mainly influenced by organic matter content, clay mineral composition, iron-oxide content, moisture content, salinity, texture and surface roughness. Typically, soils have broad, shallow absorption features at wavelengths between 400 nm and 2500 nm that are related to iron oxide and organic matter (Figure 2). In general, reflectance decreases with increasing organic matter and/or moisture content. Increases in particle size also cause a decrease in overall reflectance. Even small amounts of iron oxides can alter VNIR spectra significantly, causing broad absorption features particularly around 400 nm, 700 nm and 870 nm (Ben-Dor et al., 1999). In contrast, several clay minerals (e.g., montmorillonite, kaolinite, illite, smectite) and carbonates display distinctive narrow-band absorption features in the SWIR range between 2000 nm and 2500 nm (Ustin et al., 2004). Recent studies on soil properties focused on soil degradation, genesis and formation, contamination, classification and mapping, as well as on soil water content and swelling soils (Ben-Dor et al., 2009).

Imaging spectroscopy has been widely used to monitor oceans and inland waters, which are characterized by an overall high absorption of radiant energy compared to land surfaces (Figure 2). This characteristic makes water suitable to isolate and measure its optical constituents, such as pigments (e.g., chlorophyll), a wide range of phytoplanktonic species, dissolved organic matters, and suspended non-algal particles (e.g., minerogenic sediments). Coastal and inland waters are optically more complex as compared to open oceanic waters, which can be characterized mainly by one optical parameter and are generally referred to as case-1 waters (Morel and Prieur, 1977). In contrast, inland and coastal waters are influenced by multiple parameters.

Snow cover and its subsequent melt can dominate local to regional climate and hydrology in the world's mountainous and Polar Regions. To model the snowmelt distribution and its impact, hyperspectral remote sensing allows for the retrieval of snow properties, such as snow-covered area, albedo, grain size, very near surface liquid water, and impurities (Dozier and Painter, 2004). Among natural materials at the Earth's surface, snow has a huge range of spectral reflectance values depending on its physical characteristics, primarily the grain size but also dust or soot content, organic substances such as algae, and liquid water (Dozier et al., 2009). Clean, deep snow is highly reflective in the VIS spectrum, whereas reflectance in the NIR and SWIR wavelengths shows a general decrease, but varies considerable depending primarily on the grain size (Figure 2).

Urban areas are characterized by a wide range of spectrally distinct surface materials, whose spectral signature is determined by its chemical composition (Heiden et al., 2012). For example, roofing tiles and polyethylene exhibit pronounced absorption features and high-spectral variation, whereas other urban surfaces, such as concrete and asphalt, are characterized by low reflectance and low spectral variation. Heldens et al. (2011) identified the following current major topics regarding urban applications: urban development and planning, urban growth assessment, risk and vulnerability assessment, and urban climate.

EnMAP has the capability to detect individual absorption features in the spectra of many materials, solids, liquids, or gases. Actual detection depends on the instrument´s spectral coverage, spectral resolution, signal-to-noise ratio, the abundance of the material, and the strength of the material's absorption features in the measured wavelength region. The spectral molecular absorption and scattering properties of materials, as mentioned in the previous paragraphs, form the basis for the identification and determination of the abundances of surface and atmospheric constituents. Accordingly, research and development efforts within the EnMAP mission employ these fundamental spectral characteristics as a basis for the extraction of information from spaceborne hyperspectral data.

1.2 Current scenario in imaging spectroscopy and EnMAP

More than three decades of effort have been devoted to the development of imagers capable of acquiring contiguous spectra in different wavelength regions, thereby permitting precise and quantitative analysis of terrestrial and aquatic ecosystems. These imaging spectrometers have primarily been flown in aircrafts for experimental and commercial purposes, e.g., AIS, (Vane et al., 1983), FLI and *casi* (Gower et al., 1992), AVIRIS (Vane et al., 1993; Green et al. 1998), GER/DAIS (Collins and Chang, 1990), SFSI (Neville and Powell, 1992), Hydice (Rickard et al., 1993), MIVIS (Bianchi et al., 1994), HyMap (Cocks et al., 1998), APEX (Itten et al., 2008; Schaepman et al., 2004 and 2015), AVIS (Oppelt and Mauser, 2007), AISA (www.spectralcameras.com/aisa), HySpex (www.hyspex.no), and Hyperspec (www.headwallphotonics.com) (Figure 3). However, data acquisition from an aircraft platform cannot provide a synoptic view of extended areas and repeated acquisitions are costly. For a more complete overview of airborne imaging spectroscopy sensors and their history refer to Schaepman (2009).

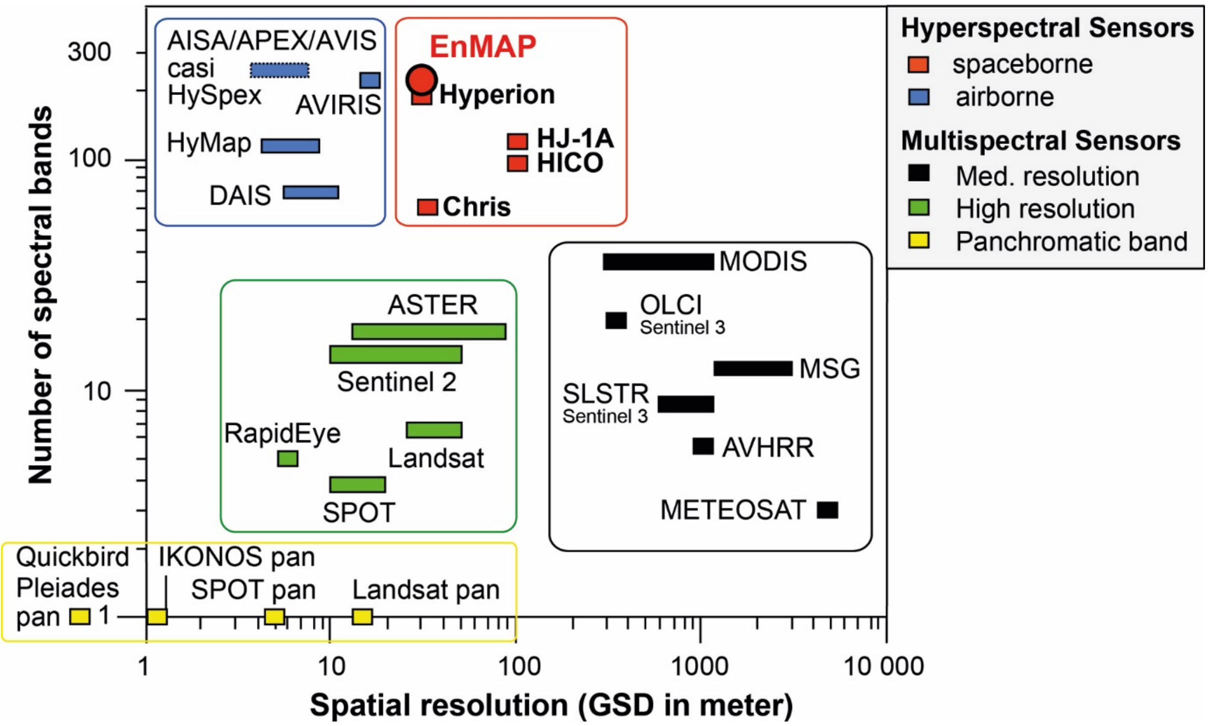

Fig. 3: Overview of the spectral and spatial resolution of selected airborne and spaceborne hyperspectral and multispectral sensors.

In general, operational optical satellite sensors have been multispectral instruments, operating in selected discrete bands in the VNIR region including in some cases bands in the SWIR and thermal infrared (TIR) region of the spectrum (e.g., Landsat, ASTER). The panchromatic sensors provide only spatial information, while the multispectral instruments, such as the broadband systems Landsat, SPOT, IRS, CBERS, ASTER, ALI, or recently Sentinel 2 augment the spatial data with mainly qualitative information about the surface materials. Exceptions are the few launched hyperspectral sensors NASA's Hyperion (from 2000 to likely 2016; Ungar et al., 2003, Pearlman et al., 2003), NASA's HICO (from 2009 to 2015; Corson et al., 2008; Lucke et al., 2011), and ESA's CHRIS (since 2001; Barnsley et al., 2004) (Figure 3). Considering that Hyperion and CHRIS were designed for a 1-year lifetime, they have provided exceptional results. Nonetheless, CHRIS and HICO are limited to the VNIR region, while Hyperion is characterized by a low signal-to-noise ratio. Both of these factors limit the sensors in their feature detection capabilities. Therefore, current spaceborne sensors provide only limited information on biochemical and geochemical parameters, which are required for detailed environmental studies.

In view of these developments, the EnMAP mission represents a milestone towards a comprehensive hyperspectral observation from space. Other imaging spectroscopy missions are prepared by ASI (Italian Space Agency) in the form of PRISMA (PRecursore IperSpettrale della Missione Operative; Pignatti et al., 2013), by JAXA (Japanese Aerospace Exploration Agency) in the form of HISUI (Hyperspectral Imager Suite; Iwasaki et al., 2011), by NASA in the form of HyspIRI (Hyperspectral Infrared Imager; Green et al., 2008), and by CNES (Centre National d'Études Spatiales) in the form of HYPXIM (Michel et al., 2011), among others. A comprehensive overview on all running and future Earth Observation IS missions is available for download from the EnMAP website.

EnMAP is a German hyperspectral satellite mission that aims at monitoring and characterising the Earth's environment on a global scale. EnMAP serves to measure and model key dynamic processes of the Earth's ecosystems by extracting geochemical, biochemical and biophysical parameters, which provide information on the status and evolution of various terrestrial and aquatic ecosystems. An overview of the EnMAP mission is provided in Guanter et al. (2015). Once operating, EnMAP will provide unique data needed to address major environmental issues related to human activity and climate change. The mission's main objective is to study and decipher coupled environmental processes and to assist and promote the sustainable management of the Earth's resources. Despite being a primarily scientific mission, EnMAP has a clear potential to evolve towards an operational service.

The EnMAP mission consortium comprises the Helmholtz Centre Potsdam - German Research Centre for Geosciences (GFZ) as the principal scientific investigator, OHB Systems AG as the industrial prime contractor in charge of providing the instrument and satellite service module, the Space Administration at the German Aerospace Agency (DLR) managing the project, and DLR Oberpfaffenhofen responsible for the ground segment.

1.3 EnMAP mission objectives

The main scientific goal of the hyperspectral EnMAP mission is to study environmental changes, investigate ecosystem responses to human activities, and monitor the management of natural resources. By measuring diagnostic parameters that quantify the state and trend of environmental change, the stability of ecosystems, and the sustainability of resource use, the EnMAP mission aims to provide critical information for an improved understanding and management of the Earth System.

The primary mission objectives are:

- to provide high-quality calibrated hyperspectral data for advanced remote sensing analyses;
- to foster and develop novel methodologies that improve the accuracy of currently available remote sensing information and to provide advanced science-driven information products;
- to obtain diagnostic geochemical, biochemical and biophysical parameters that describe the status and dynamics of various ecosystems to improve our understanding of complex environmental processes;
- to provide information products that can serve as input for ecosystem models;
- to significantly contribute to environmental research studies, particularly in the fields of ecosystem functions, natural resource management, natural hazards and Earth system modelling; and
- to develop new concepts and techniques for data extraction and assimilation to achieve synergies with other sensors.

EnMAP will significantly increase the availability of currently infrequent hyperspectral measurements. To understand and fully exploit the information content provided by EnMAP, novel evaluation techniques need to be developed, which fully utilize EnMAP's regional coverage on a global scale. EnMAP data will provide a unique opportunity to adapt and extrapolate existing hyperspectral data analysis approaches derived from laboratory, field, and airborne measurements to spaceborne imagery. Their integration in regional ecosystem models will allow to complement, enhance, and extend current local case study findings to a regional scale. Consolidated and improved regional scale science on the state and evolution of ecosystems is the prerequisite for improvements in global ecosystem models. Such upscaling studies require a sensible generalisation of the derived quantitative ecosystem parameters and the synergistic analysis with other spaceborne imagery, such as provided by ESA's Sentinels.

Due to the 30° across track off-nadir pointing capability, EnMAP is suited for repeated coverage of multiple key target sites with a maximum revisit cycle of 4 days. This ability allows EnMAP to repeatedly observe a globally distributed network of local to regional key target sites during its five years of mission operation.

1.4 Overarching research themes for EnMAP

EnMAP's repeated observations with an advanced spectral coverage and resolution will provide new insights into multiple interrelated environmental subjects. The EnMAP Science Advisory Group (EnSAG) identified several research topics for which EnMAP data can provide a substantial contribution. Because hyperspectral image analysis is applicable to a wide range of research topics, this selection focuses only on some of the most challenging environmental and societal questions.

Climate Change Impact and Measures

- How does climate change affect state, composition and seasonal cycles of terrestrial and aquatic ecosystems?
- What measures can effectively combat climate change, and how can their implementation be monitored?

Land-Cover Changes and Surface Processes

- Where and to what extent do land degradation processes and land-use / land-cover changes occur from local to global scale?

- Which processes drive land degradation, and how efficient are countermeasures?
- What are the consequences of land degradation and land-use / land-cover changes in view of food security and environmental sustainability?

Biodiversity and Ecosystem Processes

- What is the spatial pattern of ecosystem and diversity distributions from local to global scale?
- How do ecosystems change over time in their composition and health?
- How are ecosystem processes affected by human activities or natural causes, and how can harmful consequences on their biodiversity be reduced or prevented?

Water Availability and Quality

- Which areas are affected by water scarcity and water quality problems from local to global and from seasonal to decadal scales?
- How do climate change and human activities, such as intensive agriculture, water demanding industries and high population density, reinforce water scarcity and water quality problems?

Natural Resources

- How can natural resources, such as mineral deposits, energy sources and ground water sources, be explored and managed in a sustainable way?
- What impact do human activities, such as industry, mining and agriculture, have on natural resources?
- How can environmentally harmful impact, such as water and air pollution, land contamination and mine waste, be minimized in order to conserve and sustain natural resources?

Hazard and Risk Assessment

- Which areas are to what extent vulnerable to natural and man-made hazards?
- In case of a natural or man-made disaster, which areas are to what extent affected?

1.5 Impact on international programs

The products and information generated from EnMAP data will be of substantial interest for the scientific community, several European and international organizations, and the general public.

First and foremost, researchers need EnMAP data to improve their understanding of Earth surface processes and reduce uncertainties in associated ecosystem models. Scientific requirements for terrestrial and aquatic observations have long been articulated, especially at the international level, by the International Geosphere-Biosphere Program (IGBP), the Land Ocean Interaction in the Coastal Zone Program (LOICZ), the International Human Dimensions Program (IHDP), DIVERSITAS, the World Climate Research Program (WCRP), the Global Land Project (GLP), the Global Biodiversity Information Facility (GBIF), the Global Environment Outlook (GEO), the UN Agenda for Sustainable Development defining 17 Sustainable Development Goals (SDGs), and others. The major new “Future Earth” alliance on Earth system research for global sustainability integrates and consolidates international expertise in environmental and social science under one umbrella and forms a programmatic and societal justification for Earth observation research and development. This is underlined by the welcoming of Future Earth as a participating organization in the Group on Earth Observations (GEO) in 2015. GEO aims at building the Global Earth Observation System of Systems (GEOSS) that will link global Earth observation resources contributed by organizations and countries within GEO across multiple Societal Benefit Areas (SBAs) to facilitate access to the data for better informed decision-making. The SBAs include biodiversity and ecosystem sustainability, disaster resilience, energy and mineral resources management, food security and sustainable agriculture, infrastructure and transportation management, public health surveillance, sustainable urban development, and water resources management (GEO, 2015).

Key international stakeholders with a potential interest in the scientific results of the EnMAP mission, include organizations that make up the United Nations System (e.g., UNEP, FAO, UNESCO and WMO) as well as global observing systems, such as the Global Climate Observing Systems (GCOS), Global Ocean Observing System (GOOS) and Global Terrestrial Observing System (GTOS). Furthermore, EnMAP observations may be a valuable source of quantified information needed for multilateral environmental agreements, such as REDD+, UNFCCC, UNCCD, and CBD, as well as by key international entities, such as the Intergovernmental Panel on Climate Change (IPCC), the Intergovernmental Platform on Biodiversity & Ecosystem Services (IPBES) and the International Union for Conservation of Nature (IUCN).

At the level of the European Union, several Commission directories (e.g., DG VI - Agriculture, DG VIII - Development, DG XI - Environment, DG XII - Transport, and DG XVI - Regional policy) are anticipated to require continuous remotely sensed land observations, because these governmental departments need to set, monitor, and enforce their policy agenda. For example, specified biological, hydromorphological and physico-chemical parameters of water bodies have to be monitored on a regular basis according to the EU Water Framework Directive. In addition, national/local authorities will need increasingly detailed information for implementing local measures to combat desertification and to plan alternative land uses. In view of these developments, data products (e.g., soil status, vegetation cover, change detection maps, degradation index maps) will be beneficial for decision makers. In particular, the European Copernicus programme provides users with reliable and up-to-date information through a set of services related to environmental and security issues (European Commission, 2015).

2 EnMAP system and data products

2.1 Technical parameters and observational requirements

The EnMAP satellite carries a push-broom type hyperspectral imager, that records reflected radiation from the Earth surface in the wavelength region from 420 nm to 2450 nm in 242 contiguous bands. The mean bandwidth is 6.5 nm the VNIR range and 10 nm in the SWIR range. Accurate radiometric and spectral responses are ensured by a reference signal-to-noise ratio (SNR) of ≥400:1 in the VNIR and ≥170:1 in the SWIR (based on an albedo of 30 % and a solar zenith angle of 30°), a radiometric calibration accuracy of better than 5 %, and a spectral calibration uncertainty of 0.5 nm in the VNIR and SWIR.

The sensor is characterized by a ground sampling distance of 30 m (nadir at sea level) and provides a swath width of 30 km. EnMAP can record strip lengths between 30 km and 1000 km (subject to potential conflicts in the acquisition plan) with a capacity of 5000 km per day. The nominal target revisit time of 27 days can be reduced to 4 days by use of an across-track off-nadir pointing capability of ±30°. EnMAP will be launched in a sun-synchronous orbit (653 km altitude at 48°N; 97.96° inclination) with a local equatorial crossing time of 11:00 hr. The satellite launch is scheduled for 2019 with an Indian "Polar Satellite Launch Vehicle" and has a designed lifetime of five years. A summary of the main mission and instrument specifications is given in Table 1. Further descriptions can be found in Guanter et al. (2015) and Kaufmann et al. (2016).

Table 1: EnMAP mission and instrument specifications.

Hyperspectral instrument	
Imaging principle	Push-broom-prism
Spectral range	VNIR: 420 nm - 1000 nm SWIR: 900 nm - 2450 nm
Mean spectral sampling distance	VNIR: 6.5 nm SWIR: 10 nm
Spectral oversampling	1.2
SNR at reference radiance	VNIR: > 400:1 at 495 nm (nadir looking, 30° solar zenith angle, SWIR: > 180:1 at 2200 nm 0.3 earth albedo)
Spectral calibration accuracy	VNIR: 0.5 nm SWIR: 1.0 nm
Spectral stability	0.5 nm
Radiometric calibration accuracy	< 5 %
Radiometric stability	< 2.5 %
Radiometric resolution	14 bit, dual gain in VNIR
Sensitivity to polarization	< 5 %
Spectral smile/keystone effect	< 20 % of a pixel
Co-registration VNIR-SWIR	< 20 % of a pixel
Mission	
Ground sampling distance	30 m
Swath width	30 km
Swath length	up to 1000 km/orbit and 5000 km/day
Coverage	Global in near-nadir mode (VZA ≤5°)
Orbit	Sun-synchronous,11:00 local time descending node
Target revisit time	27 days (4 days with 30° across track pointing)
Pointing accuracy (knowledge)	500m (100m) at sea level

2.2 Data products and access

During the operational phase, the following EnMAP data products will be delivered to the user community: Product Level 1B, Product Level 1C, and Product Level 2A. Please, note that the raw data and the subsequent Level 0 (Figure 4) products are not available to the user community. This section provides a short definition of these products, while a more detailed description can be found in Guanter et al. (2015) and Kaufmann et al. (2016).

The Level 1B product represents top-of-atmosphere radiance. This product is radiometrically corrected, spectrally- and geometrically characterized, quality controlled, and annotated with preliminary pixel classification (usability mask). The auxiliary information (e.g., position and pointing values, interior orientation parameters) necessary for further processing is attached, but not applied. The Level 1B processor corrects the hyperspectral image for known effects, e.g., radiometric non-uniformities, and converts the system corrected data to physical at-sensor radiance values based on the up to date radiometric calibration values.

The Level 1C product represents geocoded top-of-atmosphere radiance. This product is derived from the Level 1B product, which is subsequently geometrically corrected (orthorectified) and re-sampled to a specified grid. Auxiliary data for further processing are attached, but not applied. The Level 1C processor creates orthoimages by direct geo-referencing, utilizing an adequate digital elevation model. The extraction of ground-control-points from existing reference images using image matching techniques serve to improve the line-of-sight vector and, therefore, to increase the geometric accuracy of the orthoimages. The Level 1C processor orthorectifies image tiles from the VNIR and SWIR instrument independently. The co-registration error is expected to be better than 0.2 pixels.

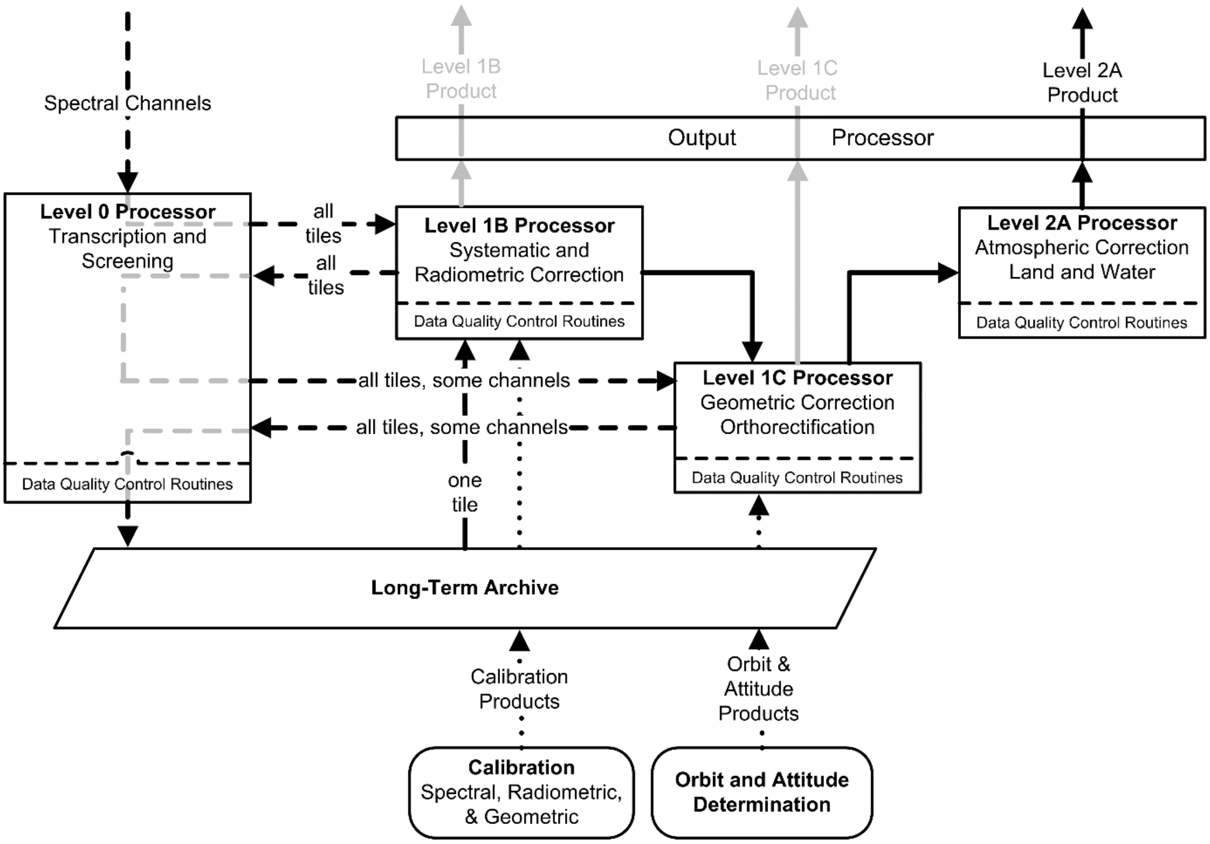

Fig. 4: The EnMAP data processing chain from the raw data to the geometrically and atmospherically corrected Level 2A product (reproduced from Guanter et al., 2015).

Finally, the Level 2A processor will convert the Level 1C products to surface reflectances separately for land and water applications. The atmospheric correction involves generation of sun glint maps for water surfaces by identification of specular reflections, detection (and correction) of haze and cirrus, estimation of aerosol optical thickness and columnar water vapor and retrieval of surface reflectance after adjacency correction. Auxiliary data for further processing are attached, but not applied. Most applications are envisioned to use the Level 2A product for further analysis.

Typically, Level 0 products will be in the archive within 24 h after completion of the corresponding downlink, and processing and delivery of Level 2A products are to be conducted within a maximum of eight hours. Thereby, the user can choose the image format (BSQ, BIL BIP, JPEG2000 or GeoTIFF). The metadata is always in Extensible Markup Language (XML) format, and the product is accompanied by a report in portable document format (PDF).

EnMAP data distribution differentiates between several user categories to set acquisition priorities. In summary, Category 1 users (Cat. 1) will be scientific users. Scientists can submit research proposals that will be evaluated by the EnSAG and potential external reviewers. Category 2 users (Cat. 2) will be non-registered international public or private entities. The priorities for data requests are, in decreasing order: internal (high priority, e.g., calibration), emergency Cat. 2 (e.g., international charter on space and major disasters), Cat. 1 users, non-emergency Cat. 2, internal (low priority, e.g., to fill up or extend requests). Requests of the first two priorities are scheduled regardless of their success concerning, for example, cloud probabilities or quota. Thus, especially requests of the last four priorities are advised to take the revisit times into account when planning the acquisition time period in order to increase the probability that the scheduling meets their requirements.

The EnMAP website (www.enmap.org) is the central entry point for all users interested in the EnMAP mission, its objectives, status, data products and processing chains. Additionally, this platform informs about the conditions and requirements for the EnMAP data access and the ongoing scientific program and activities.

2.3 Sensor calibration and product validation

In order to ensure a high data quality, EnMAP requires a well-characterized primary sensor, on-board calibration facilities, and ongoing vicarious calibration measurements throughout the entire mission lifetime. The derived data products also require independent validation by means of field and image measurements. The pre-flight sensor characterization is performed in the laboratory for both the individual subsystems and the complete end-to-end sensor system. It includes spectral, radiometric, and geometric calibrations. The spectral measurements include the band centres, bandwidths, and spectral response profiles for each band of each pixel in the array. The radiometric measurements encompass the detector array responsivity, linearity, uniformity, noise characterization, straylight, and optics transmittance with the objective of properly characterising the instrument's performance. The geometric measurements include the total field-of-view, the view angle for each pixel and each band, and the modulation transfer function. After launch, in-flight calibration is carried out using on-board calibration devices, such as the solar full aperture diffuser for the absolute radiometric calibration using the sun as the known reference, a main sphere for the relative radiometric calibration, a small sphere for spectral characterization, focal plane assembly LEDs for non-linearity calibration and a shutter for dark current calibration. Additionally, residual signals caused by thermal emissions from the shutter mechanism are regularly determined by looking into deep space.

These measurements will be complemented by vicarious calibration experiments on demand. As the imaging spectrometer and the on-board calibration instrumentation age, there is a growing need for periodic in-flight calibration, vicarious and on-board calibrations.

Validation of the EnMAP products will be performed during the commissioning phase and the operational mission period. The validation procedure includes ground- and scene-based techniques for the product evaluation to derive characteristic error estimates for the final EnMAP products and detailed information to track potential error sources back to instrument and processing chain levels. These validation results will be incorporated in calibration activities and will be provided as additional information on the instrument spectral and radiometric performance.

2.4 Synergies of EnMAP with other Earth observation missions

While EnMAP is conceived as a stand-alone mission with scientific objectives driven by the user community, valuable synergies exist between EnMAP and optical and radar imagery.

A large potential for synergies exists between EnMAP and Copernicus's Sentinel missions (Berger et al., 2012). The Sentinels aim at providing global coverage of high quality data in the optical and microwave domain in both high and medium spatial resolution. These missions will serve the Copernicus programme by providing continuous and global Earth observation from space on an operational basis.

Sentinel-2 will provide Landsat/SPOT-like imagery in a high spatial (10 m – 60 m) resolution and a moderate temporal (<5 days) and spectral (13 bands) resolution (Drusch et al., 2012). Its global coverage in a comparable spatial resolution to that of EnMAP (30 m) holds the synergistic potential to expand EnMAP's advanced regional information to a global scale. Complementary, Sentinel-3 and similar medium-spatial-resolution optical missions, which will operate concurrently with EnMAP, provide global coverage data in an almost daily temporal resolution (Donlon et al., 2012). Synergies between EnMAP and these missions include more frequent ecosystem observations allowing to resolve surface processes with high temporal variations.

In addition to optical sensors, Synthetic Aperture Radar (SAR) missions also provide complementary information to EnMAP data. For example, Sentinel-1 operationally provides C-band SAR-data of the Earth's surface with spatial resolutions of up to 10 m – 20 m (Torres et al., 2012). This ability allows for analysing the state and variation of physical parameters, such as surface roughness and soil moisture, which complements EnMAP's strength to derive bio-geochemical properties of the Earth surface. Furthermore, digital elevation model (DEM) data as retrieved from TerraSAR-X or Tandem-X using InSAR techniques may serve for data correction purposes, such as the removal of geometric distortion effects in mountainous terrain (Krieger et al., 2007).

The high spectral resolution of EnMAP can be combined with the current and future panchromatic and multispectral satellite systems like IKONOS, QuickBird, WorldView, RapidEye, and Pleiades, which are characterized by a high to very high spatial resolution. Such sensors offer additional options to improve object recognition, product validation, and temporal coverage. For example, the high temporal and spatial resolution data provided by RapidEye (one day revisit, 6.5 m ground sampling distance) can be combined with EnMAP to augment temporal coverage, which is suitable to monitor damage or infestations in agricultural crops and forests.

For the development and utilization of such synergies profound understandings of small-scale interactions between irradiation and complex 3D surface objects are required. Airborne data, especially in-flight fusion of hyperspectral and LiDAR data, delivers this understanding by their expanded data dimensionality (X, Y, Z, λ) and its very high spectral and spatial information content (Asner et al., 2012). Thus, this data can serve as a small-scale link between EnMAP and other Earth observation missions. Especially the comparability and the transferability of derived surface parameters to larger scales can be refined and evaluated based on such airborne data.

3 Main application fields for EnMAP

Accurate, quantitative information on the state and evolution of terrestrial and aquatic ecosystems is needed to support resource management, conservation strategies, rehabilitation measures, and ecosystem services. Hyperspectral image analysis can support a wide range of environmental applications, ranging, for example, from the assessment of vegetation state over mineral assemblages to water constituents and environmental hazards. EnSAG identified some of the most challenging environmental issues to which EnMAP can contribute (see section 1.4). Addressing these environmental issues requires interdisciplinary approaches across the Earth's spheres, because they are interconnected by various links and interactions (Figure 5). Fluxes of energy, water, carbon and sediment affect multiple spheres through complex feedback mechanisms and can be assessed by direct and indirect means with imaging spectroscopy. This chapter provides an overview of the relevance, current areas of research, and potential contribution of EnMAP for major environmental fields of application, including vegetation, geology and soils, coastal and inland waters, cryosphere, urban areas, atmosphere and hazards.

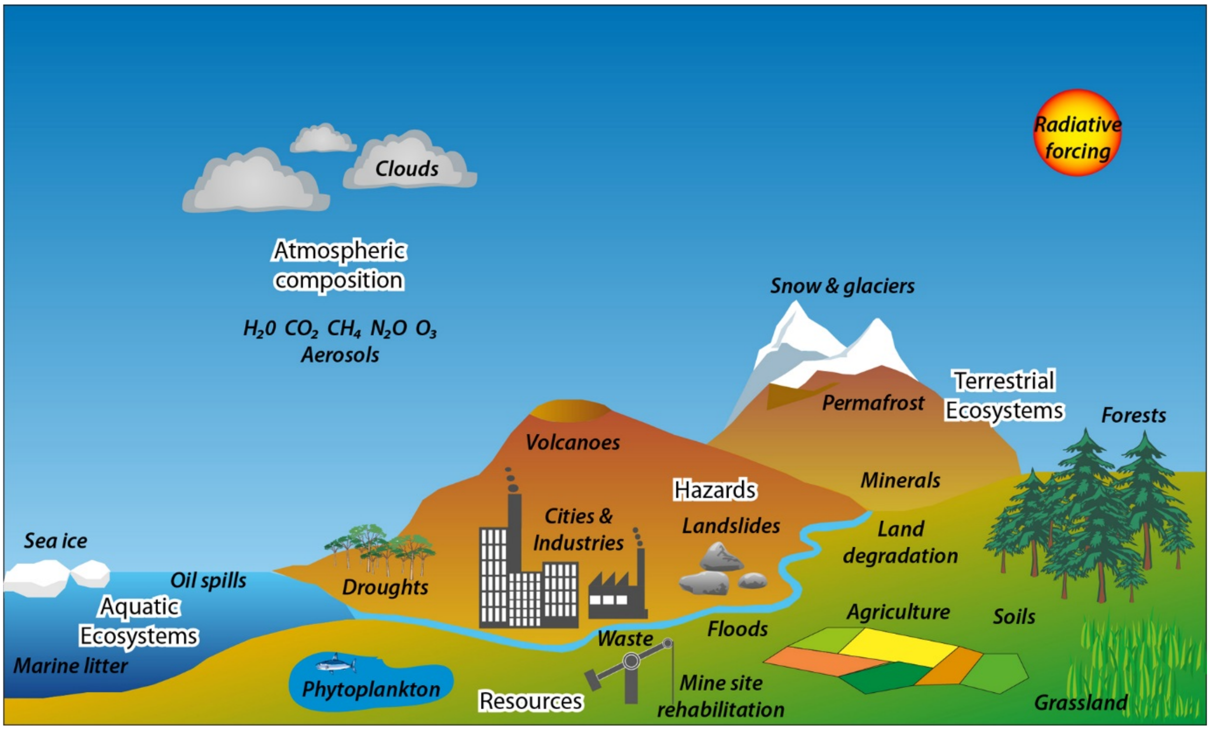

Fig. 5: Major research themes and associated application areas for imaging spectroscopy.

3.1 Vegetation

3.1.1 Natural ecosystems and ecological gradients

Pristine ecosystems on Earth are scarce (Kareiva et al., 2007) and global environmental change impacts even remote areas of our planet. Within this context, it is referred to ecosystems that are largely untouched by human land use and unmanaged or protected. Unlike managed ecosystems, these are mostly characterised by a large heterogeneity with multiple ecological gradients, as well as gradual transitions between different ecosystem types and conditions.

Specifically, monitoring and better characterizing natural or close to natural vegetation is essential to support sustainability of human-environment systems from local to global scales. Moreover, analysing and monitoring processes related to unmanaged land are crucial to deepen our understanding of indirect global environmental impacts and help to improve environmental models.

Quantifying ecosystem characteristics and the services they provide require using information at the meso- to macro-scale, which needs to be consistent and reproducible through space and time. Such information can only be obtained by means of remote sensing (Defries et al., 2005). EnMAP data and products derived from them will overcome current limitations, particularly in respect to the quantification of complex processes and gradual changes, which are prevalent in natural ecosystems (Asner et al., 2005; Leitão et al., 2015a). Concepts for the description of heterogeneous vegetated surfaces and floristic composition become possible, e.g., plant traits (Oldeland et al., 2012) or the plant functional types concept (Ustin and Gamon, 2010; Lavorel et al., 2011).

Previous studies made use of field-based or airborne hyperspectral data for quantifying biophysical parameters of natural vegetation, such as primary production, leaf area index or photosynthetic activity (Lee et al., 2004; Smith et al., 2002), biomass (Mutanga and Skidmore, 2004; Cho et al., 2007), carbon storage and water fluxes (Fuentes et al., 2006), ecosystem structure (Asner et al., 2005), or vegetation successional stage (Oldeland et al., 2010). Further uses of hyperspectral imagery have been on biodiversity mapping, both at the single species and at the community level (Cochrane, 2000; Clark et al., 2005; Feilhauer and Schmidtlein, 2009; Leitão et al., 2015b), including, for example, the monitoring of invasive species (Underwood et al., 2003; Somers and Asner, 2013). However, most of these studies are limited to one acquisition per year or less and none of them could make use of high quality hyperspectral data as EnMAP will provide. While the relatively coarse spatial resolution of hyperspectral satellite data will add challenges to such applications, data quality and availability will open up new pathways for parameter retrieval.

In this sense, high temporal data and systematic coverage by hyperspectral satellite systems, such as EnMAP, will allow for continuous monitoring of natural processes as demonstrated by pilot studies using data from experimental spaceborne systems (Asner et al., 2004; Stagakis et al., 2010; Leitão et al., 2015a) and, thus, will improve our understanding of these processes (Ustin et al. 2004). Phenological studies, previously based on existing platforms (Hoare and Frost, 2004; Fisher et al., 2006), are likely to reveal new insights by improved information that can be retrieved from high spectral resolution data. These data should be fundamental in improving existing carbon emission accounts and monitoring efforts (Numata et al., 2011), necessary to make mechanisms, such as REDD (UN Collaborative Initiative on Reducing Emissions from Deforestation and Forest Degradation) effective. EnMAP data will also be determinant in deriving Essential Biodiversity Variables (EBV; Pereira et al., 2013; Skidmore et al., 2015), this way contributing to monitor progresses towards the Aichi Targets set by the Convention on Biological Diversity (Petrou et al., 2015).

Physical-based modelling concepts are not particularly advantageous for the work in natural environments, because model calibration of such heterogeneous surfaces is mostly too complex. However, advances in statistical and machine learning provide a set of methods that are capable of coupling qualitative and quantitative analyses without being affected by collinearity effects in contagious datasets. Such new developments, such as self-learning decision trees, partial least square regressions, sparse ordination methods, Gaussian processes or support/import vector machines (Breiman, 2001; Helland, 1990; Vapnik, 1998; Witten et al., 2009; Zhu and Hastie, 2005) have high potential in making best use of the extended information in EnMAP data and allow for describing the aforementioned processes (e.g., Feilhauer et al., 2010; Verrelst et al., 2012; Schwieder et al., 2014; Leitão et al., 2015b; Suess et al., 2015).

Beyond the direct use of such generic algorithms for empirical modelling approaches, the generation of new indices and thematic transformations is of utmost importance. For example, multi-band indices and non-linear transformations may be developed based on insights derived from empirical studies with a non-linear kernel-based approach. Such developments have to be robust and transferable. However, in most cases a biome-specific calibration procedure will be required. Such calibration will be a key aspect in algorithm development in the near future.

EnMAP imagery will thus be extremely useful for monitoring natural ecosystems and their services, by allowing the accurate quantification of gradual biophysical and biochemical parameters, and the description of heterogeneous landscapes through the estimation of natural composition and pixel fractional cover.

The following main scientific tasks are related to natural ecosystems:

- Retrieval of biochemical and biophysical parameters as input into ecosystems and species habitat models to improve the understanding of ecosystems and ecological processes;
- Assessment of spatial pattern of ecosystems and biodiversity from local to global scales in the context of nature protection legislation, such as the European Special Areas of Conservation (Habitats Directive) within the Natura 2000 Network;
- Mapping and quantification of species traits, which can relate to ecological processes, ecosystem functioning and their provided services;
- Assessment of the state of biodiversity and ecosystems, as well as the services they provide, such as the above-ground carbon sequestration potential, and thus, contributing to international initiatives, such as the regional and global assessments being done by the Intergovernmental Platform on Biodiversity and Ecosystem Services (IPBES);
- Monitoring of natural or quasi-natural vegetation areas (such as nature protection areas, naturalized, un-used or extensively used areas) to understand causes and driving forces of changes; for example, in the context of land abandonment, forest disturbance or land degradation processes in order to combat biodiversity loss and promote ecosystem stability (e.g. REDD);
- Deriving of Essential Biodiversity Variables (EBV) relating to species populations, species traits, community structure, ecosystem structure and ecosystem function, this way contributing to monitor progresses towards international targets such as the Aichi targets set by the Convention on Biological Diversity (CBD);
- Quantification of spatial and temporal ecosystem transitions, such as vegetation succession, habitat heterogeneity, plant or animal community transitions, and assess potential feedback mechanisms; and
- Investigation of the effect of climate change and other anthropogenic and non-anthropogenic forces on global vegetation gradients.

3.1.2 Forests

Worldwide, forests provide timber and non-timber products as well as numerous environmental goods and services, such as conservation of biological diversity and climatic control, which are crucial for local livelihoods (FAO, 2010). However, forests and forested ecosystems are being rapidly depleted under increasing pressure due to global warming (Peng et al., 2011) and expanding human populations and economies (Hansen et al., 2008). Deforestation associated with conversion of forests to agricultural land, legal and illegal timber harvesting, drought stress, biotic stress, and recurrent wildfires are some of the most important processes, which affect forested landscapes (Bond, 2010; Anderegg et al. 2013; Ciais et al. 2005).

The challenges in forest management are multiscale and intricately linked to society's needs to preserve multiple forest values and benefit from its products. The pressing need for sustainable forest management aims at combining economic interests with ecologic concerns. In this context, remote sensing data serve economically oriented assessments and management needs as well as studies of ecological processes and functions (Franklin, 2001). Applications of remote sensing contributing to sustainable forest management are generally presented in four categories that include classification of forest cover type (i.e., tree species), estimation of forest structure and available resources (i.e., timber volume, height, age, crown closure), forest change detection and forest modelling. For each category, measurable indicators are needed to quantify the effects of management activities and natural phenomena on the sustainability of forest resources. Current research is directed at quantitatively relating remotely sensed spectral information to ground-based assessments of structural and physiological aspects of forest condition.

The future EnMAP satellite can efficiently characterize the spatial distribution of forest ecosystems and provide an inventory of forest resources. Such inventories typically comprise quantitative attributes related to forest species, health, and functioning, including estimates of chlorophyll, nitrogen, lignin and canopy water content (Goodenough et al., 2003a; Matson et al., 1994; Schlerf et al., 2005 and 2010; Asner et al. 2011). Quantifying such species-specific canopy biochemistry differences is well established to map forest species and ecosystems (Goodenough et al., 2003b; Martin et al., 1998). The fusion of hyperspectral data with other remote sensing data sources like Radar or LiDAR offers additional perspectives to estimate forest structure, forest type, biomass, timber volume, tree heights, stem densities, and age classes (Anderson et al., 2008; Dalponte et al., 2008; Huang et al., 2007; Hyde et al., 2006; Buddenbaum et al. 2013). Furthermore, it is possible to estimate the above-ground carbon stored in the forests, e.g., in the context of REDD, by combining hyperspectral imagery with geographic information, field calibrations and physiological models (le Maire et al., 2005), as well as texture and object information (Blaschke, 2010; Buddenbaum et al., 2005; van der Linden et al., 2007).

Also reforestation, afforestation, and deforestation rates on regional scales can potentially be better assessed by employing hyperspectral imaging from space (Clark et al., 2011; Goodenough et al., 1998). Such measures provide an essential contribution for documenting changes in the forests over time and will be urgently required when implementing the Agreement of the Paris Summit on Climate Change from December 2015. Previous studies on forest ecosystems emphasized the role of imaging spectroscopy allowing detailed and accurate retrievals of relevant vegetation properties (Ollinger and Smith, 2005; Schaepman et al., 2004), where the most important vegetation parameters are leaf chlorophyll and nitrogen content, the fractions of photosynthetically absorbed radiation (fAPAR), canopy water content, annual maximum leaf mass per area (LMA), and annual maximum leaf area (LAI) (e.g., le Maire et al., 2008). Thus, imaging spectroscopy offers accurate ways to provide substantial contributions to forestry information as well as new indicators of vegetation health, forest biochemistry and functioning. An important requirement for some of these applications is that canopy contributions to the signal on leaf level are successfully compensated (Knyazikhin et al., 2013). Thus, it can be anticipated that EnMAP is able to estimate changes in forest structure and condition, including above-ground carbon stocks at improved accuracies. This also extends to biotic stressors, such as bark beetles; the impact on forest ecosystems is expected to increase because of global warming. Spaceborne imaging spectrometers hold the potential to identify insect attacks already at early stages when the effects on forest reflectance are subtle and cannot be detected with conventional multispectral sensors (Fassnacht et al., 2012; Niemann et al., 2015; Wulder et al., 2009).

It should also be understood that global warming will trigger a further increase of devastating wild fires in many regions of the world (e.g., Australia, US, Mediterranean Europe). The enhanced potential of imaging spectrometers to identify drought effects and critical fuel moisture levels will open additional important application perspectives (Koetz et al. 2004 and 2008; Veraverbeke et al., 2014).

Important ecological processes in forests include carbon exchange (photosynthesis and respiration), evapotranspiration, and nutrient cycling (Coops et al., 2009; Waring and Running, 2007). To model these processes on a regional to global scale, imaging spectroscopy currently provides accurate local estimates of forest structural and chemical properties, which serve as required inputs to initialize, calibrate, and validate such models (Tenhunen et al., 1998). In the mid-term perspective, these models can assist management decisions to mitigate the effects of climate change on a regional scale.

Sun-induced chlorophyll fluorescence, which is closely linked to photosynthetic activity, can also be measured using imaging spectroscopy (Rascher et al., 2009; Meroni et al., 2009; Guanter et al., 2014). However, because the spectral resolution of the sensor used is critical (Damm et al., 2014), it remains to be evaluated to which extent EnMAP's spectral band design allows to estimate vegetation fluorescence; this will be important with respect to defining instrument requirements for future spaceborne systems.

Given the complexity of hyperspectral analysis, expert systems to support the analysis for EnMAP data have been developed (Goodenough et al., 2007 and 2012). Forest reflectance models, as compared to agricultural models, require much greater attention to forest structure, clumping, shadowing and understory effects. Reflectance models ranging from simple approaches like INFORM (Atzberger, 2000) or 4-scale (Chen and Leblanc, 1997) to more complex geometric-optical radiative transfer models like FRT (Kuusk and Nilson, 2009) or raytracing models like FLIGHT (Gerard and North, 1997) have been developed and validated in order to analyse the complex hyperspectral signal of forests (Foerster et al., 2010). Despite some successful attempts (Combal et al., 2002; Koetz et al., 2004; Schlerf and Atzberger, 2006; White et al., 2000), the inversion of these models is still a challenge and a pressing research issue for the next years.

EnMAP will enable to derive spectral indices that will serve as bio-indicators of forest condition. Through repetitive sampling of selected forest condition test sites, EnMAP will add the phenological history to the full spectral sampling data to yield effective bio-indicators of forest condition. EnMAP will provide a capability to compare observations of spectral properties of forests in many different countries. This is essential in order to develop a consistent tool for monitoring the carbon state of the world's forests and their response to climate change. Frequent and broad coverage will increase our understanding of the links between pigments, canopy chemistry, stress, and forest type. For forest inventory programs, hyperspectral data from EnMAP will provide an important sampling system to ensure precise measurements of indicators for a sustainable development.

Accordingly, the following main scientific tasks are considered important concerning forest applications:

- Mapping of forest species distributions using hyperspectral, fused and multitemporal datasets, exploring the potential of advanced classification algorithms, texture and object information, and linkages to geographic databases, etc.;
- Estimation of forest biomass, above-ground carbon, and productivity;
- Assimilation of biochemical and structural forest parameters into process models;
- Enhancement and development of invertible vegetation canopy reflectance models for the extraction of forest parameters, and forest mensuration, health, and risk assessment;
- Investigation of the viability of phenological signatures through indicators of canopy pigments and chemistry with regard to ecophysiological processes;

- Development of improved optical indices that will serve as bio-indicators of forest condition;
- Development of forest monitoring procedures, including multi-temporal and multi-sensor data, for the detection of changes in forest quality and canopy cover; and
- Creation of advanced expert systems to improve the efficiency of hyperspectral information extraction within the forestry context.

3.1.3 Agricultural land

Limited bio-productive land resources, progressing land degradation, rising population numbers, an increasingly meat-prone diet, a growing demand for biofuels, and on-going climate change, coupled with more frequent extreme meteorological events, cause substantial land use conflicts between food, fiber and energy production on one hand and ecosystem services including biodiversity conservation on the other. To sustain the benefits of natural ecosystems, a growing demand for agricultural commodities can only be met by sustainable increases in global land productivity (Mauser et al., 2015b). Thereby, global scale studies highlight that large appropriation of land resources leads to low efficiencies in land management (e.g., water use; Haberl et al., 2007; Kijne et al., 2009). The challenge of sustainably satisfying the demand for agricultural goods, thus, involves a wide range of land management aspects, including the selection of suitable crops and cultivars, the monitoring and increase of water productivity, the promotion of organic farming, the optimization of fertilizer and pesticide management, the implementation of soil conservation, and the development and application of efficient irrigation systems. Because of the spatial variability in climate, soils, and topography, as well as due to societal aspects, such as culture, education, technology, and markets, agricultural management critically relies on spatial data to support management decisions. Therefore, modern farming practices incorporate the identification, analysis, and management of spatial and temporal heterogeneity and variability within regions, farms, and fields to optimize between profitability, sustainability, and environmental protection (Mauser et al., 2015a).

Moran et al. (1997) already identified key areas where remote sensing can provide spatial information for agricultural management. These include the mapping of crop yield and biomass status as well as the monitoring of seasonally variable and spatially heterogeneous soil and crop characteristics. Since this early assessment, our understanding of farming related land heterogeneity management has progressed towards the application of detailed site-specific management measures to support sustainable production and to increase productivity. Sustainable agricultural management thereby includes early detection of infections, and water or fertilizer deficits. It further includes monitoring the ecological intensification of extensive agriculture and tracing the ecological extensification of intensive agriculture. Furthermore, it includes the identification and evaluation of new land reserves, where agriculture is gradually becoming viable due to climate change induced shifts of potential cultivation belts (Zabel et al., 2014). The implementation of these land management practices has led to a new demand for more complex and integrated spatial information around the globe, for example, concerning land evaluation, determination of site and plant specific yield gaps (i.e., the differences between potentially achievable and actually harvested yields), monitoring of fertilizer use intensity as well as determination of seeding dates and detection of phenological phenomena.

Hyperspectral Earth Observation instruments, providing agricultural information more accurately and in more detail compared to multispectral sensors, can substantially support farming management decisions (Staenz et al., 1998). Conventionally, multispectral systems were applied to derive agriculturally relevant information through statistical regression analysis between laborious ground-based measurements of biophysical variables and simple spectral indices. Hyperspectral Earth Observation systems enable the application of more thorough approaches, which fully exploit the continuous spectral information provided by spectrometers. One important approach, making full use of the continuous spectral information, is the application of invertible canopy reflectance models. These models infer biochemical/biophysical parameters, such as chlorophyll and water content, from continuous canopy spectral reflectance signatures and have already been successfully applied to field crops and grasslands (Jacquemoud et al., 2000; Bach et al., 2003; Verhoef and Bach, 2003; Migdall et al., 2009; Migdall et al., 2010; Bach et al., 2011; Richter et al., 2012; Locherer et al., 2015).

Some of the parameters that control productivity and health of crops can be estimated through model inversion using hyperspectral optical measurements such as retrieved from EnMAP:

- Leaf area index (LAI) describing the size of the producing layer (Weiss et al., 2001; Locherer et al., 2015);
- Absorbed photosynthetic active radiation (APAR) providing the amount of absorbed energy usable for production (Weiss et al., 2010);
- Chlorophyll content as the chemical actor for photosynthesis, which is dependent on the crop nitrogen status (Haboudane et al., 2002; Oppelt and Mauser, 2003);
- Water content as indicator for crop water status and crop maturity (Ceccato et al., 2001; Champagne et al., 2003; Hank et al., 2010);
- Plant density as indicator of disease sensitivity (Larsolle and Hamid Muhammed, 2007); and
- Plant pigments, such as carotinoids and anthocyanins, as indicators of adaptation of the canopy to varying light conditions (Blackburn, 2007).

Assimilation of these parameters into agro-ecological models allows for an explicit simulation of crop growth, development, and yield for each location on the Earth’s surface based on spatially heterogeneous parameters retrieved from hyperspectral remote sensing data. Model-based assimilation approaches provide site-specific information on key farming parameters, such as biomass, plant height, crop yield, nitrogen or phosphorus deficit and/or uptake, which are not directly observable with remote sensing. Thus, time series of remotely sensed crop parameters account for spatiotemporal heterogeneity in agricultural production models, which then can be used to explore the suitability of different management options (Hank et al., 2012 and 2015). The assimilation of crop parameters, such as pigment concentrations or water content, that can predominantly be deferred from hyperspectral systems, can further be enriched by additional remotely sensed vegetation parameters. They can also be derived from multispectral, thermal or microwave sensor time series, such as LAI, phenology, seeding and harvesting dates or soil moisture. Ultra-high spectral resolution systems allow for the monitoring of sun-induced chlorophyll fluorescence, which could be used as a proxy for photosynthetic efficiency (Guanter et al., 2014). Thus, they offer opportunities for using remote sensing data in agricultural management also beyond the scope of EnMAP. For all of these applications of remote sensing in the context of investigating managed farmland, a continuous monitoring of temporal dynamics is crucial. EnMAP will be the first imaging spectrometer to provide high-quality multi-temporal imagery from space and, therefore, will largely contribute to enhanced process understanding.

From the large number of existing crop growth models, the CERES family (Ritchie and Otter, 1985) is one of the most prominent approaches, which relies on statistical relationships between environmental variables and plant growth and development. PROMET-V (Schneider and Mauser, 2001) is an advancement of such an agricultural model towards spatially distributed simulations that integrate remote sensing data. A further development towards process understanding is achieved by dynamic vegetation models, which simulate plant growth on the basis of eco-physiological processes and feedbacks during the photosynthesis and respiration process.

Currently, the most realistic representation of vegetation dynamics in regional agro-ecological models as well as in regional to global ecosystem and Earth system models is based on the combination of dynamic vegetation models, agricultural management models, and appropriate canopy models that simulate the distribution of assimilates among the plant constituents (i.e., roots, stem, leaves, grains) in order to allow for a realistic representation of the complex canopy layers (e.g., LPJ-mL (Bondeau et al., 2007), PROMET (Hank, 2008)). Recent studies have shown that data assimilation approaches are viable and provide good results (Weiss et al., 2001; Bach et al., 2003; Hank et al., 2012; Machwitz et al., 2014; Hank et al., 2015). Nevertheless, further research and development is needed to improve models, in particular with regard to process representation and accuracy. In order to reach an operational stage of such coupled model systems, various data assimilation methods should be in addition tested under a broad range of farming conditions, especially in regions with low-efficiency farming systems, different crops (e.g., cassava, sorghum, groundnut) and energy plants (e.g., sugar cane, oil palm, jatropha), different stresses (e.g., water, fertilizer, temperature), irrigated agriculture, and mixed silvi-agricultural systems.

Besides further improvements in modelling approaches, sophisticated agricultural applications need to be based on frequently available hyperspectral imagery with high data quality standards. Based on the knowledge already gained in numerous studies with airborne sensors, EnMAP will offer hyperspectral data in a suitable spatial and temporal resolution to approach the next major scientific steps, leading away from regression analysis and towards mechanistic process representation.

Accordingly, the following major scientific tasks are considered to be of importance for agricultural applications:

- Development and improvement of accurate, robust and reliable crop parameter retrieval methods based on inversion of improved canopy reflectance models using imaging spectroscopy data (crop type, LAI, APAR, chlorophyll content, plant water content, canopy geometrical structure);
- Development and improvement of methods for the quantitative mapping of soil parameters, also taking the spectral signal of vegetation into account;
- Development and improvement of approaches to derive complex canopy parameters, e.g., crop phenology, management intensity, or yield gap, from hyperspectral remote sensing data in conjunction with ancillary remotely sensed data;
- Development of operational methods for yield and biomass estimation and forecasting based on hyperspectral remote sensing and ancillary data;
- Mapping of crop species distribution using time series of hyperspectral information;
- Distinguishing of crop stressors like nitrogen deficiency, crop disease, insect infestation, water stress, and chlorosis; and
- Development and improvement of approaches to assimilate remote sensing derived spatial distributions of vegetation and soil parameters into dynamic agro-ecological models.

3.2 Geology and soils

Imaging spectroscopy has proven to be an effective tool to detect, monitor, and manage key abiotic natural resources including minerals, soils, and fossil fuels, which are largely non-renewable. Current research in hyperspectral remote sensing focuses on the assessment of mineral deposits (e.g., Clark et al., 2003), the detection of oil discharges on the Earth surface (e.g., Lammoglia and de Souza Filho, 2011), the deduction of soil properties (e.g., Ben-Dor et al., 2009), and the evaluation and monitoring of soil function (such as water storage, carbon storage) and threats (such as acidification, soil erosion) (e.g., Stevens et al., 2013; Schmid et al., 2015).

3.2.1 Geological exploration

Minerals, or more specifically ore minerals, contain economically valuable elements (mainly metals), which are essential to modern industry and, therefore, to the development of society. The constantly changing demand of ores and the criticality to the producing industry causes perennial re-evaluations of existing occurrences, deposits and mines, and the global detection and validation of new deposits. Among geophysical and geochemical field surveys, hyperspectral remote sensing surveys are increasingly applied to exploration investigations. The basic principle of hyperspectral remote sensing for mineral detection is the mathematical description and statistical analysis of material characteristic signals in the spectral ranges of the visible and infrared wavelength range (Hunt, 1977; Clark et al., 2003; van der Meer, 2004 and 2012). These characteristic signals (absorption bands) are physically based on electronic transitions in the d- or f-orbitals of the elements (e.g., transitions into the valence band for Fe and crystal field transitions for rare earth elements), or vibrational motions and their overtones in the molecular bonds (e.g., Fe-OH and Mg-OH in amphiboles, Al-OH in clay minerals, CO3 in calcium carbonates) (Hunt, 1977; Dieke and Crosswhite, 1963; Swayze et al., 2014). Mineral mapping tools, such as the USGS Tetracorder and its successor MICA and the EnGEOMAP 2.0, and image analysis software, such as the EnMAP-Box and ENVI-Exelis Visual Information Solutions, utilize the mineral characteristic absorption bands to spectroscopically characterize and map surface materials (Clark et al., 2003; van der Linden et al., 2015). The characteristic absorption bands of identifiable minerals serve as a proxy for the lithological units of the different deposit types. These proxy minerals include, for example, alunite, chlorite, dickite, epidote, jarosite, kaolinite, and sericite. They serve as key indicators representative for epigenetic and sedimentary hydrothermal deposits (copper, gold, iron, lead, zinc bearing) (Mielke et al., 2014; Swayze et al., 2014). Carbonatite-alkaline igneous related deposits (rare earth element, lithium, tantalum, niobium bearing) can be mapped using the ankerite, calcite, dolomite, epidote, rare earth element absorption bands and the clay mineral/carbonates ratio (Turner et al., 2014; Boesche, 2015; Boesche et al., 2015a). In this manner proxy minerals can be found for most deposit types and, thus, their occurrences can be mapped. In addition to mineral mapping for resource detection, mining monitoring, natural erosion and environmental pollution as well as Earth's crust forming processes (e.g., volcanic activities) can be assessed using the aforementioned mineral mapping methodologies.

The following main scientific tasks are related to geological exploration:

- Development of algorithms and expert systems for mineralogical mapping with emphasis on alteration zones and index minerals of metamorphic zonations;
- Analysis of the capability of hyperspectral data for the detection of rare earth minerals based on different globally distributed sites;
- Development of new algorithms and models for non-linear, weighted unmixing and mineral quantification approaches; and
- Investigation of the effects of mineral-induced stress on the spectral signature of dense vegetation canopies to establish a link between vegetation stress and specific minerals.

3.2.2 Digital soil mapping

Soil is a fundamental and irreplaceable natural resource, which is largely non-renewable. Soils are complex dynamic systems, which are formed and developed as a result of the combined effects of climate and biotic activities, and modified by topography. Soil development can be either progressive or regressive with time, and a modification of the chemical, physical, and mineralogical properties of soil surfaces can take place at variable time scales from event-based to seasonal. Soil provides a multitude of land-based ecosystem goods and services supporting and regulating life on the planet. It carries out a number of key environmental functions that are essential for human subsistence, such as food, fibre and timber production, water storage and redistribution, pollutant filtering or carbon storage. Understanding the response of soils to external drivers (global environmental changes, management) to assist in decision making at all scales requires precise spatially referenced soil data and maps. However, conventional soil surveys are scarce, expensive, time-intensive and not cross-comparable (harmonized), which precludes a meaningful assessment of the state of the soil resource at large scales. As an alternative, soil spectroscopy in the laboratory has proven to be a fast, cost-effective, non-destructive, and repeatable analytical technique that can be used to monitor the state of soils (Nocita et al., 2015). From airborne platforms, hyperspectral remote sensing (HRS) of soil has demonstrated a large potential to quantify topsoil key properties (organic carbon, texture, mineralogy) over a broad gradient of soils. In particular, the amount of organic matter and iron content, particle size distribution, clay mineralogy, water content, soil contamination, cation exchange capacity and calcium carbonate content, can be determined with imaging spectroscopy (e.g., Ben-Dor et al., 2009; Stevens et al., 2013). Due to soil's complexity as a mixture of organic and inorganic compounds and expressed in their VNIR reflectance properties, simple band assignment techniques or spectral matching, such as done in the geology HRS field, are rarely used. However, multivariate calibration (i.e. statistical) approaches, which allow full quantification of the soil properties based on field data for local calibration, are preferred.

Hyperspectral data as provided by the EnMAP satellite will hold considerable potential to characterize the pedosphere by identifying soil properties and their changes in time. Digital soil mapping toolboxes that include automatic identification and semi-quantification of key soil properties, such as organic carbon, water content, clay, iron, carbonates mineral content, are already available that are applicable at a global scale (Chabrillat et al., 2011). For the full quantification of soil properties, current EnMAP simulations allowed to develop soil maps in specific test sites where ground-reference data were available (Chabrillat et al., 2014). In view of the limited arable land area and rising population, the emerging field of precision farming is receiving increased attention and the soil science community is facing a growing need for regional, continental, and worldwide digital soil databases to monitor the status of the soil. Supported by imaging spectroscopy, soil conditions can be assessed to allow farmers to better evaluate critical needs such as irrigation, nutrient supply, and cultivation to gain increased agricultural yields (Dematte et al., 2000). Nonetheless, advances are still necessary to fully develop HRS products that can support, in a credible manner, digital mapping and monitoring of soils (Wulf et al., 2015).

The following main scientific tasks are related to digital soil mapping:

- Retrieval of soil properties, such as organic matter and iron content, particle size distribution, clay mineralogy, water content, soil contamination, cation exchange capacity and calcium carbonate content to analyse status and changes of soils;
- Improvement of methodologies and algorithms for the extraction of key soil parameters based on remote sensing spectral signal with emphasis on prediction accuracy and influence of spatial scale;
- Quantitative estimation of the influence of surface parameters in bare and semi-bare areas (such as water content, vegetation cover, surface roughness) on the spectral signature of soils and on the retrieval of soil properties;
- Analysis of the contribution of global soil databases to calibrate the remote sensing based soil condition indices against reference samples; and
- Monitoring of the state of soils and development of spatio-temporal maps of soil properties.

3.3 Coastal and inland waters

Coastal and inland water bodies are vital for recreation, food supply, commerce and human health, and they also support habitats for a large floral and faunal diversity. Since decades, these ecosystems experience high pressure from increasing social and economic human activities as well as climate change in future. As sinks for pollutants, coastal and freshwater ecosystems are among the most sensitive indicators of environmental impacts related to human activities (UNEP, 2012). For example, a major global ecological problem is the increasing eutrophication and pollution of coastal and inland water bodies caused by fluvially transported substances, such as phosphate and nitrogen compounds, which derive from intensified agricultural and industrial activities. Monitoring and managing the water quality of coastal and inland habitats is necessary as they are vital to many kinds of utilization, including urbanisation, tourism, transportation, industry, fish farming and drinking water supply. According to the EU Water Framework Directive, specified biological, hydro-morphological and physico-chemical parameters of water bodies have to be monitored on a regular basis.

A major advantage of hyperspectral data covering coastal and shallow freshwater bodies is the ability to spectrally unmix various in-column optical constituents and the sea floor or lake bottom (Carder et al., 1993; Goetz, 2011). The advanced spectral resolution of EnMAP in the VIS and NIR region will allow the assessment of water constituents including phytoplankton pigments, suspended matter, dissolved organic matter, dissolved organic carbon concentration, and water transparency. Moreover, phytoplankton taxonomic groups can be identified, which provide indications for the occurrence of harmful algal blooms (Bracher et al., 2009). Chlorophyll-a concentration is widely used as an indicator of algal biomass that depends upon nitrogen and phosphate availability in the water bodies (Carlson and Simpson, 1996; Kamarainen et al., 2009). Water transparency is a widely used indicator of the trophic state, which is influenced by the abundance of organic and inorganic suspended particulate and dissolved matter (Kirk 1994). Several researchers have developed algorithms to quantify various parameters, such as chlorophyll-a, humic substances, suspended matter, yellow substances, and water transparency (Giardino et al., 2007; Kallio et al., 2001; Schiller and Doerffer, 1999; Thiemann and Kaufmann, 2000 and 2002). EnMAP can make use of these standards for detailed observations of coastal zones and inland waters, while sensors such as MODIS, VIIRS, and the recent OLCI as part of ESA's Sentinels are designed for ocean applications with frequent observations at coarser spatial resolutions. Algorithms for coastal and inland water constituents with different phytoplankton, particulate and dissolved matter composition will be adapted and improved for EnMAP to provide water quality data at a higher spatial resolution. Water quality assessment serves both monitoring of freshwater security and the still increasing importance of aquaculturally used coastal and inland water bodies. Moreover, water quality assessment is crucial for the monitoring and management of endangered ecosystems, such as coral reefs, seagrass meadows or mangrove forests (Bell et al., 2008; Landvelde and Prins, 2007).

EnMAP data will not only offer more frequent observations of in-column constituents but will provide frequent information about the type and status of the sea floor substrate and its changes for optical shallow waters. Water column correction approaches using hyperspectral data allow the identification of bottom vegetation types and, if regularly monitored, the observation of sedimentation dynamics, as well as short- and long-term changes in species distribution and structure (Vahtmaee et al., 2011). Quantitative analyses of coastal benthic communities enable the investigation of net primary production (Dierssen et al., 2010). Moreover, many benthic species act as environmental indicators. Therefore, their frequent monitoring enables an estimate of the state of coastal marine environments and provides evidence for environmental changes (Phinn et al., 2003; Vahtmaee et al., 2006). In this context, the fusion of EnMAP data and satellite data with a high geometric resolution (e.g., Worldview, GeoEye) offers the potential to pinpoint heterogeneously distributed vegetation and sediment patches. The monitoring of benthic vegetation can support integrated coastal zone management when species of certain genera (e.g., Ulva, Laminaria, seegrasses) are grown as a food supply for humans or aquaculture of marine animals (Anderson et al., 2007; Radiarta et al., 2011). The fusion with spatially high-resolution data also offers the potential to monitor frequently invasive benthic and emergent species (Albright and Ode, 2011; Forrest et al., 2012).

Coastal ecosystems are highly productive and store large amounts of carbon (Cole et al., 2007; Pidgeon, 2009). The distribution and dynamics of organic carbon in the vegetation, in combination with dissolved organic matter, are important in understanding regional and global carbon cycles. In this context, the EnMAP data provide efficient means to characterize the role of coastal and inland water bodies in carbon uptake and release.

Coastal and freshwater ecosystem management involves modelling and monitoring, which require a reliable information base and robust analytical techniques. Conventional mapping methods are logistically constrained, while airborne campaigns are cost intensive and often are limited to a few acquisition dates. The EnMAP satellite will enable a repeatable quantitative monitoring of the water-related environmental parameters mentioned above. The combination of hyperspectral data with ecological or hydrological models, geographic information systems and in-situ measurements allows the development of advanced integrated management plans for coastal zones and catchments characterized by inland water bodies, wetlands or reservoirs (Yang, 2009; Radiarta et al., 2011). The fusion of hyperspectral data with thermal infrared data offers additional perspectives to the analysis of the trophic state of coastal or freshwater ecosystems. A combination of EnMAP derived bathymetry with RADAR, LIDAR or Laserscan data can be useful to derive underwater topography and morpho-dynamics of shallow water areas (Pleskachevsky et al., 2011). Thus, imaging spectroscopy enables an accurate estimation of water quality and sea floor parameters. Moreover, it offers the potential for new and complementary indicators for the characterization of the state of coastal and inland water bodies.

Coral Reefs

Coral reefs are mosaics of coral, algae and sand. They occupy an area of approximately 250,000 km^2 to 600,000 km^2 (Hochberg, 2011), corresponding to about 5 % – 15 % of the shallow sea areas (0 m – 30 m depth), and are spatially heterogeneous at sub-meter scales. Coral reefs host a diversity of organisms whose complex dynamics are affected by a vast range of interconnected processes. In addition to their ecological value, they also provide significant economic value, supporting, for example, fisheries, aquaculture, tourism and recreation (Andréfouët et al., 2005). Thriving in a narrow range of conditions, they are very sensitive to environmental changes and react quickly to new stressors, making them one of the most threatened coastal ecosystems in the world and a unique indicator of global change (e.g., Andréfouët et al., 2005). A decline in reef status is represented by a shift from coral- to algal-dominated community structures and accompanied by a general decrease in biodiversity. However, current reef surveys usually cover only small regions, leaving vast areas of the world’s coral reefs unsurveyed (Hochberg, 2011). Remote sensing is one technique with a huge potential for quantifying reef community status at large scales.

Historically, remote sensing approaches used the Landsat series, SPOT HRV and ASTER data for the detection of reefs and reef geomorphology from the mid-1970s (Hochberg, 2011). Development of imaging spectrometers operated on airborne platforms in the 1990s enabled identification and mapping of reef communities. While broadband data allow the discrimination of three to six classes (Mumby et al., 2004), an increased number of and narrower bands may allow more than 10 habitat types to be discriminated (Hedley, 2013). More recent developments include spectral unmixing, “wavelength feature” approaches and radiative transfer model inversion methods that require hyperspectral data (Hedley, 2013), while change detection analyses still depend on multispectral imagery due to limitations in multi-temporal hyperspectral data availability. The most ambitious objectives, such as the discrimination of live coral versus dead coral and/or macroalgae, quantification of live coral cover, or the detection of coral bleaching events, are not yet routinely achieved (Hedley, 2013).

In summary, coral reef remote sensing is a very dynamic field and upcoming sensors, such as EnMAP, are expected to have a major impact in the near future by providing data currently acquired from airplanes at great costs. Not only will EnMAP's high-spectral resolution likely allow for identification of the three basic reef bottom-types with high accuracy, spectral unmixing to discriminate sub-pixel composition, or modelling of light absorption and water optical properties, it will enable global mapping of benthic community structure and long-term monitoring of reef status, increasing the understanding of the large-scale oceanographic and ecological processes that affect reef health (Hochberg, 2011).

Accordingly, the following main scientific tasks are related to coastal and inland water body applications:

- Improvement of the identification of different substances by their spectral characteristics, such as improved chlorophyll quantification, the differentiation between ecological important phytoplankton groups, and dissolved organic compounds;
- Enhancement of the identification of different fractions of suspended mineral and organic particles;
- Monitoring of the spatio-temporal dynamics and structure of optical shallow sea/lake bottom substrate (vegetation and sediment);
- Monitoring of the distribution patterns of invasive submersed and emergent algae;
- Monitoring of the variety of algal species/genera in space and time as a bio-indicator of coastal and freshwater ecology;
- Monitoring and taxonomic identification of (potentially toxic) algal and phytoplankton blooms in eutrophicated coastal and inland waters;
- Estimation of processes, such as primary production in inland and coastal waters and suspended matter transport and its impact on coastal ecosystems;
- Monitoring of the distribution of sediments in tidal flats, wetlands, coral reefs and mangrove forests; and
- Monitoring of coastal erosion and changes in coastal morphology.

3.4 Cryosphere

The magnitude of predicted global warming is largest in high-latitude and high-altitude regions (IPCC, 2014). Retreating inland ice, decreasing sea ice extent, shorter snow cover periods, and accelerated degradation of permafrost areas testify this longstanding trend (e.g., Pritchard et al., 2009; Liston and Hiemstra, 2011; Stroeve et al., 2007; Lawrence and Slater, 2005; IPCC, 2014). Complex feedback mechanisms imply a wide range of climatic, hydrologic, ecologic, and geomorphic changes in these regions. Quantifying the state and changes of snow, glaciers, ice caps, sea ice and permafrost landscapes is strongly hampered by missing ground observations due to the challenging logistics as a result of the remote and complex terrain. Therefore, satellite observations represent a unique database to track and quantify variations in the cryosphere.

Despite the environmental limitations for optical sensors in the Polar Regions (i.e., months of polar night, high cloud coverage, and year-round low solar incidence angles), hyperspectral satellite and airborne data provide unique synoptic information on biogeochemical and -physical environmental quantities. Hyperspectral data provide the most important input and enabling from data in space and time to derive terrestrial and aquatic energy, water, sediment, and carbon fluxes. Accordingly, hyperspectral remote sensing offers the great potential to measure key diagnostic parameters that map, monitor and model the cryosphere at landscape scales.

3.4.1 Permafrost and Vegetation

Permafrost covers about 25 % of the northern hemispheric land area and, hence, represents one of the largest components of the Arctic cryosphere. Permafrost arctic environments maintain important ecosystems with unique plant communities which are particularly sensitive and responsive to climatic changes. In permafrost environments, the vegetation, thermal sub-ground conditions, geomorphology, hydrology and atmospherical fluxes highly interact with each other. Field observations of the active layer (top layer of soil that thaws during the summer) and the underlaying permanently frozen ground show a continuously warming trend with a high-spatial variability in warming rates that depend on ice content and absolute ground temperatures (Smith et al., 2010; Romanovsky et al., 2010). Large-scale permafrost degradation may provoke feedbacks, such as activation of the soil carbon pool and a northward expansion of shrubs and forests (Lawrence and Slater, 2005). Increased permafrost knowledge is particularly important for the design and maintenance of infrastructure in permafrost environments and for designing effective adaptation strategies for the local communities under warmer climatic conditions (Romanovsky et al., 2010).

Permafrost is a sub-ground thermal phenomenon which cannot be directly observed by optical remote sensing. However, there are a large number of surface indicators suited for hyperspectral remote sensing applications, such the state of the vegetation, surface morphology, hydrology, and aquatic ecosystems. In particular, the discrimination of different vegetation types, biophysical variables and the photosynthetic activity is of great interest in taiga and tundra permafrost landscape research (Rees et al., 2003; Laidler and Treitz, 2003; Hope et al., 2003). For example, Muster et al. (2012 and 2013) used the hyperspectral CHRIS-sensor and other optical remote sensing data to investigate the surface water and the moisture regime for process studies of energy and water fluxes and to extract the subpixel fraction of surface water. Buchhorn et al. (2013a) and Buchhorn (2014) provided a base for hyperspectral remote sensing of high-latitude tundra permafrost landscapes by analysing the hyperspectral and spectro-directional reflectance properties of the main tundra plant communities under changing illumination conditions, showing that they can be well distinguished spectrally. Measurements with an EnMAP-specific spectro-goniometer system (Buchhorn and Schwieder, 2012; Buchhorn et al., 2013a; Buchhorn, 2014) revealed that up to a sensor viewing zenith angle of 30°, the backshadow effect seems to dominate the gap effect, which leads to lower reflectance values in the forward viewing directions compared to the nadir or backward viewing directions. Additionally, the contrast between shadowed and illuminated surfaces is reduced, because even low-growing plant canopies can produce long shadows at high solar zenith angles. On the other hand with increasing SZA, the reflectance anisotropy changes to an azimuthally symmetrical, bowl-shaped distribution of reflectance values with the lowest ones at nadir. The explanation for these findings is that the erectophile moss and lichen understory together with widely dispersed erectophile grasses suppress the planophile-like BRDF (bidirectional reflectance distribution function) behavior. At a SZA of 55° to 60°, the gap effect starts to become dominant in the overall more erectophile tundra canopy with complete dominance at a SZA beyond 68°. This knowledge of the spectro-directional reflectance characteristics of tundra vegetation is now available for the retrieval of high-quality, consistent and, therefore, comparable and reproducible datasets from airborne and spaceborne sensors for the high-latitudes.

The following main scientific tasks are related to permafrost and vegetation:

- Assessment of the state and changes in vegetation, hydrology, and surface morphology in permafrost landscapes; and
- Discrimination of different vegetation communities and plant functional types, vegetation succession on disturbances, and phenological and photosynthetic state of Arctic vegetation.

3.4.2 Snow & Ice

Snow

Characterization of snow-covered areas and inland ice is critical for understanding the Earth's hydrology, climatology and ecology, because of their significant effect on the energy balance at the land-atmosphere boundary and their importance as fresh water sources. Distributed snow-surface energy-balance models need the following spatially distributed parameters that potentially can be provided by hyperspectral remote sensing: snow-covered area, snow albedo, grain size, and snow water equivalent (Dozier and Painter, 2004). Accurate measurements of these physical snow properties are also prerequisites to drive distributed hydrological models in order to quantify timing and magnitude of snowmelt runoff and its source areas.

However, detailed ground-based measurements of snow and inland ice properties are completely scarce due to the remoteness and challenging and often dangerous logistics. Satellite-based imaging spectroscopy can be used to retrieve key snow inland ice parameters:

Snow albedo and snowmelt are directly linked to the growth of grain size (Warren and Wiscombe, 1980). The snow reflectance decreases dramatically, especially in the NIR range, as the snow grains evolve after deposition. Liquid water inclusions of melting snow yield albedo reductions, because liquid water in snow causes the grains to form clusters (Colbeck, 1979). Repeated hyperspectral measurements of snow enable to quantify the evolution of albedo by accounting for various effects like grain size and snow contaminants.

Snow contaminants, such as dust, algae, and soot, degrade snow reflectance significantly, especially in the VIS spectrum by adsorption of incoming radiation and at longer wavelength by increases in grain size through local microscale metamorphism (Dozier et al., 2009). For example, an experiment that compared hyperspectral data to field-measured impurities showed good agreement between measured dust concentrations and snow reflectance (Tanikawa et al., 2002). The extensive glacial debris cover, which characterizes most mountain glaciers, can be spectrally analysed to decipher their origin and to improve glacial mapping as well as our understanding of glacial ablation and kinematics (Casey et al., 2012).

Organic materials in the snow may have even distinctive spectral features (Takeuchi, 2002). Snow algae (*Chlamydomonas nivalis*) may be abundant on top of the snow and inland ice causing albedo to decrease. Their distinctive reddish colour, caused by pigment absorption allows measurement of their concentration with hyperspectral data (Painter et al., 2001).

Because varying grain sizes and ablation of contaminants and organic materials translate into variability of spectral reflectance, multiple snow endmembers are necessary to characterize snow. Spectral mixture analysis enables to accurately represent the spatial distribution of snow (Nolin et al., 1993). Painter et al. (1998) improved subpixel snow mapping by allowing the spectrum of the snow endmember to vary to match the spectral shape of the pixel's snow reflectance. The authors used hyperspectral airborne AVIRIS data to estimate both subpixel snow cover and grain size over a wide range of snow conditions in the Sierra Nevada. Rosenthal and Dozier (1996) developed linear spectral mixture analysis for subpixel snow-covered area from Landsat. Although only based on multispectral data, they were able to map patchy snow cover several times during a season. This Landsat spectral mixing model was also used to map snow on glaciers. For example, Klein and Isacks (1999) applied the spectral mixture analysis to identify the ablation and accumulation zones and the transient snowline on several tropical glaciers.

Sea ice

Knowledge of properties of the sea ice is of greatest importance, because the sea ice albedo is among the most crucial parameters, which govern the climate processes.

In the context of the changing Arctic climate, knowledge on sea ice surface melting, its spatial distribution and the length of the melt season is required to predict the role of the sea ice cover in the radiative balance. Melt ponds change the radiative balance in the Arctic, because they drastically reduce the ice albedo and, therefore, increase the flux of absorbed sun light energy and speed up the melting process (positive feedback mechanism). Snow accumulation on the sea ice needs to be considered as one of the most critical variables in determining ice permeability and melt pond development (Eicken et al., 2004).

Sediment-laden sea ice, i.e., ‘dirty sea ice’, is a common phenomenon in the Arctic. The sea-ice sediments mainly consist of terrigenous sediments with clay minerals, quartz and feldspars as main components (Nuernberg et al., 1994). Due to surface melt, the sediment accumulates at the surface of multi-year sea ice, often concentrated into layers of mud several millimetres thick. The quantification of sediment transport by sea ice presents a considerable challenge due to the patchy distribution of sediments and the overall difficulty in obtaining data on the areal distribution and suspended particulate matter concentrations, while published quantitative estimates of sea-ice transported sediment loads differ significantly (Eicken et al., 2005 and further references therein). Lisitzin (2002) postulated that 10 % to 50 % of the total Arctic sea-ice area is covered by dirty sea ice.

In order to assess the change of the energy budget in the region, the sea ice reflective properties, such as pure ice or ‘dirty ice’, snow and melt pond coverage on sea ice have to be known. These products can serve as an input for Global Climate Models, hydrological models and for the estimation of sediment on sea-ice flux. In addition to these applications, knowledge of the spectral properties of sea ice surface, such as the melt pond fraction, is useful to plan ship navigations. Therefore, spectral remote-sensing potentially provides the different sea-ice albedo types, extracts melt pond fractions, maps the extent of particle-laden sea ice and assesses its particulate loading. Perovich et al. (2007) refer to direct measurements of the anisotropic reflectance factor for snow covered, bare, and ponded sea ice. Huck et al. (2007) built up a radiative transfer model for sea ice coupled with an optical model for particulates included in sea ice to model different sea ice surfaces of variable sediment load. They distinguish between different degrees of sediment loading and the melt pond fraction. Istomina et al. (2014) developed an algorithm to retrieve the melt pond fraction and different sea ice types from MERIS data and validated it against aerial, shipborne and in-situ campaign data. The developed algorithm is based on a newly developed optical model of sea ice reflection, accounting also for the bi-directional reflection from the ice/snow surface (Zege et al., 2015). This is particularly important for Polar Regions where the SZA is high. The results show the best correlation for landfast and multiyear ice of high ice concentrations. The presented melt pond fraction and sea ice albedo retrieval need various spectral bands in the VIS and NIR regions of the spectrum (Istomina et al., 2014; Zege et al., 2015).

Future snow and ice research will benefit from a synergistic data collection that combines fine spectral and spatial resolution (EnMAP) with sensors with a broad swath and daily coverage of the whole Earth (MODIS, Sentinel 3, VIIRS). Envisioned applications include regular tests of medium-spatial resolution data with EnMAP and data assimilations to improve mapping and monitoring of, sea-ice types, snow cover on inland ice and sea ice, ice algae, sediment and dust on ice, melt pond fraction and evolution on inland ice and sea ice by an increased temporal and spatial resolution.

The following main scientific tasks are related to snow and ice:

- Development and improvement of new hyperspectral approaches to retrieve snow properties (e.g., albedo, grain size and near-surface liquid water, mineral and organic contaminants) and spatial snow cover distribution;
- Exploration of synergies to multispectral sensors with varying spatial scales to improve snow mapping in forests and adapt to angular variability;
- Determination of the spatial and temporal variability of ponded ice spectral reflectance properties as a key parameter in determining the large-scale sea-ice albedo; and
- Determination of snow accumulation, melt pond areal fraction, and sediment load on sea-ice to overcome problems associated with the significant spatial inhomogeneity observed and the fact that it occurs in largely inaccessible parts of the world's oceans.

3.5 Urban areas

Over the past 50 years, anthropogenic ecosystem changes were more rapid and extensive than in any comparable period of time in history (MEA, 2005). The world currently experiences rapid urbanization and an increase in the number of megacities, particularly in developing countries. According to the United Nations Development Program, urban population growth will continue to rise substantially over the next several decades (UN, 2012). The (often uncontrolled) process of urbanization always results in changes in land use and cover and causes serious problems, such as environmental pollutions, destruction of ecosystems, waste disposal and others. Moreover, urbanization and related changes in lifestyle increase the per capita demand for energy, goods and services (Meyerson et al., 2007). Land conversions, introduced by urban consumption patterns, have regional consequences for the biophysical system that may lead to global consequences (Sanchez-Rodriguez et al., 2005). Thus, there is a critical need to map urban land cover composition and monitor urban growth. Remote sensing techniques are widely used to study urban environments. However, hyperspectral applications are comparably scarce (Xu and Gong, 2007; Cavalli et al., 2008; Weng et al., 2008), which may, to a great extent, be explained by the spectral and structural complexity of urban areas (Small, 2001 and 2003; van der Linden and Hostert, 2009) and to a limited availability of appropriate sensors covering the full reflective wavelength range (Roberts et al., 2012). EnMAP hyperspectral data of medium spatial resolution will open up new opportunities to describe and monitor land-cover composition in urban areas and along urban-suburban gradients assisting in the understanding of the dynamics of global urbanization (Heldens et al., 2011).

Classification schemes for urban areas are generally influenced by the spatial scale of analysis and the scope of related studies (Heiden et al., 2007; Herold et al., 2004). Research is needed to determine the most suitable classification scheme for EnMAP. Given the 30 m ground sampling distance of EnMAP, urban mapping will often require a quantification of the sub-pixel land-cover composition. For these types of analyses, techniques such as spectral unmixing or regression modelling that are capable of dealing with the spectral variety of urban surfaces have to be developed (Roessner et al., 2001; Franke et al., 2009; Okujeni et al., 2013). For both qualitative and quantitative analyses of urban areas, the implementation of reference spectral libraries is essential (Herold et al, 2004; Heldens et al., 2011; Heiden et al., 2012; Bieniarz et al., 2014; Jilge et al., 2015; Okujeni et al., 2015a). However, it poses a challenging step that requires extensive collaboration between international research groups (Hueni et al., 2009; Rasaiah et al., 2011). The combination of medium-spatial resolution and high-spectral information content requires new concepts for the description of land-cover composition. While the occurrences of spectrally pure surface materials are rare, urban spectral mixtures contain compositional information that might be characteristic for certain urban structures, such as inner city centres or commercial areas. Recent studies that focused on plant species variations used compositional variation to extract major vegetation gradients (Schmidtlein and Sassin, 2004; Feilhauer et al., 2011). Applying such concepts to urban areas could account for the spectral and spatial information content of EnMAP data.

One essential application with regard to urban planning is reliable mapping of imperviousness. Within this context, approaches that combine qualitative and quantitative analyses appear most suited to make full use of the additional information from EnMAP. This additional information will help make approaches based on the V-I-S concept (vegetation - impervious surface - soil, Ridd, 1995; Wu and Murray, 2003; Lu and Weng, 2006) more reliable or help to extend such models by additionally differentiating built-up and non-built-up areas. Recent analysis of simulated data showed EnMAP’s potential for improved and extended V-I-S mapping compared to broadly available multispectral Landsat data (Okujeni et al., 2015a).

Reliable surface material indicators are needed for applications, such as urban climate studies and other approaches that require knowledge on the biophysical properties of the urban land cover. Remote sensing data is more and more used to study the urban climate at meso and macro scales. Especially physical properties of urban areas, such as reflection, absorption, emissivity, specific heat capacity, but also height and spatial arrangement of urban objects, are needed to parameterize climate models (Jin et al., 2007; Yang, 2000; De Foy et al., 2006). Spaceborne hyperspectral EnMAP data will have the potential to provide this information (Okujeni et al., 2015b) on an operational basis. However, suitable concepts are needed to derive urban ecological indicators (Behling et al., 2015) and to integrate the surface information into urban climate models. Local climate zones (LCZ) are a concept especially developed for climate studies in urban areas (Stewart and Oke, 2012).

In this context, fusion of spectral and thermal data (at the feature or knowledge level) may reveal the relationship between thermal patterns, urban surface materials, and urban structure and, thus, helps to understand their influences on the urban climate (Oke, 1988). Such data fusion studies have already been carried out at local scales with airborne thermal and hyperspectral data (e.g., Xu et al., 2008). Novel fusion techniques combining future EnMAP data with thermal sensors (e.g., ASTER, HyspIRI) can open up new opportunities for urban climate studies on larger scales. Another challenging task is the combined analysis of hyperspectral data and spatially high-resolution remote sensing data, which enables a detailed analysis of urban structures combined with surface material information. In this context, image data fusion (Zhang, 2010) is a promising technique to retrieve further information from EnMAP data. However, methodological gaps exist for spatial upscaling techniques that preserve spectral information content. Overall, the synergistic use of hyperspectral, thermal, and optical data with advanced data analysis techniques may result in enhanced socioeconomic and environmental indicators to model urban dynamics and their social and environmental consequences.

Accordingly, main scientific tasks related to urban areas include:

- Mapping and monitoring of urbanization and its dynamics with high spectral detail worldwide;
- Development of comprehensive urban spectral libraries for universal urban land-cover mapping based on EnMAP data;
- Development and improvement of classification algorithms to quantify urban land cover, including classes that are spectrally ambiguous in multispectral data;
- Investigation of new concepts for information extraction based on spectral mixtures;
- Application and extension of the V-I-S concept to produce biophysical surface maps with respect to the needs of urban environmental process models , e.g., on urban climate and hydrology; and
- Mapping of the abundance of hazardous materials such as asbestos, e.g., in the context of risk analyses.

3.6 Atmosphere

Although EnMAP is not specifically designed for atmospheric research, variables that describe atmospheric conditions and constituents may be retrieved from EnMAP data. These variables include atmospheric levels of methane, atmospheric water vapour, mineral dust, particulate matter clouds, and pollen.

Methane is among the most important greenhouse gases and its concentration was increased three fold since pre-industrial times (e.g., IPCC, 1995; Bousquet et al., 2006). Besides large-scale emissions e.g. from wetlands or due to land-use changes, small-scale emissions play an important role in the total amount and variability of current day methane emissions (e.g., Katey et al., 2006; Cao et al., 1998). Satellite observations with coarse spatial resolution were a key to identify previously unknown emission sources of methane (e.g., Houweling et al., 2006). Smaller scale anthropogenic and natural sources can contribute significantly to the total global emissions (Katey et al., 2007; Kort et al., 2014) and their monitoring can significantly reduce uncertainties on their budget estimates. Small-scale methane sources could be identified from hyperspectral aircraft measurement using techniques which are in principle applicable to EnMAP measurements in the SWIR spectral region (e.g., Bradley, 2011; Thorpe et al., 2014; Thompson et al., 2015). Thus, retrievals of atmospheric methane concentrations from EnMAP observations could bridge the current gap between airborne campaigns and coarse spatial resolution spaceborne observations. Initial tests have demonstrated the feasibility of methane column content retrievals with EnMAP, which suggests that one can leave the realm of methane anomaly detection and start to monitor and quantify small spatial scale methane emissions either from natural sources, such as lakes and fires, or anthropogenic sources, such as mines or industrial sites. The detection limit and absolute retrieval accuracy from algorithms for EnMAP observations are currently an active field of research and remain to be determined.

Atmospheric water vapour is important for many environmental applications, because it constitutes one of the most effective greenhouse gases in the atmosphere. It shows a high-spatial and temporal variability, depending on meteorological conditions and land use at the underlying Earth's surface. Information on the regional distribution of atmospheric water vapour may, for example, facilitate the analysis of SAR data, because the radar signal transit time depends on the atmospheric conditions. A few algorithms for the retrieval of columnar water vapour content from hyperspectral remote sensing data have already been developed (e.g., Barducci et al., 2004).

Atmospheric constituents such as mineral dust and particulate matter clouds originating from sand storm areas or biomass-burning activities also show a highly variable temporal and spatial distribution. Mineral composition of such transported dust is essential to our understanding of climate forcing, mineralogy of dust sources, aerosol optical properties, and mineral deposition to the ground. Furthermore, the differentiation of spectral signals from the ground and from mineral dust may allow separating atmospheric influences from the actual ground signal by determining their mineral composition. Chudnovsky et al. (2009) showed that, for the suspended dust, the absorption signature could be decoupled from scattering, allowing detection of key minerals. For vegetation and phenological studies, temporal and spatial pattern of pollen spread may be retrieved from hyperspectral data as few studies have already demonstrated (e.g., Kaleita et al., 2006).

Accordingly, scientific tasks related to atmospheric applications include:

- Development of a retrieval algorithms for total column methane concentration from EnMAP observations;
- Establishment of figures on the detection limit and total accuracy of a potential methane product;
- Development and improvement of algorithms to retrieve columnar water vapour based on hyperspectral data;

- Development and improvement of algorithms to characterise mineral dust, particulate matter clouds and pollen based on hyperspectral data; and
- Development and improvement of algorithms to separate the spectral signal of mineral dust from the actual ground signal.

3.7 Hazards and Risks

EnMAP data can contribute to various information needs, originating from the goal of an improved hazard and risk assessment. These include process-related (hazard) as well as damage-related (vulnerability and risk) aspects and apply to both, natural and man-made hazards. Overall, the main benefit of hyperspectral data lies on their potential for a more differentiated characterization of predisposing (contributing) factors as well as changes caused by hazardous phenomena in regard to environmental conditions and affected infrastructures.

Landslides

In mountainous areas, landslides of various forms and composition impose a constant threat to local communities and infrastructures. Landslide inventories (Guzzetti et al., 2012) and hazard assessment (Guzzetti et al., 2005) studies have long been based on the analysis of remote sensing data for an improved characterization of predisposing factors as well as for the establishment of up-to-date landslide inventories (Metternicht et al., 2005 and references therein; Behling et al., 2014; Scaioni, 2014). Remote sensing based landslide analysis can be improved with hyperspectral data, especially for an improved characterization of environmental factors predisposing landslides. For example, this includes a better differentiation of the lithological conditions and an improved identification of inhomogeneities within landslide-prone slopes, indicating an increased potential for the onset of slope failures. This way, hyperspectral data can contribute to a better characterization of active unstable slopes, such as debris-covered areas, fractured/disjointed rock walls, landslide accumulation borders and individual structural features and landforms, such as major faults and fractures, trenches, elongated depressions, and counterslope scarps (Mondino et al., 2009).

Swelling soils

Expansive clays and clay-shales cause costly damages world-wide every year. The distribution of reported instances of heaving (Chen, 1988) indicates that the problem of expansive soil is widespread throughout the five continents, mostly confined to semi-arid regions of the world. Soil spectroscopy has been shown to be a useful tool for evaluation of expansive potential (e.g., Goetz et al., 2001) and hyperspectral remote sensing with its potential for direct identification of constituent minerals in soils allowed detection and mapping of expansive clays in different locations and at different spatial scales (e.g., Chabrillat et al., 2002; Chabrillat and Goetz, 2006; Kariuki et al., 2004). Hyperspectral imagery can identify heaving soils and map their spatial distribution and, thus, offer practical help to planners.

Floods

Many riverine and coastal areas in the world are threatened by floods caused by rainstorms, snowmelt, cyclones, tidal waves or dam-failures. A major challenge related to flood monitoring is the timely detection and the broad regional extent. Consequently, satellite imagery has been extensively used since the 1970s to detect and monitor floods allowing for a more rapid emergency response, the assessment of damaged areas, and the study of water quality changes (Ip et al., 2006). Hyperspectral remote sensing has proven to be particularly suited to estimate soil contamination in floodplains (e.g., Goetze et al., 2010).

Droughts

Droughts can have a substantial impact on the ecosystem and agriculture of the affected area. For example, large-scale agricultural losses can have local to global socioeconomic implications in the form of income losses and increasing commodity prices (Simelton et al., 2012; Ubilava, 2012). In general, drought periods lead to an increased fire susceptibility and tree mortality, whereas carbon uptake decreases significantly (Nepstad et al., 1999; Asner et al., 2000; Williamson et al., 2000). Spaceborne imaging spectroscopy has a large potential to study climate–vegetation interactions by detecting the state of vegetation on a regional scale (Asner et al., 2004). Such ecosystem studies may yield an increased accuracy of ecological models and could result in drought-preventive measures for agricultural areas.

Volcanoes

In concert with seismic and geodetic measurements, hyperspectral information on volcanic debris flows, pyroclastic materials, and gas emissions are fundamental to the understanding of eruptive systems (Crowley et al., 2003; Tralli et al., 2005). In particular, hyperspectral information may provide valuable insights into volcanic activity (Cipar et al., 2010). While these studies illustrate the potential of a hyperspectral sensor in volcanic research, the approaches need to be fine-tuned and tailored to the information needs of crisis management. For example, the differentiation between various crater types, lava flow types and volcanic deposits would significantly improve the risk assessment to enable a timely planning of evacuation measures.

Land degradation and soil erosion

As a result of climatic variations and human mismanagement, deterioration in soil and plant cover has adversely affected nearly 70 % of the world´s dry-lands that cover approximately one third of the continental surface of the Earth. These facts have led to the ratification, by almost 180 nations, of the UN Convention to Combat Desertification (UNCCD, 1994), which emphasizes the need to monitor and assess land degradation processes worldwide. Combating desertification requires accurate knowledge of the current land-degradation status and the magnitude of the potential hazard. It is widely agreed that accelerated erosion is one of the most important sources of land degradation that, together with the destruction of vegetation cover and structure, contributes to the potential increase of land degradation and desertification (Pickup, 1989).

EnMAP data holds considerable potential to assess various degrees of land degradation by retrieving important variables that control the susceptibility to soil erosion, such as soil compaction, surface roughness, infiltration rate, and soil moisture (Haubrock et al., 2004 and 2008). Due to distinct topsoil characteristics, soils previously affected by erosion can be spectrally distinguished from intact soils (Dematte et al., 2000), and soil erosion and deposition stages can be mapped with hyperspectral remote sensing (Schmid, 2015). Another manifestation of soil degradation is increased salinity, which is commonly caused by rising water tables induced by land clearing or irrigation. In this case, imaging spectroscopy proved to be an effective tool to infer the degree of soil salinity as indicated by the shape of the hydroxyl absorption feature at 2200 nm and by the presence of indicator minerals such as gypsum or smectite (Taylor et al., 2001; Taylor, 2004). Further applications to investigate land degradation based on hyperspectral imagery include the analysis of spatial patterns and temporal dynamics of desertification (Asner and Heidebrecht, 2005) and the identification and mapping of dry senescent vegetation cover, thus, providing an accurate vegetation cover in arid areas (e.g., Chabrillat, 2006). Overall, EnMAP will open up new possibilities to assist agricultural land use and to combat land degradation and soil erosion processes.

Oil spills

Imaging spectroscopy has been employed to detect the occurrence and migration of oil spills and contamination. Oil seepages may occur naturally within onshore or offshore basins or result from leaks and spills during the extraction, transportation, storage, and utilization of petroleum. In marine environments hyperspectral data can be used to track an oil spill's areal extent, the oil thickness, and oil categories. For example, Salem (2001) developed methods to detect oil-polluted surfaces (soil and water) and to predict oil spill trajectories and migration rates for a quick disaster response. However, the spectral behaviour of oil in water is inherently a highly non-linear and variable phenomenon that changes depending on oil thickness and oil/water ratios (Rand et al., 2011). In addition, hyperspectral imagery has been used to detect ecosystem changes by weathered oil in coastal littoral zones (Bostater et al., 2011; Salem, 2005) and by oil-induced vegetation stress (Li et al., 2005).

Marine litter

The pollution of marine and coastal environments with marine litter, which is mainly composed of plastics, has been identified as a long-term hazard for associated ecosystems (Galgani et al., 2010; UNEP, 2009). Continuously increasing disposal quantities and low plastic degrading rates (on the order of centuries) caused an increasing litter accumulation in these environments over the past decades. Marine litter causes several harms including entanglement of and ingestion by marine organisms (e.g., fishes, seabirds) (Gregory, 2009). Because persistent toxic substances, such as organochlorines (e.g., PCB, DDE, DDT) and others, are accumulating at high concentrations on the surface of plastics (e.g., Mato et al., 2001; Ogata et al., 2009), the ingestion of plastics by marine organisms represents the entrance point of those substances into the food chain (e.g., Bjorndal et al., 1994; Eriksson and Burton, 2003; Graham and Thompson, 2009; Boerger et al., 2010). However, whether there is enrichment or depletion within the food chain is subject to on-going research (Zarfl et al., 2011). Despite a basic understanding of principle sources and sinks of plastic pollution, a detailed assessment of their quantities and transport pathways is still lacking (Zarfl et al., 2011). Therefore, the monitoring of marine litter is prescribed as a mandatory task in the Marine Strategy Framework Directive (MSDF-indicator 10.1.3) and, consequently, on EU level as well as on the global level guidelines which have been compiled for the best practices of conducting this monitoring (Cheshire et al., 2009; JRC, 2013). Given that imaging spectroscopy is suitable to identify marine plastics (e.g., Thompson et al., 2004; Kuriyama et al., 2002), EnMAP might contribute to the localization of major pollution sources, sinks and pathways of marine litter. A potential application to localize marine litter is related to natural hazards like tsunamis and floods, which can act as transport agents for large amounts of artificial materials into the marine environment. A major challenge in such a scenario is the timely acquisition and analysis of remote sensing images, which requires the development of efficient image processing techniques for a near-real-time support to enable the removal of marine litter.

Industrial and mine waste and environmental rehabilitation

The extraction of natural resources is frequently associated with environmental degradation due to the dispersion of potentially toxic substances. For example, numerous abandoned mines (e.g., open pit coal, copper and gold mines) have left an environmental legacy of acidic drainage and toxic metals in downstream watersheds with adverse effects to human and ecosystem health (Swayze et al., 2000). Acid mine drainage derives from an enhanced sulfide hydro-oxidation process due to the increased effective surface of crushed and milled rocks during the mining process. Sulfuric acid enters the food chain through contaminated soils and water, which can ultimately result in the collapse of wetlands (McCarthy et al., 2007) and the decline of ecosystems in general (Wepener et al., 2011). In addition, technical accidents or illegal dumpings that release toxic industrial waste can contaminate the surrounding environment (Mayes et al., 2011; Minh et al., 2003; Okoronkwo et al., 2006; Wong et al., 2007). Imaging spectroscopy can effectively identify contaminations and determine its sources and impacts on the water cycle and vegetation health (Clark et al., 2003; Kemper and Sommer, 2004).

For example, hyperspectral mapping of areas affected by acid mine drainage has accelerated the site clean-up and saved millions of dollars in clean-up costs (EPA, 1998). Based on an improved understanding of environmental impacts, many countries strengthened legislation to enforce environmental protection and to implement rehabilitation measures (MMSD, 2002). In this context, imaging spectroscopy represents a comprehensive monitoring tool to assess the mining related environmental impacts and to monitor the progress of ecosystems restoration. Regarding waste management, hyperspectral applications provided information on the concentration and distribution of asbestos and other debris materials in the aftermath of the September 11th terrorist attacks (Clark et al., 2001). Therefore, EnMAP has the potential to become an efficient operational tool to monitor both the effects of environmental pollution and the progress made in the rehabilitation of affected sites.

The following main scientific tasks are related to hazards and risks:

- Monitoring of tectonic, lithological and soil parameters for better characterization of factors predisposing landslide formation to improve hazard assessments;
- Detection and mapping of swelling soils occurrences to assess swelling potential and to improve hazard assessment and application of adequate countermeasures;
- Detection and monitoring of flood occurrences to assess flood risks, damaged areas, and water quality;
- Monitoring of the state of vegetation during drought periods to improve the accuracy of ecological models and to develop drought-preventive measures for agricultural areas;
- Investigation of volcanic systems with regard to their crater types, lava flow types and volcanic deposits to improve risk assessment and evacuation measures;
- Monitoring land degradation processes (erosion and deposition) by providing regular maps of vegetation distribution and characteristics (taking into account highly variable background substrates) and soil status, such as organic matter (TOC), $CaCO_3$, iron content, infiltration rate, salinity, and physical crusting development;
- Identification and quantification of various soil contaminants through their specific spectral signatures or indicators (e.g., bio-indicators based on eco-toxicological effects on vegetation) linked to change in chemical composition of the polluted soil;
- Investigation of oil spills with respect to type, distribution, migration rates, and environmental impacts;
- Identification of sources, sinks and pathways of marine litter during large-scale plastics discharge events;
- Monitoring of mining sites for their sustainable management; and
- Monitoring and quantification of the distribution of toxic materials in waste dumping sites and assess the degree of environmental contamination and the success of remediation strategies.

4 Scientific exploitation strategy

In the preparatory phase of the EnMAP mission, a considerable effort is dedicated to develop tools for data processing and build an expert scientific community around imaging spectroscopy to ensure exploitation of the full information content of the EnMAP data once operational. This chapter provides a brief overview of the various activities.

4.1 Information and training

The primary source of information about the EnMAP mission is the EnMAP website (www.enmap.org). In addition, a mailing list was established to spread EnMAP-specific news and announcements. One can subscribe to the list by sending an email to EnMAP_wiss-on[at]gfz-potsdam.de. As of May 2016, the list has approx. 300 subscribers from research, administration and business.

Key documents of the EnMAP mission, targeting the scientific community and other users, are highlighted in Table 2. Note that some of these documents are under preparation and will be available at a later stage. Research results related to EnMAP are frequently published in scientific journals and presented at international conferences. To raise public awareness, relevant information about the mission and its status are spread through the media.

EnMAP science workshops and organized conference sessions are held regularly with the objectives to inform about the progress of the mission, to present and discuss EnMAP-related research, and to raise awareness of the mission.

The YoungEnMAP group represents a research community of PhD students, early PostDocs and undergraduate students based at various universities and research institutes in Germany and elsewhere. To promote and train these junior scientists, EnMAP schools are conducted by the EnSAG on a regular basis covering a broad range of topics.

4.2 EnMAP preparatory flight campaigns

In the framework of the EnMAP preparatory program, a large number of hyperspectral airborne flight campaigns have been and will be carried out in the future to support scientific application development in a wide range of environments. These campaigns facilitate the evaluation of the potential performance for the retrieval of key environmental parameters, the exploitation of synergies with other sensors, and the development and testing of new image processing algorithms and calibration/ validation methods (Guanter et al., 2015). In addition, the datasets are input for EnMAP end-to-end scene simulations (see section 4.3). In the future, methods developed and experiences gained from the work with these airborne and simulated EnMAP datasets can be readily employed during the mission operation period.

Most of the test sites were covered by multi-seasonal flights to support the analysis of multi-temporal process studies. Furthermore, acquisitions at different flight altitudes were obtained, which facilitate spatial scaling studies. In some occasions, the simultaneous data collection with other sensors (e.g., LiDAR) enables multi-sensoral studies. Most campaigns were accompanied by extensive ground-data sampling to calibrate and validate the airborne data acquisitions.

Table 2: Key documents of the EnMAP mission.

Document	Author	Target group	Language	Objectives	Availability
EnMAP Science Plan	PI, EnSAG	Scientists, funding institutions, environmental stakeholders and govern-mental bodies	eng	Describe the scientific background, requirements and activities related to the EnMAP mission	www.enmap.org (2016, continuously updated)
EnMAP flyer	PI, EnSAG	General public	eng	Brief information about mission, objectives and application fields	www.enmap.org (2015)
EnMAP brochure	PI, EnSAG	General public	eng/ger	Information about scientific objectives and application fields	www.enmap.org (2014/12)
Hyperspectral algorithms report	PI, EnSAG	Hyperspectral community	eng	Overview of algorithms for hyperspectral analyses	www.enmap.org (2010)
EnMAP Algorithms Theoretical Baseline Document (ATBD)	Ground segment	(potential) users of EnMAP data	eng	Detailed information on algorithms and databases used by the ground segment for data processing	www.enmap.org (at launch)
EnMAP Mission Handbook	DLR Space Administra-tion	(potential) users of EnMAP data	eng	Give mission overview, inform about data access (general and AO process), main aspects of data policies (priorities, contingents), data (level, formats, processing etc.)	www.enmap.org (due 1 year ahead of launch)
EnMAP User Manual of the Instrument Planning	Ground segment	(potential) users of EnMAP data	eng	Information about the instrument planning	www.enmap.org (at launch)
EnMAP User Manual of the Planning Portal	Ground segment	(potential) users of EnMAP data	eng	Information about EOWEB data access portal	www.enmap.org (at launch)
The EnMAP Spaceborne Imaging Spectroscopy Mission for Earth Observation	PI, EnSAG	(potential) users of EnMAP data	eng	Overall mission overview	Guanter et al. (2015)
Environmental Mapping and Analysis Program – A German Hyperspectral Mission	PI, OHB, EnSAG	(potential) users of EnMAP data	eng	Detailed technical description	Kaufmann et al. (2016)

The datasets are successively made freely available to the scientific community as DOI-referenced data publications which are under a Creative Commons Licence. An overview of all available datasets at http://www.enmap.org/?q=flights provides details about the campaigns, such as information about recorded airborne hyperspectral datasets, other data associated with the respective campaigns such as field and laboratory measurements, and availability of simulated EnMAP and Sentinel-2 imagery. In addition, all datasets are accompanied by data reports (EnMAP Technical Reports), describing in detail how the data were acquired and (pre)processed and which ground truth and additional data are available.

In addition to these campaign data, a number of field sampling guides and spectral libraries developed within the mission's preparatory program are made available as EnMAP Technical Reports via the EnMAP website.

4.3 EnMAP end-to-end scene simulations

Preparatory activities involve the simulation of the entire image generation and processing chain using the EnMAP end-to-end scene simulator (EeteS; Segl et al., 2012). EeteS comprises four main modules (atmospheric, spatial, spectral, and radiometric) to generate EnMAP-like raw data and is capable of simulating EnMAP-like data products using a L1B, L1C and L2A processor. These simulated data are important for activities related to the optimization of fundamental instrument configurations, allowing the effect of parameter changes to be tested using simulated benchmark datasets. In addition, these datasets support the development and evaluation of data pre-processing algorithms as well as the testing of new algorithms for the improved scientific exploitation of future EnMAP data, such as tools for geometric alignment of EnMAP to co-existing Earth observation missions, facilitating synergetic uses, for example, with Sentinel-2 data. Sample datasets generated with EeteS are provided upon request to scientific users.

4.4 EnMAP-Box

Full exploitation of the high-spectral information content of EnMAP data requires the availability of state-of-the-art image processing approaches for all users and application fields. Therefore, the EnMAP-Box is developed targeting both, novices as well as experienced users, and offers basic processing and visualization functionality as well as advanced approaches for image analysis. Moreover, the open source code may easily be extended by individual applications. This way, the exchange and centralized distribution of latest developments shall be fostered within the EnMAP user community. From the first versions in 2009, the conceptual development of the EnMAP-Box was driven by the following objectives:

- User-friendliness: for example, achieved by an intuitive graphical user interface (GUI) (Figure 6), focusing on the handling and visualization of data with high-spectral dimension, widget controlled machine learning algorithms, common file formats, selected basic tools and easy-to-use advanced methods, and the possible integration into ENVI;
- Comprehensiveness: the set of available tools and applications as well as interfaces to scripting languages make the constant switch between different software obsolete;
- Standardization: the implementation and use of applications is standardized to assist external developers and provide the users a common look-and-feel, which also constitutes a key component for user-friendliness; and
- Addressing external developers: availability of well-documented source code, offering an application programming interface (API) and an application wizard.

A detailed description of the concept and status of the EnMAP-Box is given in van der Linden et al. (2015).

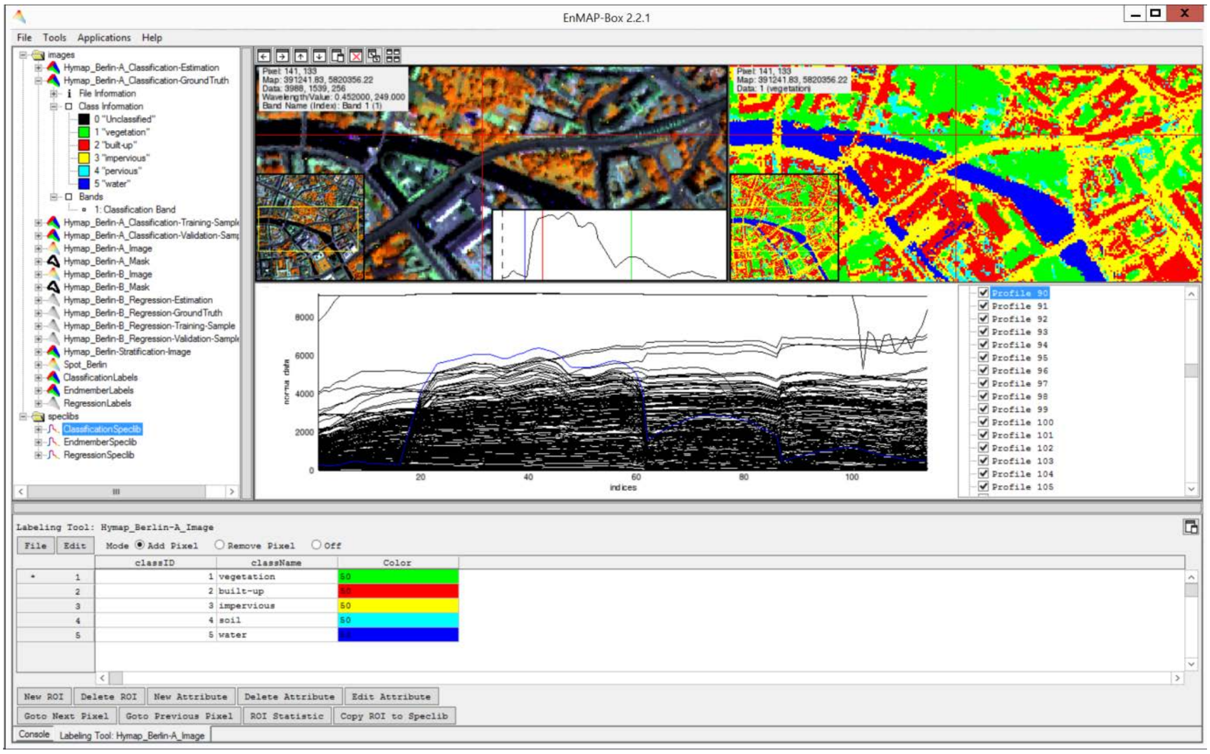

Fig. 6: Graphical user interface of the EnMAP-Box 2.2.1, showing simulated EnMAP data and mapping results of Berlin, Germany.

The EnMAP-Box (Version 2.2 released in January 2016 at www.enmap.org) works stand-alone, but may be integrated into the ENVI classic menu. It can also be used with any multispectral imagery. It combines functionality for spectrally high-dimensional data with latest machine learning and interfaces to R or Python. The toolbox is delivered together with an API for a standardized integration of new developments independent from the respective programming language. Since 2012, more and more external applications were added, all following the idea of a standardized implementation (Table 3).

Prior to the start of EnMAP, the toolbox will be converted into a Python plug-in to be used in Q-GIS. It will be extended by a set of sensor product specific tools including additional pre-processing tools, e.g., for a locally adapted atmospheric correction to transfer data from level 1B to 2A. In addition, import filters for complementary sensors, e.g., Sentinel-2/3 or Landsat OLI, will be included.

Table 3: List of available applications in the EnMAP-Box version 2.2.

Type of application	Application name(s) and reference	Reference	Contributor*
General applications			
Support vector machine classification and regression incl. adapted learning strategy for gradual class transitions	imageSVM	Janz et al. (2007); Suess et al. (2015)	HUB
Random forests for classification and regression	imageRF	Waske et al. (2012)	UB, HUB
Partial least squares regression	autoPLSR	Wold et al. (2001)	UB
Spectral feature clustering	Feature Clustering	Held et al. (2015)	HUB
Spectral index data mining tool	SpInMine		UT
Iterative spectral mixture analysis	iterativeSMA	Rogge et al. (2006)	UT
SVR-based unmxing using synthetic libraries	syntMix-SVR	Okujeni et al. (2013)	HUB
Maximum entropy analysis	MaxEntWrapper		UB
Calculator for spatial and spectral image processing	imageMath		HUB
Application related tools			
Agricultural applications (including tools for estimating (i) the red-edge inflection point, (ii) a suite of 65 agricultural vegetation indices, (iii) spectral integrals and advanced statistical evaluation, and (iv) the estimation of optical active water thickness in vegetation	iREIP , AVI, ASI, ASE, OAWI		LMU
Soil properties mapping	EnSoMAP	Chabrillat et al. (2016)	GFZ
Mineral detection and mapping	EnGeoMAP - Base	Mielke et al. (2014)	GFZ
Rare earth element detection and mapping	EnGeoMAP – REE	Boesche et al. (2015b)	GFZ
Ocean related parameter retrieval	Phytobenthos Index, Ocean Color Chlorophyll		HZG
Data specific tools			
Surface water body detection	EnWaterMap	Bochow et al. (2012)	GFZ

* HUB – Humboldt-Universität zu Berlin, UB – University of Bonn, UT – Trier University, LMU - Ludwig-Maximilians-Universität München, HZG - Helmholtz-Zentrum Geesthacht, GFZ - Helmholtz Centre Potsdam - German Research Centre for Geosciences.

References

Albright, T. P., and D. J. Ode (2011), Monitoring the dynamics of an invasive emergent macrophyte community using operational remote sensing data, Hydrobiologia, 661, 469–474.

Anderegg, W. R. L., J. M. Kane, and L. D. L. Anderegg (2013), Consequences of widespread tree mortality triggered by drought and temperature stress, Nature Climate Change, 3, 30-36.

Anderson, R. J., A. Rand, R. Share, A. u. Bolton, and J. J (2007), Mapping and quantifying the South African kelp resource, African Journal of Marine Science, 29, 369–378.

Anderson, J., L. Plourde, M. Martin, B. Braswell, M.-L.Smith, R. Dubayah, M. Hofton, and J. Blair (2008), Integrating waveform lidar with hyperspectral imagery for inventory of a northern temperate forest, Remote Sensing of Environment, 112, 1856–1870.

Andréfouët, S., E. J. Hochberg, C. Chevillon, F. E. Muller-Karger, J. C. Brock, and C. Hu (2005), Multi-scale remote sensing of coral reefs, In, Miller, R. L. et al. (eds.), Remote Sensing of Coastal Aquatic Environments, Springer

Asner, G. P., A. R. Townsend, and B. H. Braswell (2000), Satellite observation of el nino effects on amazon forest phenology and productivity, Geophysical Research Letters, 27 (7), 981–984.

Asner, G. P., D. Nepstad, G. Cardinot, and D. Ray (2004), Drought stress and carbon uptake in an amazon forest measured with spaceborne imaging spectroscopy, Proceedings of the National Academy of Sciences of the United States of America, 101 (16), 6039–6044.

Asner, G. P., and K. B. Heidebrecht (2005), Desertification alters regional ecosystem-climate interactions, Global Change Biology, 11 (1), 182–194.

Asner, G. P., A. J. Elmore, R. F. Hughes, A. S. Warner, and V. P. M. (2005), Ecosystem structure along bioclimatic gradients in Hawaii from imaging spectroscopy, Remote Sensing of Environment, 96, 3–4.

Asner, G. P., D. E. Knapp, T. Kennedy-Bowdoin, M. O. Jones, R. E. Martin, J. Boardman, and R. F. Hughes (2008), Invasive species detection in Hawaiian rainforests using airborne imaging spectroscopy and LiDAR, Remote Sensing of Environment, 112 (5), 1942–1955.

Asner, G. P., R. E. Martin, D. E. Knapp, R. Tupayachi, C. Anderson, L. Carranza, P. Martinez, M. Houcheime, F. Sinca, and P. Weiss (2011), Spectroscopy of canopy chemicals in humid tropical forests, Remote Sensing of Environment, 115, 3587-3598.

Asner, G. P., D. E. Knapp, J. Boardman, R. O. Green, T. Kennedy-Bowdoin, M. Eastwood, R. E. Martin, C. Anderson, and C. B. Field (2012), Carnegie Airborne Observatory-2: Increasing science data dimensionality via high-fidelity multi-sensor fusion, Remote Sensing of Environment, 124, 454–465.

Atzberger, C. (2000), A decade of trans-european remote sensing cooperation., chap. Development of an invertible forest reflectance model: The INFOR-Model, pp. 39–44 Balkema.

Bach, H., W. Mauser, and K. Schneider (2003), The use of radiative transfer models for remote sensing data assimilation in crop growth models, pp. 35–40, Wageningen Academic Publishers, Wageningen, NL.

Bach, H., S. Migdall, W. Mauser, W. Angermair, A. J. Sephton, and G. Martin-de Mercado (2011), An integrative approach of using satellite-based information for precision farming: Talkingfields, in 61st International Astronautical Congress, vol. 6, pp. 4669–4676, Curran Associates, Inc., Red Hook, NY.

Barducci, A., D. Guzzi, P. Marcoionni, and I. Pippi (2004), Algorithm for the retrieval of columnar water vapor from hyperspectral remotely sensed data, Appl. Opt., 43 (29), 5552–5563.

Barnosky, A. D., N. Matzke, S. Tomiya, G. O. U. Wogan, B. Swartz, T. B. Quental, C. Marshall, J. L. McGuire, E. L. Lindsey, K. C. Maguire, B. Mersey, and E. A. Ferrer (2011), Has the earth's sixth mass extinction already arrived? Nature, 471 (7336), 51–57.

Barnsley, M. J., J. J. Settle, M. A. Cutter, D. R. Lobb, and F. Teston (2004), The PROBA/CHRIS mission: A lowcost smallsat for hyperspectral multiangle observations of the Earth surface and atmosphere, IEEE Transactions on Geoscience and Remote Sensing, 42, 1512–1520.

Behling, R., S. Roessner, H. Kaufmann, and B. Kleinschmit (2014), Automated Spatiotemporal Landslide Mapping over Large Areas Using RapidEye Time Series Data, Remote Sensing, 6 (9), 8026–8055.

Behling, R., M. Bochow, S. Foerster, S. Roessner, and H. Kaufmann (2015), Automated GIS-based derivation of urban ecological indicators using hyperspectral remote sensing and height information, Ecological Indicators, 48, 218-234.

Bell, S. S., M. S. Fonseca, and W. J. Kenworthy (2008), Dynamics of a subtropical seagrass landscape: links between disturbance and mobile seed banks, Landscape Ecol, 23, 67–74.

Ben-Dor, E., J. A. Irons, and A. Epema (1999), Manual of Remote Sensing, chap. Soil Reflectance, pp. 111–188, NewYork: J. Wiley & Sons, Inc.

Ben-Dor, E., S. Chabrillat, J. A. M. Dematte, G. Taylor, J. Hill, and M. L. Whiting (2009), Using imaging spectroscopy to study soil properties, Remote Sensing of Environment, 113 (Suppl. 1), 38–55.

Berger, M., J. Moreno, J. A. Johannessen, P. F. Levelt, and R. F. Hanssen (2012), ESA's sentinel missions in support of earth system science, Remote Sensing of Environment, 120 (0), 84–90.

Bianchi, R., C. Marino, and S. Pignatti (1994), Airborne hyperspectral remote sensing in Italy, Proceedings of the European symposium on Satellite Remote Sensing, Europto Series, pp. 26–30, Rome, Italy.

Bieniarz, J., E. Aguilera, X. Zhu, R. Mueller, U. Heiden, and P. Reinartz (2014), Spectral-spatial joint sparsity unmixing of hyperspectral data using overcomplete dictionaries, Whispers Conference proceedings.

Bjorndal, K. A., A. B. Bolten, and C. J. Lagueux (1994), Ingestion of marine debris by juvenile sea-turtles in coastal Florida habitats, Marine Pollution Bulletin, 28 (3), 154–158.

Blackburn, G. A. (2007), Hyperspectral remote sensing of plant pigments, Journal of Experimental Botany, 58 (4), 855–67.

Blaschke, T. (2010), Object based image analysis for remote sensing, ISPRS Journal of Photogrammetry and Remote Sensing, 65 (1), 2–16.

Boerger, C. M., G. L. Lattin, S. L. Moore, and C. J. Moore (2010), Plastic ingestion by planktivorous fishes in the north pacific central gyre, Marine Pollution Bulletin, 60 (12), 2275–2278.

Boesche, N. K. (2015), Detection of Rare Earth Elements and Rare Earth Oxides with Hyperspectral Spectroscopy - Near-Field and Spaceborne Investigations in Preparation of the EnMAP Mission, Dissertation,University of Potsdam, Potsdam.

Boesche, N. K., C. Rogass, C. Mielke, S. Herrmann, F. Körting, A. Papenfuß, C. Lubitz, M. Brell, S. Tonn, and U. Altenberger (2015a), Hyperspectral Rare Earth Element Mapping of Three

Outcrops at the Fen Complex, Norway: Calcitic, Dolomitic, and Ankeritic Carbonatites, In Rare Earths Industry, Technological, Economic, and Environmental Implications, 1 edition, Elsevier.

Boesche, N., C. Rogaß, C. Lubitz, M. Brell, S. Herrmann, C. Mielke, S. Tonn, O. Appelt, U. Altenberger, and H. Kaufmann (2015b): Hyperspectral REE (Rare Earth Element) Mapping of Outcrops—Applications for Neodymium Detection, Remote Sensing, 7 (5), 5160-5186.

Bochow, M., B. Heim, T. Küster, C. Rogaß, I. Bartsch, K. Segl, S. Reigber, and H. Kaufmann (2012), On the use of airborne imaging spectroscopy data for the automatic detection and delineation of surface water bodies, In, Chemin, Y., (Ed), Remote sensing of planet earth, InTech - Open Access Publisher, 3-22.

Bond, I. (2010), Redd+ in dryland forests: issues and prospects for pro-poor REDD in the miombo woodlands of southern Africa, Tech. rep., International Institute for Environment and Development (UK).

Bondeau, A., P. C. Smith, S. Zaehle, S. Schaphoff, W. Lucht, W. Cramer, D. Gerten, H. Lotze-Campen, C. Mueller, M. Reichstein, and B. Smith (2007), Modelling the role of agriculture for the 20th century global terrestrial carbon balance, Global Change Biology, 13 (3), 679–706.

Bostater, C. R., J. Jones, H. Frystacky, G. Coppin, F. Levaux, and X. Neyt (2011), Airborne Imaging Sensors for Environmental Monitoring & Surveillance In Support Of Oil Spills & Recovery Efforts, in Remote Sensing of the Ocean, Sea Ice, Coastal Waters, and Large Water Regions 2011, Proceedings of SPIE, vol. 8175, edited by Bostater, CR and Mertikas, SP and Neyt, X and VelezReyes, M, SPIE.

Bousquet, P., P. Ciais, J.B. Miller, E.J. Dlugokencky, D.A. Hauglustaine, C. Prigent, G.R. Van der Werf, P. Peylin, E.-G. Brunke, C. Carouge, R.L. Langenfelds, J. Lathiere, F. Papa, M. Ramonet, M. Schmidt, L.P. Steele, S.C. Tyler, and J. White (2006), Contribution of anthropogenic and natural sources to atmospheric methane variability. Nature, 443 (7110), 439-443.

Bracher, A., M. Vountas, T. Dinter, J. P. Burrows, R. Roettgers, and I. Peeken (2009), Quantitative observation of cyanobacteria and diatoms from space using PhytoDOAS on SCIAMACHY data, Biogeosciences, 6 (5), 751–764.

Bradley, E.S., I. Leifer, D.A. Roberts, P.E. Dennison, and L. Washburn (2011), Detection of marine methane emissions with AVIRIS band ratios. Geophysical Research Letters, 38 (10).

Breiman, L. (2001), Random forests, Machine Learning, 45 (1).

Buchhorn, M., and M. Schwieder (2012), Expedition "EyeSight-NAAT-Alaska" 2012. In: Expeditions to Permafrost 2012: "Alaskan North Slope/ Itkillik", "Thermokarst in Central Yakutia", "EyeSight-NAAT-Alaska". Alfred-Wegener-Institut für Polar- und Meeresforschung. Bremerhaven (Reports on Polar and Marine Research, 655), 41–65.

Buchhorn, M., D.A. Walker, B. Heim, M.K. Raynolds, H.E. Epstein, and M. Schwieder (2013a), Ground-Based Hyperspectral Characterization of Alaska Tundra Vegetation along Environmental Gradients, Remote Sensing, 5(8), 3971–4005.

Buchhorn, M., R. Petereit, and B. Heim (2013b), A Manual Transportable Instrument Platform for Ground-Based Spectro-Directional Observations (ManTIS) and the Resultant Hyperspectral Field Goniometer System, Sensors, 13(12), 16105–16128.

Buchhorn, M. (2014): Ground-Based Hyperspectral and Spectro-Directional Reflectance Characterization of Arctic Tundra Vegetation Communities - Field Spectroscopy and Field Spectro-Goniometry of Siberian and Alaskan Tundra in Preparation of the EnMAP Satellite Mission. Dissertation Universität Potsdam.

Buddenbaum, H., M. Schlerf, and J. Hill (2005), Classification of coniferous tree species and age classes using hyperspectral data and geostatistical methods, International Journal of Remote Sensing, 26, 5453–5465.

Buddenbaum, H., S. Seeling, and J. Hill (2013), Fusion of full-waveform lidar and imaging spectroscopy remote sensing data for the characterization of forest stands, International Journal of Remote Sensing, 34, 4511-4524.

Ciais, P., M. Reichstein, N. Viovy, A. Granier, J. Ogee, V. Allard, M. Aubinet, N. Buchmann, C. Bernhofer, A. Carrara, F. Chevallier, N. de Noblet, A. D. Friend, P. Friedlingstein, T. Grunwald, B. Heinesch, P. Keronen, A. Knohl, G. Krinner, D. Loustau, G. Manca, G. Matteucci, F. Miglietta, J. M. Ourcival, D. Papale, K. Pilegaard, S. Rambal, G. Seufert, J. F. Soussana, M. J. Sanz, E. D. Schulze, T. Vesala, and R. Valentini (2005), Europe-wide reduction in primary productivity caused by the heat and drought in 2003, Nature, 437, 529-533.

Cao, M.K., K. Gregson, and S. Marshall (1998), Global methane emission from wetlands and its sensitivity to climate change. Atmospheric Environment, 32 (19), 3293-3299.

Carder, K. L., P. Reinersman, R. F. Chen, F. Mullerkarger, C. O. Dans, and M. K. Hamilton (1993), AVIRIS calibration and application in coastal oceanic environments, Remote Sens Environ, 44, 205–216.

Carlson, R., and J. Simpson (1996), A coordinator's guide to volunteer lake monitoring methods, Tech. rep.

Casey, K. A., A. Kaab, and D. I. Benn (2012), Geochemical characterization of supraglacial debris via in situ and optical remote sensing methods: a case study in Khumbu Himalaya, Nepal, Cryosphere, 6 (1), 85–100.

Cavalli, R. M., L. Fusilli, S. Pascucci, S. Pignatti, and F. Santini (2008), Hyperspectral sensor data capability for retrieving complex urban land cover in comparison with multispectral data: Venice city case study, Sensors, 8, 3299–3320.

Ceccato, P., S. Flasse, S. Tarantola, S. Jacquemoud, and J.-M. Gregoire (2001), Detecting vegetation leaf water content using reflectance in the optical domain, Remote Sensing of Environment, 77 (1), 22–33.

Chabrillat, S., A. F. H. Goetz, H. W. Olsen, and L. Krosley (2002), Use of hyperspectral images in the identification and mapping of expansive clay soils and the role of spatial resolution, Remote Sensing of Environment, 82 (2-3), 431-445.

Chabrillat, S. and A. F. H. Goetz (2006), Remote sensing of expansive soils: Use of hyperspectral methodology for clay mapping and hazard assessment, I,: Ali Al-Rawas, A., and M.F.A. Goosen (eds), Expansive Soils: Recent Advances in Characterization and Treatment, Taylor & Francis, London, UK, 187-209.

Chabrillat, S. (2006), Land degradation indicators: spectral indices, Annals of Arid Zone, Special issue Land quality assessment, 45 (3-4), 331-354.

Chabrillat, S., A. Eisele, S. Guillaso, C. Rogaß, E. Ben-Dor, and H. Kaufmann (2011), HYSOMA: An easy-to-use software interface for soil mapping applications of hyperspectral imagery, Proceedings of the 7th EARSeL SIG Imaging Spectroscopy Workshop, Edinburgh, Scotland, UK, 11-13 April 2011.

Chabrillat, S., S. Foerster, A. Steinberg, and K. Segl (2014), Prediction of common surface soil properties using airborne and simulated EnMAP hyperspectral images: Impact of soil algorithm and sensor characteristic, 2014 IEEE International Geoscience and Remote Sensing Symposium, IGARSS 2014 & 35th Canadian Symposium on Remote Sensing, Québec city, QC, Canada, 13-18 July 2014, 2914-2917.

Chabrillat, S., S. Guillaso, A. Rabe, S. Foerster, and L. Guanter (2016), From HYSOMA to ENSOMAP – A new open source tool for quantitative soil properties mapping based on hyperspectral imagery from airborne to spaceborne applications, General Assembly European Geosciences Union, Vienna, Austria, 2016, Geophysical Research Abstracts, Vol. 18, EGU2016-14697.

Champagne, C. M., K. Staenz, A. Bannari, H. McNairn, and J.-C. Deguise (2003), Validation of a hyperspectral curve-fitting model for the estimation of plant water content of agricultural canopies, Remote Sensing of Environment, 87 (2-13), 148–160.

Chen, F.H. (1988), Foundations on Expansive Soils, 2nd ed., Elsevier, Amsterdam, p. 463

Chen, J. M., and S. G. Leblanc (1997), A four-scale bidirectional reflectance model based on canopy architecture, Geoscience and Remote Sensing, IEEE Transactions on, 35 (5), 1316–1337.

Cheshire, A. C., E. Adler, J. Barbière, Y. Cohen, S. Evans, S. Jarayabhand, L. Jeftic, R. T. Jung, S. Kinsey, E. T. Kusui, I. Lavine, P. Manyara, L. Oosterbaan, M. A. Pereira, S. Sheavly, A. Tkalin, S. Varadarajan, B. Wenneker, and G. Westphalen, (2009), UNEP/IOC Guidelines on Survey and Monitoring of Marine Litter, UNEP Regional Seas Reports and Studies, No. 186; IOC Technical Series No. 83: xii + 120 pp.

Cho, M. A., A. Skidmore, F. Corsi, S. E. Van_Wieren, and I. Sobhan (2007), Estimation of green grass/herb biomass from airborne hyperspectral imagery using spectral indices and partial least squares regression, International Journal of Applied Earth Observation and Geoinformation, 9, 414–424.

Chudnovsky, A., E. Ben-Dor, A. B. Kostinski, and I. Koren (2009), Mineral content analysis of atmospheric dust using hyperspectral information from space, Geophysical Research Letters, 36 (15), L15,811.

Cipar, J., R. Dunn, and T. Cooley (2010), Active volcano monitoring using a space-based hyperspectral imager, in American Geophysical Union, Fall Meeting.

Clark, R. N., R. O. Green, G. A. Swayze, G. Meeker, S. Sutley, T. M. Hoefen, K. E. Livo, G. Plumlee, B. Pavri, C. Sarture, S. Wilson, P. Hageman, P. Lamothe, J. S. Vance, J. Boardman, I. Brownfield, C. Gent, L. C. Morath, J. Taggart, P. M. Theodorakos, and M. Adams (2001), Environmental studies of the World Trade Center area after the September 11, 2001 attack, Open File Report OFR-01-0429, version 1.1 ed., U.S. Geological Survey, Denver, Colorado.

Clark, R. N., G. A. Swayze, K. E. Livo, R. F. Kokaly, S. J. Sutley, J. B. Dalton, R. R. McDougal, and C. A. Gent (2003), Imaging spectroscopy: Earth and planetary remote sensing with the USGS tetracorder and expert systems, 108 (E12), 5131–5175.

Clark, M. L., D. A. Roberts, and D. B. Clark (2005), Hyperspectral discrimination of tropical rain forest tree species at leaf to crown scales, Remote Sensing of Environment, 96, 375–398.

Clark, M. L., D. A. Roberts, J. J. Ewel, and D. B. Clark (2011), Estimation of tropical rain forest aboveground biomass with small-footprint lidar and hyperspectral sensors, Remote Sensing of Environment, 115 (11), 2931–2942.

Cochrane, M. A. (2000), Using vegetation reflectance variability for species level classification of hyperspectral data, International Journal of Remote Sensing, 21, 2075–2087.

Cocks, T., R. Jenssen, A. Stewart, I. Wilson, and T. Shields (1998), The hymap airborne hyperspectral sensor, the system, calibration and performance., in Proceedings 1st EARSEL Workshop on imaging spectrometry, pp. 37–42, Zurich.

Colbeck, S. (1979), Grain clusters in wet snow, Journal of Colloid and Interface Science, 72 (3), 371–384.

Cole, J. J., Y. T. Prairie, N. F. Caraco, W. H. McDowell, L. J. Tranvik, and G. H. Striegl (2007), Plumbing the global carbon cycle, Integrating Inland Waters into the Terrestrial Carbon Budget; Ecosystems, 10, 171–184.

Collins, W., and S.-H. Chang (1990), Commercial spectroscopy with the geophysical research imaging spectrometer (geris), in Proceedings of the Technical Symposium on Optical Engineering and Photonics in Aerospace Sensing, vol. 1298, pp. 61–72, Society of Photo-Optical Instrumentation Engineers (SPIE).

Combal, B., F. Baret, M. Weiss, A. Trubuil, D. Mace, A. Pragnere, R. Myneni, Y. Knyazikhin, and L. Wang (2002), Retrieval of canopy biophysical variables from bidirectional reflectance using prior information to solve the ill-posed inverse problem, Remote Sensing of Environment, 84, 1–15.

Coops, N. C., C. J. Ferster, R. H. Waring, and J. Nightingale (2009), Comparison of three models for predicting gross primary production across and within forested ecoregions in the contiguous united states, Remote Sensing of Environment, 113 (3), 680–690.

Corson, M. R., D. R. Korwan, R. L. Lucke, S. W. A., and C. O. Davis (2008), The hyperspectral imager for the coastal ocean (hico) on the international space station, in IEEE Proceedings of the International Geoscience and Remote Sensing Symposium.

Crowley, J., B. Hubbard, and J. Mars (2003), Analysis of potential debris flow source areas on mount shasta, california, by using airborne and satellite remote sensing data, Remote Sensing of Environment, 87 (2-13), 345–358.

Dalponte, M., L. Bruzzone, and D. Gianelle (2008), Fusion of hyperspectral and lidar remote sensing data for classification of complex forest areas, IEEE Transactions on Geoscience and Remote Sensing, 46, 1416–1427.

Damm, A., L. Guanter, V. C. E. Laurent, M. E. Schaepman, A. Schickling, and U. Rascher (2014), FLD-based retrieval of sun-induced chlorophyll fluorescence from medium spectral resolution airborne spectroscopy data, Remote Sensing of Environment, 147, 256-266.

Defries, R., S. Pagiola, W. L. Adamowicz, H. Resit Akcakaya, A. Arcenas, S. Babu, D. Balk, U. Confalonieri, W. Cramer, F. Falconi, S. Fritz, R. Green, E. Gutierrez-Espeleta, K. Hamilton, R. Kane, J. Latham, E. Matthews, T. Ricketts, and T. Xiang Yue (2005), Analytical approaches for assessing ecosystem condition and human well-being., chap. Ecosystems and human well-being: current state and trends, pp. 37–71, Island Press, Washington.

De Foy, B., L. T. Molina, and M. J. Molina (2006), Satellite-derived land surface parameters for mesoscale modelling of the Mexico City basin. Atmospheric Chemistry and Physics, 6.

Dematte, J. A. M., J. Morelli, E. Nelly, and R. Negrao (2000), Precision agriculture applied to sugar cane cultivation in Sao Paulo, Brazil, in Second International Conference on Geospatial Information in Agriculture and Forestry, vol. 2, pp. 388–394, Lake Buena Vista, Florida.

Dieke, G. H., and H. M. Crosswhite (1963), The Spectra of the Doubly and Triply Ionized Rare Earths, Applied Optics 2 (7), 675–686.

Dierssen, H. M., R. C. Zimmerman, D. Lisa, and A (2010), Benthic ecology from space: optics and net primary production in seagrass and benthic algae across the great bahama, Marine Ecology Progress Series, 411, 1–15.

Dirzo, R., and P. H. Raven (2003), Global state of biodiversity and loss, Annual Review of Environment and Resources, 28 (1), 137–167.

Donlon, C., B. Berruti, A. Buongiorno, M.-H. Ferreira, P. Femenias, J. Frerick, P. Goryl, U. Klein, H. Laur, C. Mavrocordatos, J. Nieke, H. Rebhan, B. Seitz, J. Stroede, and R. Sciarra (2012), The global monitoring for environment and security (gmes) sentinel-3 mission, Remote Sensing of Environment, 120 (0), 37–57.

Dozier, J., and T. Painter (2004), Multispectral and hyperspectral remote sensing of alpine snow properties, Annual Review of Earth and Planetary Sciences, 32, 465–494.

Dozier, J., R. O. Green, A. W. Nolin, and T. H. Painter (2009), Interpretation of snow properties from imaging spectrometry, Remote Sensing of Environment, 113, 25–37.

Eicken, H., R. Gradinger, A. Graves, A. Mahoney, and I. Rigor (2005), Sediment transport by sea ice in the Chukchi and Beaufort Seas: Increasing importance due to changing ice conditions? Deep-Sea Res. II, 52, 3281-3302.

Eicken, H., T. C. Grenfell, D. K. Perovich, J. A. Richter-Menge, and K. Frey (2004), Hydraulic controls of summer Arctic pack ice albedo, J. Geophysical Research, 109 (C08007)

EPA (1998), Advanced measurement initiative workshop report: advanced measurement and site characterization of mining impacts on public health and the environment, Tech. Rep. EPA-235-R-98-002, United States Environmental Protection Agency, Colorado School of Mines,Golden, Colorado:.

Eriksson, C., and H. Burton (2003), Origins and biological accumulation of small plastic particles in fur seals from Macquarie Island, Ambio, 32 (6), 380–384.

ESA (2015), Earth Observation Science Strategy for ESA: A new Era for Scientific Advances and Societal Benefits, ESA SP-1329/1, 2015, European Space Agency.

European Commission (2015) Copernicus. Europe’s eyes on Earth. Copernicus Brochure.

FAO (2010), Guidelines on sustainable forest management in drylands of sub-Saharan Africa, In, Arid Zone Forests and Forestry. Rome.

FAO (2011), The state of the world’s land and water resources for food and agriculture (SOLAW) – Managing systems at risks, Food and Agriculture Organization of the United Nations, Rome and Earthscan, London.

Fassnacht, F.E., H. Latifi, and B. Koch (2012), An angular vegetation index for imaging spectroscopy data — Preliminary results on forest damage detection in the Bavarian National Park, Germany, International Journal of Applied Earth Observation and Geoinformation, 19, 308-321.

Feilhauer, H. and S. Schmidtlein (2009), Mapping continuous fields of forest alpha and beta diversity, Applied Vegetation Science, 12, 429-439.

Feilhauer, H., G. Asner, R. Martin, and S. Schmidtlein (2010), Brightness-normalized partial least squares regression for hyperspectral data, Journal of Quantitative Spectroscopy and Radiative Transfer, 111, 1947–1957.

Feilhauer, H., U. Faude, and S. Schmidtlein (2011), Combining isomap ordination and imaging spectroscopy to map continuous floristic gradients in a heterogeneous landscape, Remote Sensing of Environment, 115 (10), 2513–2524.

Fisher, J. I., J. F. Mustard, and M. A. Vadeboncoeur (2006), Green leaf phenology at Landsat resolution: Scaling from the field to the satellite, Remote Sensing of Environment, 100, 265–279.

Foerster, M., D. Spengler, H. Buddenbaum, J. Hill, and B. Kleinschmit (2010), A review of the combination of spectral and geometric modelling for the application in forest remote sensing - Ein Überblick über die Kombination spektraler und geometrischer Modellierung zur Anwendung in der forstlichen Fernerkundung, Photogrammetrie - Fernerkundung - Geoinformation, 2010 (4), 253–265.

Forrest, M. E., V. Wittmann, N. A. Schmidt, A. Raineault, W. Hamilton, S. G. Pike, J. E. Schladow, B. E. Reuter, and A. C. Trembanis (2012), Quantitative assessment of invasive species in lacustrine environments through benthic imagery analysis, Limnol. Oceanogr. Methods, 10, 65–74.

Framework-Document (2008), UN collaborative initiative on reducing emissions from deforestation and forest degradation, Tech. rep., FAO, UNDP, UNEP.

Franke, J., D. A. Roberts, K. Halligan, and G. Menz (2009), Hierarchical multiple endmember spectral mixture analysis (MESMA) of hyperspectral imagery for urban environments, Remote Sensing of Environment, 113, 1678–1690.

Franklin, S. (2001), Remote sensing for sustainable forest management, Lewis Publishers, Boca Raton, London, New York, Washington, D.C.

Fuentes, D. A., J. A. Gamon, Y. Cheng, H. C. Claudio, H. lie Qiu, Z. Mao, D. A. Sims, A. F. Rahman, W. Oechel, and H. Luo (2006), Mapping carbon and water vapor fluxes in a chaparral ecosystem using vegetation indices derived from AVIRIS, Remote Sensing of Environment, 103 (3), 312–323.

Galgani, F., D. Fleet, J. Van Franeker, S. Katsanevakis, T. Maes, J. Mouat, L. Oosterbaan, I. Poitou, G. Hanke, R. Thompson, E. Amato, A. Birkun, and C. Janssen (2010), JRC Scientific and Technical Reports, chap. Marine Strategy Framework Directive, Task Group 10 Report: Marine Litter, Publications Office of the European Union.

GEO (2015), GEO Strategic Plan 2016-2025: Implementing GEOSS, Group on Earth Observation.

Gerard, F. F., and P. R. J. North (1997), Analyzing the effect of structural variability and canopy gaps on forest BRDF using a geometric-optical model, Remote Sensing of Environment, 62 (1), 46–62.

Giardino, C., V. E. Brando, A. G. Dekker, N. Strombeck, and G. Candiani (2007), Assessment of water quality in lake Garda (Italy) using Hyperion, Remote Sensing of Environment, 109 (2), 183–195.

Goetz, A. F., G. Vane, J. E. Solomon, and B. N. Rock (1985), Imaging spectrometry for earth remote sensing, 228 (4704), 1147–1153.

Goetz, A.F.H., S. Chabrillat, and Z. Lu (2001), Field reflectance spectrometry for detection of swelling clays at construction sites, Field Analytical Chemistry and Technology, 5 (3), 143-155.

Goetz, A. F. H. (2011), Measuring the Earth from Above: 30 Years (and Counting) of Hyperspectral Imaging, Photonics Spectra, 45 (6), 42.

Goetze, C., A. Jung, I. Merbach, R. Wennrich, and C. Gläßer (2010), Spectrometric analyses in comparison to the physiological condition of heavy metal stressed floodplain vegetation in a standardised experiment, Central European Journal of Geosciences, 2 (2), 132-137.

Goodenough, D., D. Charlebois, A. Bhogal, and N. Daley (1998), An improved planner for intelligent monitoring of sustainable development of forests, in Geoscience and Remote Sensing Symposium Proceedings, IGARSS, vol. 1, pp. 397–399.

Goodenough, D., H. Chen, A. Dyk, T. Han, S. McDonald, M. Murdoch, K. Niemann, J. Pearlman, and C. West (2003a), EVEOSD forest information products from AVIRIS and Hyperion, in Geoscience and Remote Sensing IEEE International Symposium - IGARSS, vol. I, pp. 284–287.

Goodenough, D. G., A. Dyk, K. O. Niemann, J. Pearlman, H. Chen, T. Han, M. Murdoch, and C. West (2003b), Processing Hyperion and ALI for forest classification, IEEE Transactions on Geoscience and Remote Sensing, 41 (6), 1321–1331.

Goodenough, D. G., A. Dyk, G. Hobart, and C. Hao (2007), Forest information products from hyperspectral data - Victoria and Hoquiam test sites, in IEEE Transactions on Geoscience and Remote Sensing, IGARSS ’07, 1532–1536.

Goodenough, D., H. Chen, P. Gordon, K. O. Niemann, and G. Quinn (2012), Forest applications with hyperspectral imaging, in Proc. IGARSS 2012, pp. 7309–7312, Munich, Germany.

Gower, J. F. R., G. A. Borstad, C. D. Anger, and H. Edel (1992), CCD-based imaging spectroscopy for remote sensing: the FLI and CASI programs, Canadian Journal of Remote Sensing, 18, 199–208.

Graham, E. R., and J. T. Thompson (2009), Deposit- and suspension-feeding sea cucumbers (echinodermata) ingest plastic fragments, Journal of Experimental Marine Biology and Ecology, 368 (1), 22–29.

Green, R.O., M. Eastwood, C. Sarture, T. Chrien, M. Aronsson, B. Chippendale, J. Faust, B. Pavri, C. Chovit, M. Solis, et al. (1998), Imaging spectroscopy and the airborne visible/infrared imaging spectrometer (AVIRIS), Remote Sensing of Environment, 65, 227–248.

Green, R., G. P. Asner, S. Ungar, and R. Knox (2008), NASA mission to measure global plant physiology and functional types, Proceedings of the 2008 IEEE Aerospace Conference, Big Sky, MT, USA, 1–8 March 2008, 1–7.

Green R. O. (2014), Lessons and key results from 30 years of imaging spectroscopy, Proc. SPIE 9222, Imaging Spectrometry.

Gregory, M. R. (2009), Environmental implications of plastic debris in marine settings-entanglement, ingestion, smothering, hangers-on, hitch-hiking and alien invasions, Philosophical Transactions of the Royal Society B-Biological Sciences, 364 (1526), 2013–2025.

Guanter, L., Y. Zhang, M. Jung, J. Joiner, M. Voigt, J. A. Berry, C. Frankenberg, A. R. Huete, P. Zarco-Tejada, J.-E. Lee, M. S. Moran, G. Ponce-Campos, C. Beer, G. Camps-Valls, N. Buchmann, D. Gianelle, K. Klumpp, A. Cescatti, J. M. Baker, and T. J. Griffis (2014), Global and time-resolved monitoring of crop photosynthesis with chlorophyll fluorescence. Proceedings of the National Academy of Sciences of the United States of America (PNAS), 111, E1327-E1333.

Guanter, L. H. Kaufmann, K. Segl, S. Foerster, C. Rogass, S. Chabrillat, T. Kuester, A. Hollstein, G. Rossner, C. Chlebek, C. Straif, S. Fischer, S. Schrader, T. Storch, U. Heiden, A. Mueller, M. Bachmann, H. Muehle, R. Mueller, M. Habermeyer, A. Ohndorf, J. Hill, H. Buddenbaum, P. Hostert, S. van der Linden, P. J. Leitao, A. Rabe, R. Doerffer, H. Krasemann, H. Xi, W. Mauser, T. Hank, M. Locherer, M. Rast, K. Staenz, and B. Sang (2015), The EnMAP Spaceborne Imaging Spectroscopy Mission for Earth Observation, Remote Sensing, 7 (7), 8830-8857.

Guzzetti, F., P. Reichenbach, M. Cardinali, M. Galli, and F. Ardizzone (2005), Probabilistic landslide hazard assessment at the basin scale, Geomorphology, 72, 272–299.

Guzzetti, F., A. C. Mondini, M. Cardinali, F. Fiorucci, M. Santangelo, and K.-T. Chang, (2012), Landslide inventory maps: New tools for an old problem, Earth-Science Reviews 112, 42–66.

Haberl, H., K. H. Erb, F. Krausmann, V. Gaube, A. Bondeau, C. Plutzar, S. Gingrich, W. Lucht, and M. Fischer-Kowalski (2007), Quantifying and mapping the human appropriation of net primary production in earth’s terrestrial ecosystems, Proceedings of the National Academy of Sciences, 104 (31), 12,942–12,947.

Haboudane, D., J. R. Miller, N. Tremblay, P. J. Zarco-Tejada, and L. Dextraze (2002), Integrated narrow-band vegetation indices for prediction of crop chlorophyll content for application to precision agriculture, Remote Sensing of Environment, 81 (2-13), 416–426.

Hank, T. (2008), A biophysically based coupled model approach for the assessment of canopy processes under climate change conditions, Dissertation.

Hank, T., P. Marzahn, F. Schlenz, and W. Mauser (2010), Assessing Moisture Conditions of Heterogeneous Land Surfaces through Hyperspectral Analysis of Water Absorption Features, ESA Special Publication 683.

Hank, T. B., H. Bach, K. Spannraft, M. Friese, T. Frank, and W. Mauser (2012), Improving the process-based simulation of growth heterogeneities in agricultural stands through assimilation of earth observation data, IEEE Explore, 1006-1009.

Hank, T., H. Bach, and W. Mauser (2015), Using a Remote Sensing-Supported Hydro-Agroecological Model for Field-Scale Simulation of Heterogeneous Crop Growth and Yield: Application for Wheat in Central Europe, Remote Sensing, 7 (4), 3934-3965.

Hansen, M., D. Roy, E. Lindquist, B. Adusei, C. Justice, and A. Altstatt (2008), A method for integrating MODIS and Landsat data for systematic monitoring of forest cover and change in the congo basin, Remote Sensing of Environment, 112, 2495–2513.

Haubrock, S., S. Chabrillat, and H. Kaufmann (2004), Application of hyperspectral imaging and laser scanning for the monitoring and assessment of soil erosion in a recultivation mining area, in Remote sensing and GIS for environmental studies: Application in geography, vol. 113, edited by S. Erasmi, B. Cyffka, and M. Kappas, pp. 230–237, Goettinger Geographische Abhandlungen.

Haubrock, S., S. Chabrillat, C. Lemmnitz, and H. Kaufmann (2008), Surface soil moisture quantification models from reflectance data under field conditions, 29 (1), 3–29.

Hedley, J. D. (2013), Chapter 4 – Hyperspectral Applications, In, Goodman, J.A. et al. (eds.), Coral Reef Remote Sensing, Springer.

Heiden, U., K. Segl, S. Roessner, and H. Kaufmann (2007), Determination of robust spectral features for identification of urban surface materials in hyperspectral remote sensing data, Remote Sensing of Environment, 111 (4), 537–552.

Heiden, U., W. Heldens, S. Roessner, K. Segl, T. Esch, and A. Mueller (2012), Urban structure type characterization using hyperspectral remote sensing and height information, Landscape and Urban Planning, 105 (4), 361 – 375.

Held, M., A. Rabe, C. Senf, S. van der Linden, and P. Hostert (2015), Analyzing hyperspectral and hypertemporal data by decoupling feature redundancy and feature relevance, IEEE Geoscience and Remote Sensing Letters, 12, 983-987.

Heldens, W., U. Heiden, T. Esch, E. Stein, and A. Mueller (2011), Can the future EnMAP mission contribute to urban applications - a literature survey, Remote Sensing, 3, 1817–1846.

Heldens, W., H. Taubenboeck, T. Esch, U. Heiden, and M. Wurm (2013), Analysis of Surface Thermal Patterns in Relation to Urban Structure Types: A Case Study for the City of Munich, In, Thermal Infrared Remote Sensing - Sensors, Methods, Applications Remote Sensing and Digital Image Processing, Springer, 475-494.

Helland, I. S. (1990), PLS regression and statistical models, Scandivian Journal of Statistics, 17, 97–114.

Herold, M., D. A. Roberts, M. E. Gardner, and P. E. Dennison (2004), Spectrometry for urban area remote sensing - development and analysis of a spectral library from 350 to 2400 nm, Remote Sensing of Environment, 91 (3-14), 304–319.

Hoare, D., and P. Frost (2004), Phenological description of natural vegetation in southern Africa using remotely-sensed vegetation data, Applied Vegetation Science, 7, 19–28.

Hochberg, E. J. (2011), Remote Sensing of Coral Reef Processes, In, Dubinsky, Z. and E. Stambler (eds.), Coral Reefs: An Ecosystem in Transition, Springer.

Hope, A., W. Boynton, D. Stow, and D. Douglas (2003), Interannual growth dynamics of vegetation in the Kuparuk River watershed, Alaska based on the Normalized Difference Vegetation Index, International Journal of Remote Sensing, 24 (17), 3413–3425.

Houweling, S., T. Roeckmann, I. Aben, F. Keppler, M. Krol, J.F. Meirink, E.J. Dlugokencky, and C. Frankenberg (2006), Atmospheric constraints on global emissions of methane from plants. Geophysical Research Letters 33 (15).

Huang, S., C. Potter, R. Crabtree, S. Hager, and P. Gross (2007), Fusing optical and radar data to estimate sagebrush, herbaceous, and bare ground cover in Yellowstone Remote Sensing of Environment, 114, 251–264.

Huck, P., B. Light, H. Eicken, and M. Haller (2007), Mapping sediment-laden sea ice in the Arctic using AVHRR remote-sensing data: Atmospheric correction and determination of reflectances as a function of ice type and sediment load, Remote Sensing of Environment, 107, 484-495.

Hueni, A., J. Nieke, J. Schopfer, M. Kneubuehler, and K. Itten (2009), The spectral database specchio for improved long-term usability and data sharing, Computers & Geosciences, 35 (3), 557–565.

Hunt, G. R., and J. W. Salisbury (1970), Visible and near infrared spectra of minerals and rocks. I. Silicate minerals, Modern Geology, 1, 282–300.

Hunt, G. R. (1977), Spectral Signatures of Particulate Minerals in the Visible and near Infrared, Geophysics, 42 (3), 501–513.

Hyde, P., R. Dubayah, W. Walker, J. B. Blair, M. Hofton, and C. Hunsaker (2006), Mapping forest structure for wildlife habitat analysis using multi-sensor (LiDAR, SAR/InSAR, ETM+, Quickbird) synergy, Remote Sensing of Environment, 102 (1-2), 63–73.

Ip, F., J. Dohm, V. Baker, T. Doggett, A. Davies, R. Castavo, S. Chien, B. Cichy, R. Greeley, R. Sherwood, D. Tran, and G. Rabideau (2006), Flood detection and monitoring with the autonomous sciencecraft experiment onboard EO-1, Remote Sensing of Environment, 101 (4), 463–481.

IPCC (2007), Climate Change 2007: Impacts, Adaptation and Vulnerability, Cambridge Univ. Press, Contribution of Working Group II to the Fourth Assessment Report of the Intergovernmental Panel on Climate Change, (M.L. Parry, O.F. Canziani, J.P. Palutikof, P.J. van der Linden and C.E. Hanson).

IPCC (1995), Radiative Forcing of Climate Change, Cambridge University Press, New York (1995), pp. 85–87

IPCC (2012), Summary for policymakers, in: Managing the risks of extreme events and disasters to advance climate change adaptation, Tech. rep., Cambridge, UK and New York, NY, USA.

IPCC (2014), Climate Change 2014: Synthesis Report. Contribution of Working Groups I, II and III to the Fifth Assessment Report of the Intergovernmental Panel on Climate Change, IPCC, Geneva, Switzerland, 151 pp.

Istomina, L., G. Heygster, M. Huntemann, P. Schwarz, G. Birnbaum, R. Scharien, C. Polashenski, D. Perovich, E. Zege, A. Malinka, A. Prikhach, and I. Katsev, (2015), Melt pond fraction and spectral sea ice albedo retrieval from MERIS data - Part 1: Validation against in situ, aerial, and ship cruise data, The Cryosphere, 9, 1551-1566.

Itten, K.I., F. Dell'Endice, A. Hueni, M. Kneubuehler, D. Schlaeper, D. Odermatt, F. Seidel, S. Huber, J. Schopfer, T. Kellenberger et al. (2008), APEX—The hyperspectral ESA airborne prism experiment, Sensors, 8, 6235–6259.

Iwasaki, A., N. Ohgi, J. Tanii, T. Kawashima, and H. Inada (2011), Hyperspectral Imager Suite (HISUI) — Japanese hyper-multi spectral radiometer, Proceedings of the 2011 IEEE International Geoscience and Remote Sensing Symposium (IGARSS), Vancouver, BC, USA, 24–29 July 2011; pp. 1025–1028.

Jacquemoud, S., C. Bacour, H. Poilve, and J. P. Frangi (2000), Comparison of four radiative transfer models to simulate plant canopies reflectance: Direct and inverse mode, Remote Sensing of Environment, 74 (3), 471–481.

Janz, A., S. van der Linden, B. Waske, and P. Hostert (2007), ImageSVM - a user-oriented tool for advanced classification of hyperspectral data using support vector machines, In Reusen, I., and J. Cools (Eds.) (2007), Proceedings 5th EARSeL Workshop on Imaging Spectroscopy - "Imaging Spectroscopy: Innovation in environmental research", 23-25 April, 2007. Bruges, Belgium

Jilge, M., U. Heiden, M. Habermeyer, and C. Jürgens (2015), Global Learning Spectral Archive - A new Way to deal with Unknown Urban Spectra, AGU Fall Meeting, 14 – 18 December 2015, San Francisco, USA.

Jin, M., J. M. Shepherd, and C. Peters-Lidard (2007), Development of a parameterization for simulating the urban temperature hazard using satellite observations in climate model, Natural Hazards, 43, 257–271.

JRC, MSFD Technical Subgroup on Marine Litter (2013), Guidance on Monitoring of Marine Litter in European Seas - A guidance document within the Common Implementation Strategy for the Marine Strategy Framework Directive, JRC Scientific and Policy Reports: Report EUR 26113 EN, Luxembourg, Publications Office of the European Union.

Kaleita, A. L., B. L. Steward, R. P. Ewing, D. A. Ashlock, M. E. Westgate, and J. L. Hatfield (2006), Novel analysis of hyperspectral reflectance data for detecting onset of pollen shed in maize, American Society of Agricultural and Biological Engineers, 49 (6), 8.

Kallio, K., T. Kutser, T. Hannonen, S. Koponen, J. Pulliainen, J. Vepsalainen, and T. Pyhalahti (2001), Retrieval of water quality from airborne imaging spectrometry of various lake types in different seasons, 268 (1-3), 59–77.

Kamarainen, A., R. Penczykowski, M. Van de Bogert, P. Hanson, and S. Carpenter (2009), Phosphorus sources and demand during summer in a eutrophic lake, Biomedical and Life Sciences, 71 (2), 214–227.

Kareiva, P., S. Watts, R. McDonald, and T. Boucher (2007), Domesticated nature: Shaping landscapes and ecosystems for human welfare, Science, 316, 1866–1869.

Kariuki P. C., T. Woldai, and F. van der Meer (2004), Effectiveness of spectroscopy in identification of swelling indicator clay minerals. International Journal of Remote Sensing, 25 (2), 455-469.

Katey, W.M., S. A. Zimov, J. P. Chanton, D. Verbyla, and F. S. Chapin (2006), Methane bubbling from Siberian thaw lakes as a positive feedback to climate warming, Nature 443(7107), 71-75.

Katey, W.M., L.C. Smith, and F.S. Chapin (2007), Methane bubbling from northern lakes: present and future contributions to the global methane budget. Philosophical Transactions of the Royal Society of London A: Mathematical, Physical and Engineering Sciences, 365 (1856), 1657-1676.

Kaufmann H., B. Sang, T. Storch, K. Segl, S. Foerster, L. Guanter, M. Erhard, B. Heider, S. Hofer, H.-P. Honold, B. Penné, M. Bachmann, M. Habermeyer, A. Mueller, R. Mueller, M. Rast, K. Staenz, C. Straif and C. Chlebek (2016), Chapter seven, Environmental Mapping and Analysis Program – A German Hyperspectral Mission. In, Qian, S.-E. (edt), Optical Payloads for Space Missions, First Edition. John Wiley & Sons.

Kemper, T., and S. Sommer (2004), Use of airborne hyperspectral data to estimate residual heavy metal contamination and acidification potential in the Guadiamar floodplain Andalusia, Spain after the Aznacollar mining accident, Proceedings of SPIE on Remote Sensing for Environmental Monitoring, GIS Applications, and Geology IV, 5574, 224–234.

Kijne, J., J. Barron, H. Hoff, J. Rockstroem, L. Karlberg, J. Gowing, S. Wani, and D. Wichelns (2009), Opportunities to increase water productivity in agriculture with special reference to Africa and South Asia, A report prepared by Stockholm Environment Institute, for the Swedish Ministry of Environment presentation at CSD 16, New York, SEI, Stockholm.

Kirk, J. O. T. (1994), Light and photosynthesis in aquatic ecosystems, Cambridge University Press, Cambridge.

Klein A.G., and B. L. Isacks (1999), Spectral mixture analysis of Landsat Thematic Mapper images applied to the detection of the transient snowline on tropical Andean glaciers, Global Planetary Change 22, 139–54.

Knipling, E. B. (1970), Physical and physiological basis for the reflectance of visible and near-infrared radiation from vegetation, Remote Sensing of Environment, 1 (3), 155–159.

Knyazikhin, Y., M. A. Schull, P. Stenberg, M. Mõttus, M. Rautiainen, Y. Yang, A. Marshak, P. Latorre Carmona, R. K. Kaufmann, P. Lewis, M. I. Disney, V. Vanderbilt, A. B. Davis, F. Baret, S. Jacquemoud, A. Lyapustin, and R. B. Myneni (2013), Hyperspectral remote sensing of foliar nitrogen content, Proceedings of the National Academy of Sciences, 110, E185–E192.

Koetz, B., M. Schaepman, F. Morsdorf, P. Bowyer, K. Itten, and B. Allgoewer (2004), Radiative transfer modeling within a heterogeneous canopy for estimation of forest fire fuel properties, Remote Sensing of Environment, 92, 332–344.

Koetz, B., F. Morsdorf, S. van der Linden, T. Curt, and B. Allgoewer (2008), Multi-source land cover classification for forest fire management based on imaging spectrometry and LiDAR data, Forest Ecology and Management, 256, 263-271.

Kollmair, M., and S. Banerjee (2011), Drivers of migration in mountainous regions of the developing world, Tech. rep., UK Governments Foresight Project, Migration and Global Environmental Change.

Kort, E.A., C. Frankenberg, K.R. Costigan, R. Lindenmaier, M.K. Dubey, and D. Wunch (2014), Four corners: The largest US methane anomaly viewed from space. Geophysical Research Letters 41 (19), 6898-6903.

Krieger, G., A. Moreira, H. Fiedler, I. Hajnsek, M. Werner, M. Younis, and M. Zink (2007), TanDEM-X: A satellite formation for high-resolution SAR interferometry, Geoscience and Remote Sensing, IEEE Transactions on, 45 (11), 3317–3341.

Krueger, G., J. Erzinger, and H. Kaufmann (1998), Laboratory and airborne reflectance spectroscopic analyses of lignite overburden dumps, Journal of Geochemical Exploration, 64 (1-3), 47–65.

Kumar, A., A. Saha, and V. K. Dadhwal (2010), Some issues related with sub-pixel classification using HYSI data from IMS-1 satellite, Journal of the Indian Society of Remote Sensing, 38, 203–210.

Kuriyama, Y., K. Konishi, H. Kanehiro, C. Otake, T. Kaminuma, Y. Mato, H. Takada, and A. Kojima (2002), Plastic pellets in the marine environment of Tokyo bay and Sagami Bay, Nippon Suisan Gakkaishi, 68 (2), 164–171.

Kuusk, A., and T. Nilson (2009), Forest reflectance and transmittance - FRT user guide, version 08.2009.

Laidler, G., and P. Treitz (2003), Biophysical remote sensing of arctic environments, Progress in Physical Geography, 27 (1), 44–68.

Lammoglia, T., and C. R. de Souza Filho (2011), Spectroscopic characterization of oils yielded from Brazilian offshore basins: Potential applications of remote sensing, Remote Sensing of Environment, 115 (10), 2525–2535.

Landvelde, F., and H. Prins (2007), Resilience and restoration of soft-bottom near shore ecosystems, Hydrobiologica, 591, 1–4.

Larsolle, A., and H. Hamid Muhammed (2007), Measuring crop status using multivariate analysis of hyperspectral field reflectance with application to disease severity and plant density, Precision Agriculture, 8 (1), 37–47.

Lavorel, S., K. Grigulis, P. Lamarque, M.-P. Colace, D. Garden, J. Girel, G. Pellet, and R. Douzet (2011), Using plant functional traits to understand the landscape distribution of multiple ecosystem services, Journal of Ecology, 99 (1), 135–147.

Lawrence, D. M., and A. G. Slater (2005), A projection of severe near-surface permafrost degradation during the 21st century, Geophysical Research Letters, 32 (24), L24,401–5.

le Maire, G., H. Davi, K. Soudani, C. Francois, V. Le Dantec, and E. Dufrene (2005), Modeling annual production and carbon fluxes of a large managed temperate forest using forest inventories, satellite data and field measurements, Tree Physiology, 25 (7), 859–872.

le Maire, G., C. Francois, K. Soudani, D. Berveiller, J.-Y. Pontailler, N. Breda, H. Genet, H. Davi, and E. Dufrene (2008), Calibration and validation of hyperspectral indices for the estimation of broadleaved forest leaf chlorophyll content, leaf mass per area, leaf area index and leaf canopy biomass, Remote Sensing of Environment, 112 (10), 3846– 3864.

Lee, Z., K. Carder, C. Mobley, R. Steward, and J. Patch (1999), Hyperspectral remote sensing for shallow waters: 2. Deriving bottom depths and water properties by optimization, Applied Optics, 38 (18), 3831–3843.

Lee, K. S., W. B. Cohen, R. E. Kennedy, T. K. Maiersperger, and S. T. Gower (2004), Hyperspectral versus multispectral data for estimating leaf area index in four different biomes, Remote Sensing of Environment, 91, 508–520.

Leitão, P. J., M. Schwieder, S. Suess, A. Okujeni, L. S. Galvão, S. van der Linden, and P. Hostert (2015a), Monitoring natural ecosystem and ecological gradients: perspectives with EnMAP, Remote Sensing, 7, 13098-13119.

Leitão, P. J., M. Schwieder, S. Suess, I. Catry, E. J. Milton, F. Moreira, P. E. Osborne, M. J. Pinto, S. van der Linden, and P. Hostert (2015b), Mapping beta diversity from space: sparse generalised dissimilarity modelling (SGDM) for analysing high-dimensional data, Methods in Ecology and Evolution, 6, 764-771.

Li, L., S. L. Ustin, and M. Lay (2005), Application of AVIRIS data in detection of oil-induced vegetation stress and cover change at Jornada, New Mexico, Remote Sensing of Environment, 94 (1), 1–16.

Lisitzin, A.P. (2002), Sea-Ice and Iceberg Sedimentation in the Ocean - Recent and Past, Springer-Verlag Berlin Heidelberg (Original Russian edition published by Nauka, Moscow, 1994).

Liston, G. E., and C. A. Hiemstra (2011), The Changing Cryosphere: Pan-Arctic Snow Trends (1979-2009), Journal of Climate, 24 (21), 5691–5712.

Locherer, M., T. Hank, M. Danner, and W. Mauser (2015), Retrieval of Seasonal Leaf Area Index from simulated EnMAP data through optimized LUT-based Inversion of the PROSAIL Model, Remote Sensing, 7 (8), 10321-10346.

Loreau, M., S. Naeem, P. Inchausti, J. Bengtsson, J. Grime, A. Hector, D. Hooper, M. Huston, D. Raffaelli, B. Schmid, D. Tilman, and D. Wardle (2001), Biodiversity and ecosystem functioning: Current knowledge and future challenges, 294 (5543), 804–808.

Lu, D., and Q. Weng (2006), Use of impervious surface in urban land-use classification, Remote Sensing of Environment, 102 (1-12), 146–160.

Lucke, R.L., M. Corson, N. R. McGlothlin, S. D. Butcher, D. L. Wood, D. R. Korwan, R. R. Li, W. A. Snyder, C. O. Davis, and D. T. Chen (2011), Hyperspectral imager for the coastal ocean: Instrument description and first images, Applied Optics, 50, 1501–1516.

Machwitz, M., L. Giustarini, C. Bossung, D. Frantz, M. Schlerf, H. Lilienthal, L. Wandera, P. Matgen, L. Hoffmann, and T. Udelhoven (2014), Enhanced biomass prediction by assimilating satellite data into a crop growth model, Environmental Modelling & Software, 62, 437-453.

Martin, M., S. Newman, J. Aber, and R. Congalton (1998), Determining forest species composition using high spectral resolution remote sensing data, Remote Sensing of Environment, 65, 249–254.

Mato, Y., T. Isobe, H. Takada, H. Kanehiro, C. Ohtake, and T. Kaminuma (2001), Plastic resin pellets as a transport medium for toxic chemicals in the marine environment, Environmental Science & Technology, 35 (2), 318–324.

Matson, P., L. Johnson, C. Billow, J. Miller, and R. Pu (1994), Seasonal patterns and remote spectral estimation of canopy chemistry across the Oregon transect, Ecological Applications, 4 (2), 280–298.

Mauser, W., T. Hank, and H. Bach (2015a), Earth Observation for food security and sustainable agriculture, In JAXA (edt.): Applications of Satellite Earth Observations: Serving society, science, & industry, Full Report, 2015 Edition, Committee On Earth Observation Satellites, 169-174.

Mauser, W., F. Zabel, G. Klepper, R. Delzeit, T. Hank, B. Putzenlechner, and A. Calzadillo (2015b), Global biomass production potentials exceed expected future demand without the need for cropland expansion, Nature Communications, 6, 8946.

Mayes, W. M., A. P. Jarvis, I. T. Burke, M. Walton, V. Feigl, O. Klebercz, and K. Gruiz (2011), Dispersal and Attenuation of Trace Contaminants Downstream of the Ajka Bauxite Residue (Red Mud) Depository Failure, Hungary, Environmental Science & Technology, 45 (12), 5147–5155.

McCarthy, T. S., V. Arnold, J. Venter, and W. N. Ellery (2007), The collapse of Johannesburg's klip river wetland, South African Journal of Science, 103, 391–408.

MEA (2005), Urban systems - current state and trends, Assessment report, Millennium Ecosystem Assessment.

Meroni, M., M. Rossini, L. Guanter, L. Alonso, U. Rascher, R. Colombo, and J. Moreno (2009), Remote sensing of solar-induced chlorophyll fluorescence: Review of methods and applications, Remote Sensing of Environment, 113, 2037-2051.

Metternicht, G., L. Hurni, and R. Gogu (2005), Remote sensing of landslides: An analysis of the potential contribution to geo-spatial systems for hazard assessment in mountainous environments, Remote Sensing of Environment, 98 (2-13), 284–303.

Meyerson, F. A. B., L. Merino, and J. Durand (2007), Migration and environment in the context of globalization, Frontiers in Ecology and the Environment, 5 (4), 182–190.

Michel, S., P. Gamet, and M. J. Lefevre-Fonollosa (2011), HYPXIM—A hyperspectral satellite defined for science, security and defence users, Proceedings of the 2011 3rd Workshop on

Hyperspectral Image and Signal Processing: Evolution in Remote Sensing (WHISPERS), Lisbon, Portugal, 6–9 June 2011, pp. 1–4.

Mielke, C., N. K. Boesche, C. Rogass, H. Kaufmann, C. Gauert, and M. de Wit (2014), Spaceborne Mine Waste Mineralogy Monitoring in South Africa, Applications for Modern Push-Broom Missions: Hyperion/OLI and EnMAP/Sentinel-2, Remote Sensing 6 (8), 6790–6816.

Migdall, S., H. Bach, J. Bobert, M. Wehrhan, and W. Mauser (2009), Inversion of a canopy reflectance model using hyperspectral imagery for monitoring wheat growth and estimating yield, Precision Agriculture, 10 (6), 508–524.

Migdall, S., N. Ohl, and H. Bach (2010), Parameterisation of the land surface reflectance model SLC for winter rape using spaceborne hyperspectral CHRIS data, in Hyperspectral Workshop 2010 From CHRIS/Proba to PRISMA & EnMAP and beyond, edited by H. Lacoste-Francis.

Minh, N., T. Minh, M. Watanabe, T. Kunisue, I. Monirith, S. Tanabe, S. Sakai, A. Subramanian, K. Sasikumar, P. Viet, B. Tuyen, T. Tana, and M. Prudente (2003), Open dumping site in Asian developing countries: A potential source of polychlorinated dibenzo-p-dioxins and polychlorinated dibenzofurans, Environmental Science & Technology, 37 (8), 1493–1502.

MMSD (2002), Breaking new ground: Mining, minerals and sustainable development, Tech. rep., London.

Mondino, E. B., M. Giardino, and L. Perotti (2009), A neural network method for analysis of hyperspectral imagery with application to the cassas landslide (Susa valley, NW-Italy), Geomorphology, 110 (1-12), 20–27.

Moran, M. S., A. Vidal, D. Troufleau, J. Qi, T. R. Clarke, P. J. Pinter Jr, T. A. Mitchell, Y. Inoue, and C. M. U. Neale (1997), Combining multifrequency microwave and optical data for crop management, Remote Sensing of Environment, 61 (1), 96–109.

Morel, A., and L. Prieur (1977), Analysis of variations in ocean color, Limnology and Oceanography, 22 (4), 709–722.

Mumby P. J., W. Skirving, A. E. Strong, J. T. Hardy, E. F. LeDrew, E. J. Hochberg, R. P. Stumpf, and L. T. David (2004), Remote sensing of coral reefs and their physical environment, Marine Pollution Bulletin, 48, 219-228.

Muster, S., M. Langer, B. Heim, S. Westermann, and J. Boike (2012), Subpixel heterogeneity of ice-wedge polygonal tundra: a multi-scale analysis of land cover and evapotranspiration in the Lena river delta, Siberia, Tellus B, 64 (17), 301.

Muster, S., B. Heim, A. Abnizova, and J. Boike, (2013), Water Body Distributions Across Scales: A Remote Sensing Based Comparison of Three Arctic Tundra Wetlands, Remote Sensing, 5(4), 1498-1523.

Mutanga, O., and A. Skidmore (2004), Narrow band vegetation indices overcome the saturation problem in biomass estimation, International Journal of Remote Sensing, 25, 3999–4014.

Nepstad, D., A. Verissimo, A. Alencar, C. Nobre, E. Lima, P. Lefebvre, P. Schlesinger, C. Potter, P. Moutinho, E. Mendoza, M. Cochrane, and V. Brooks (1999), Large-scale impoverishment of Amazonian forests by logging and fire, Nature, 398 (6727), 505–508.

Neville, R. A., and I. Powell (1992), Design of SFSI: An imaging spectrometer in the SWIR, Canadian Journal of Remote Sensing, 18 (4), 210–222.

Niemann, K.O., G. Quinn, R. Stephen, F. Visintini, and D. Parton (2015), Hyperspectral Remote Sensing of Mountain Pine Beetle with an Emphasis on Previsual Assessment, Canadian Journal of Remote Sensing, 41, 191-202.

Nocita, M., A. Stevens, B. van Wesemael, M. Aitkenhead, M. Bachmann, B. Barthès, E. Ben Dor, D. J. Brown, M. Clairotte, A. Csorba, P. Dardenne, J. A. M. Dematte, V. Genot, C. Guerrero, M.

Knadel, L. Montanarella, C. Noon, L. Ramirez-Lopez, J. Robertson, H. Sakai, J. M. Soriano-Disla, K. D. Shepherd, B. Stenberg, E. K. Towett, R. Vargas, and J. Wetterlind (2015), Chapter Four – Soil Spectroscopy: An Alternative to Wet Chemistry for Soil Monitoring, Advances in Agronomy,132, 139–159.

Nolin, A. W., J. Dozier, and L. A. K. Mertes (1993), Mapping alpine snow using a spectral mixture modelling technique, Annals of Glaciology, 17, 121–124.

Numata, I., M. A. Cochrane, C. M. Souza, and S. M. H. (2011), Carbon emissions from deforestation and forest fragmentation in the Brazilian Amazon, Environmental Research Letters, 6, 044,003.

Nuernberg, D., I. Wollenburg, D. Dethleff, H. Eicken, H. Kassens, T. Letzig, E. Reimnitz, and J. Thiede (1994), Sediments in Arctic sea ice — Implications for entrainment, transport and release, Marine Geology, 119, 185–214.

Ogata, Y., H. Takada, K. Mizukawa, H. Hirai, S. Iwasa, S. Endo, Y. Mato, M. Saha, K. Okuda, A. Nakashima, M. Murakami, N. Zurcher, R. Booyatumanondo, M. P. Zakaria, L. Q. Dung, M. Gordon, C. Miguez, S. Suzuki, C. Moore, H. K. Karapanagioti, S. Weerts, T. McClurg, E. Burres, W. Smith, M. Van Velkenburg, J. S. Lang, R. C. Lang, D. Laursen, B. Danner, N. Stewardson, and R. C. Thompson (2009), International pellet watch: Global monitoring of persistent organic pollutants (pops) in coastal waters. 1. initial phase data on pcbs, ddts, and hchs, Marine Pollution Bulletin, 58 (10), 1437–1446.

Oke, T. (1988), Street design and urban canopy layer climate, Energy and Buildings, 11 (1-13), 103 – 113.

Okoronkwo, N. E., S. A. Odemelam, and O. A. Ano (2006), Levels of toxic elements in soils of abandoned waste dump site, African Journal of Biotechnology, 5 (13), 1241–1244.

Okujeni, A., S. van der Linden, L. Tits, B. Somers, and P. Hostert (2013), Support vector regression and synthetically mixed training data for quantifying urban land cover, Remote Sensing of Environment, 137, 184-197.

Okujeni, A., S. van der Linden, and P. Hostert (2015a), Extending the vegetation–impervious–soil model using simulated EnMAP data and machine learning, Remote Sensing of Environment, 158, 69-80.

Okujeni, A., S. van der Linden, and P. Hostert (2015b), On the use of extended vegetation-impervious-soil maps from simulated EnMAP data for characterizing urban functional areas, ESA-ESRIN conference on Mapping Urban Areas from Space (MUAS). Frascati, Rome, Italy.

Oldeland, J., W. Dorigo, D. Wesuls, and N. Juergens (2010), Mapping bush encroaching species by seasonal differences in hyperspectral imagery, Remote Sensing, 2, 1416–1438.

Oldeland, J., D. Wesuls, and N. Jürgens (2012), RLQ and fourth-corner analysis of plant species traits and spectral indices derived from HyMap and CHRIS-PROBA imagery, International Journal of Remote Sensing, 33, 6459–6479.

Ollinger, S., and M.-L. Smith (2005), Net primary production and canopy nitrogen in a temperate forest landscape: An analysis using imaging spectroscopy, modeling and field data, Ecosystems, 8 (7), 760–778.

Oppelt, N., and W. Mauser (2003), Hyperspectral remote sensing - a tool for the derivation of plant nitrogen and its spatial variability within maize and wheat canopies, in 4th European Conference on Precision Agriculture, edited by J. Stafford and A. Werner, Precision Agriculture, pp. 493–498, Wageningen Academic Publishers.

Oppelt, N., and W. Mauser (2007), The airborne visible infrared imaging spectrometer AVIS: Design, characterization and calibration, Sensors, 7, 1934–1953.

Painter, T.H., D. A. Roberts, R. O. Green, and J. Dozier (1998), The effect of grain size on spectral mixture analysis of snow-covered area from AVIRIS data, Remote Sensing of Environment 65, 320–32.

Painter, T.H., B. Duval, W. H. Thomas, M. Mendez, S. Heintzelman, and J. Dozier (2001), Detection and quantification of snow algae with an airborne imaging spectrometer, Applied Environmental Microbiology 67, 5267–72.

Painter, T.H., J. Dozier, D. A. Roberts, R. E. Davis, and R. O. Green (2003), Retrieval of subpixel snow-covered area and grain size from imaging spectrometer data, Remote Sensing of Environment 85, 64–77.

Pearlman, J. S., P. S. Barry, C. C. Segal, J. Shepanski, D. Beiso, and S. L. Carman (2003), Hyperion, a space-based imaging spectrometer, in IEEE Transactions on Geoscience and Remote Sensing, 1, vol. 41, pp. 1160– 1173.

Peng, C., X. Ma, Z. Lei, Q. Zhu, H. Chen, W. Wang, S. Liu, W. Li, X. Fang, and X. Zhou (2011), A drought-induced pervasive increase in tree mortality across Canada’s boreal forests, Nature Climate Change, 1, 467–471.

Pereira, H.M., S. Ferrier, M. Walters, G. N. Geller, R. H. G. Jongman, R. J. Scholes, M. W. Bruford, N. Brummitt, S. H. M. Butchart, A. C. Cardoso, N. C. Coops, E. Dulloo, D. P. Faith, J. Freyhof, R. D. Gregory, C. Heip, R. Hoeft, G. Hurtt, W. Jetz, D. S. Karp, M. A. Mcgeoch, D. Obura, Y. Onoda, N. Pettorelli, B. Reyers, R. Sayre, J. P. W. Scharlemann, S. N. Stuart, E. Turak, M. Walpole, and M. Wegmann (2013), Essential biodiversity variables, Science, 339, 277-278.

Perovich, D.K., B. Light, H. Eicken, K. F. Jones, K. Runciman, and S. V. Nghiem (2007), Increasing solar heating of the Arctic Ocean and adjacent seas, 1979-2005: Attribution and role in the ice-albedo feedback, Geophysical Research Letters, 34, L19505.

Petrou, Z.I., I. Manakos, and T. Stathaki (2015), Remote sensing for biodiversity monitoring: a review of methods for biodiversity indicator extraction and assessment of progress towards international targets, Biodiversity and Conservation, 24, 2333-2363.

Phinn, S. R., A. G. Dekker, V. C. Brando, and M. Roelfsema (2003), Mapping water quality and substrate cover in optically complex coastal and reef waters: An integrated approach, Mar Pollut Bull, 51, 459–469.

Pickup, G. (1989), New land degradation survey techniques for arid Australia - problems and prospects, The Rangeland Journal, 11 (2), 74–82.

Pidgeon, E. (2009), Carbon sequestration by coastal marine habitats: Important missing sinks, In: The Management of Natural Coastal Carbon Sinks, pp. 47–51, Gland, Switzerland.

Pignatti, S, P. Angelo, P. Simone, R. Filomena, S. Federico, S. Tiziana, A. Umberto, C. Vincenzo, N. Acito, D. Marco et al. (2013), The PRISMA hyperspectral mission: Science activities and opportunities for agriculture and land monitoring, Proceedings of the 2013 IEEE International Geoscience and Remote Sensing Symposium (IGARSS), Melbourne, Australia, 21–26 July 2013, pp. 4558–4561.

Pleskachevsky, A., S. Lehner, T. Heege, and C. Mott (2011), Synergy and fusion of optical and synthetic aperture radar satellite data for underwater topography estimation in coastal areas, Ocean Dynamics, 61, 2099–2120.

Pritchard, H. D., R. J. Arthern, D. G. Vaughan, and L. A. Edwards (2009), Extensive dynamic thinning on the margins of the Greenland and Antarctic ice sheets, Nature, 461 (7266), 971–975.

Radiarta, I. N., S.-I. Saitoh, and H. Yasui (2011), Aquaculture site selection for Japanese kelp (Laminaria japonica) in southern Hokkaido, japan, using satellite remote sensing and GIS-based models, ICES Journal of Marine Science, 68, 773–780.

Rand, R. S., R. N. Clark, and K. E. Livo (2011), Feature-based and statistical methods for analyzing the Deepwater Horizon oil spill with AVIRIS imagery, in Imaging Spectroscopy XVI, Proceedings of SPIE, vol. 8158, edited by Shen, SS and Lewis, PE, SPIE.

Rasaiah, B., T. Malthus, S. D. Jones, and C. Bellman (2011), The role of hyperspectral metadata, in Hyperspectral Data Exchange. Proceedings of the 7th EARSeL Workshop, Edinburgh.

Rascher, U., G. Agati, L. Alonso, G. Cecchi, S. Champagne, R. Colombo, A. Damm, F. Daumard, E. de Miguel, G. Fernandez, B. Franch, J. Franke, C. Gerbig, B. Gioli, J. A. Gómez, Y. Goulas, L. Guanter, O. Gutiérrez-de-la-Cámara, K. Hamdi, P. Hostert, M. Jiménez, M. Kosvancova, D. Lognoli, M. Meroni, F. Miglietta, A. Moersch, J. Moreno, I. Moya, B. Neininger, A. Okujeni, A. Ounis, L. Palombi, V. Raimondi, A. Schickling, J. A. Sobrino, M. Stellmes, G. Toci, P. Toscano, T. Udelhoven, S. van der Linden, and A. Zaldei (2009), CEFLES2: the remote sensing component to quantify photosynthetic efficiency from the leaf to the region by measuring sun-induced fluorescence in the oxygen absorption bands, Biogeosciences, 6, 1181-1198.

Rees, W., M. Williams, and P. Vitebsky (2003), Mapping land cover change in a reindeer herding area of the Russian Arctic using Landsat TM and ETM+ imagery and indigenous knowledge, Remote Sensing of Environment, 85 (4), 441–452.

Richter, K., C. Atzberger, T. Hank, and W. Mauser (2012), Derivation of biophysical variables from Earth Observation data: validation and statistical measures, Journal of Applied Remote Sensing, 6 (1), 063557.

Rickard, L. J., R. W. Basedow, E. F. Zalewski, P. R. Silverglate, and M. Landers (1993), Hydice: an airborne system for hyperspectral imaging, Proceedings of SPIE, 1937, 173–179.

Ridd, M. K. (1995), Exploring a v-i-s (vegetation-impervious surface-soil) model for urban ecosystem analysis through remote sensing: comparative anatomy for cities, International Journal of Remote Sensing, 16 (12), 2165–2185.

Ritchie, J., and S. Otter (1985), Description and performance of CERES-Wheat: A user-oriented wheat yield model, NAL Call No. AS21 R44A7, vol. 38, USDA, Agricultural Research Service.

Roberts, D. A. Quattrochi, G. C. Hulley, S. J. Hook, and R. O. Green (2012), Synergies between VSWIR and TIR data for the urban environment: An evaluation of the potential for the hyperspectral infrared imager (HyspIRI) decadal survey mission, Remote Sensing of Environment, 117, 83–101.

Roessner, S., K. Segl, U. Heiden, and H. Kaufmann (2001), Automated differentiation of urban surfaces based on airborne hyperspectral imagery, Geoscience and Remote Sensing, IEEE Transactions on, 39 (7), 1525 –1532.

Rogge, D.M., B. Rivard, J. Zhang, and J. Feng (2006), Iterative spectral unmixing for optimizing per-pixel endmember sets. IEEE Transactions on Geoscience and Remote Sensing, 44, 3725-3736.

Romanovsky, V. E., S. L. Smith, and H. H. Christiansen (2010), Permafrost thermal state in the polar northern hemisphere during the international polar year 2007-2009: a synthesis, Permafrost and Periglacial Processes, 21 (2), 106–116.

Rosenthal W., and J. Dozier (1996), Automated mapping of montane snow cover at subpixel resolution from the Landsat Thematic Mapper. Water Resource Research 32,115–30.

Salem, F. (2001), Hyperspectral image analysis for oil spill mitigation, in 22nd Asian Conference on Remote Sensing, pp. 748–753, Singapore.

Salem, F. (2005), Hyperspectral image assessment of oil-contaminated wetland, International Journal of Remote Sensing, 26, 811–821.

Sanchez-Rodriguez, R., K. C. Seto, D. Simon, W. D. Solecki, F. Kraas, and G. Laumann (2005), Science plan - urbanization and global environmental change, IHDP Report 15, International Human Dimension Programme on Global Environmental Change, Bonn.

Scaioni, M. (2014), Remote Sensing for Landslide Investigations: An Overview of Recent Achievements and Perspectives, Remote Sensing, 6 (12), 12666–12666.

Schaepman, M., K. Itten, D. Schlaepfer, J. Kaiser, J. Brazile, W. DeBruyn, A. Neukom, H. Feusi, P. Adolph, R. Moser, T. Schilliger, L. d. Vos, G. Brandt, P. Kohler, M. Meng, J. Piesbergen, P. Strobl, J. Gavira, G. Ulbrich, and R. Meynart (2004), Apex: current status of the airborne dispersive pushbroom imaging spectrometer, in Sensors, Systems, and Next-Generation Satellites VII, SPIE Remote Sensing Conference, Barcelona.

Schaepman, M. E. (2007), Spectrodirectional remote sensing: From pixels to processes, International Journal of Applied Earth Observation and Geoinformation, 9 (2), 204–223.

Schaepman, M. E. (2009), The SAGE Handbook of Remote Sensing, chap. Imaging Spectrometers, pp. 166–178, SAGE, London (UK).

Schaepman, M. E., S. L. Ustin, A. J. Plaza, T. H. Painter, J. Verrelst, and S. Liang (2009), Earth system science related imaging spectroscopy - an assessment, 113 (Suppl.1), 123–137.

Schaepman, M.E., M. Jehle, A. Hueni, P. D'Odorico, A. Damm, J. Weyerrnann, F. D. Schneider, V. Laurent, C. Popp, F. C. Seidel et al. (2015), Advanced radiometry measurements and Earth science applications with the Airborne Prism Experiment (APEX), Remote Sensing of Environment, 158, 207–219.

Schiller, H., and R. Doerffer (1999), Neural network for emulation of an inverse model - operational derivation of case II water properties from MERIS data, 20 (9), 1735–1746.

Schlerf, M., and C. Atzberger (2006), Inversion of a forest reflectance model to estimate structural canopy variables from hyperspectral remote sensing data, Remote Sensing of Environment, 100, 281–294.

Schlerf, M., C. Atzberger, and J. Hill (2005), Remote sensing of forest biophysical variables using HyMap imaging spectrometer data, Remote Sensing of Environment, 95, 177–194.

Schlerf, M., C. Atzberger, J. Hill, H. Buddenbaum, W. Werner, and G. Schueler (2010), Retrieval of chlorophyll and nitrogen in Norway spruce (picea abies l. karst.) using imaging spectroscopy, International Journal of Applied Earth Observation and Geoinformation, 12 (1), 17–26.

Schmid, T., M. Rodríguez-Rastrero, P. Escribano, A. Palacios-Orueta, E. Ben-Dor, A. Plaza, R. Milewski, M. Huesca, A. Bracken, V. Cicuéndez, M. Pelayo, and S. Chabrillat (2015), Characterization of soil erosion indicators using hyperspectral data from a Mediterranean rainfed cultivated region, IEEE Journal of Selected Topics in Applied Earth Observation and Remote Sensing (JSTARS).

Schmidtlein, S., and J. Sassin (2004), Mapping of continuous floristic gradients in grasslands using hyperspectral imagery, Remote Sensing of Environment, 92 (1), 126–138.

Schneider, K., and W. Mauser (2001), Using remote sensing data to model water, carbon and nitrogen fluxes with PROMET-V, in Remote sensing for agriculture, ecosystems, and hydrology II, pp. 12–23.

Schwieder, M., P. J. Leitão, S. Suess, C. Senf, and P. Hostert (2014), Estimating fractional shrub cover using simulated EnMAP data: a comparison of three machine learning regression techniques, Remote Sensing, 6, 3427-3445.

Segl, K., L. Guanter, C. Rogaß, T. Kuester, S. Roessner, H. Kaufmann, B. Sang, V. Mogulsky, and S. Hofer (2012), EeteS - The EnMAP End-to-End Simulation Tool, IEEE Journal of Selected Topics in Applied Earth Observations and Remote Sensing, 5 (2), 522-530.

Simelton, E., E. D. G. Fraser, M. Termansen, T. G. Benton, S. N. Gosling, A. South, N. W. Arnell, A. J. Challinor, A. J. Dougill, and P. M. Forster (2012), The socioeconomics of food crop production and climate change vulnerability: a global scale quantitative analysis of how grain crops are sensitive to drought, Food Security, 4 (2), 163–179.

Skidmore, A.K., N. Pettorelli, N. C. Coops, G. N. Geller, M. Hansen, R. Lucas, C.A. Muecher, B. O'connor, M. Paganini, H. M. Pereira, M. E. Schaepman, W. Turner, T. Wang, and M. Wegmann (2015), Agree on biodiversity metrics to track from space, Nature, 523, 403-405.

Small, C. (2001), Spectral dimensionality and scale of urban radiance, in AVIRIS Workshop Proceedings.

Small, C. (2003), High spatial resolution spectral mixture analysis of urban reflectance, Remote Sensing of Environment, 88, 170–186.

Smith, M. L., S. V. Ollinger, M. E. Martin, J. D. Aber, R. A. Hallett, and C. L. Goodale (2002), Direct estimation of aboveground forest productivity through hyperspectral remote sensing of canopy nitrogen, Ecological Applications, 12, 1286–1302.

Smith, S., V. Romanovsky, A. Lewkowicz, C. Burn, M. Allard, G. Clow, K. Yoshikawa, and J. Throop (2010), Thermal state of permafrost in north America: a contribution to the international polar year, Permafrost and Periglacial Processes, 21 (2), 117–135.

Somers, B. and G. P. Asner (2013), Invasive species mapping in Hawaiian rainforests using multi-temporal Hyperion spaceborne imaging spectroscopy, IEEE Journal of Selected Topics in Applied Earth Observations and Remote Sensing, 6, 351-359.

Staenz, K., T. Szeredi, and J. Schwarz (1998), ISDAS - a system for processing/analyzing hyperspectral data, Canadian Journal of Remote Sensing, 24 (2), 99–113.

Stagakis, S., N. Markos, O. Sykioti, and A. Kyparissis (2010), Monitoring canopy biophysical and biochemical parameters in ecosystem scale using satellite hyperspectral imagery: An application on a phlomis fruticosa mediterranean ecosystem using multiangular CHRIS/PROBA observations, Remote Sensing of Environment, 114, 977–994.

Stewart, I. D., and T. R. Oke (2012), Local Climate Zones for Urban Temperature Studies, Bulletin of the American Meteorological Society, 93, 1879–1900.

Stevens, A., M. Nocita, G. Toth, L. Montanarella, and B. van Wesemael (2013), Prediction of Soil Organic Carbon at the European Scale by Visible and NearInfraRed Reflectance Spectroscopy, PLoS ONE, 8(6): e66409.

Stroeve, J., M. M. Holland, W. Meier, T. Scambos, and M. Serreze (2007), Arctic sea ice decline: Faster than forecast, Geophysical Research Letters, 34 (9), L09,501–6.

Suess, S., S. van der Linden, A. Okujeni, M. Schwieder, P. J. Leitão, and P. Hostert, (2015), Using class-probabilities to map gradual transitions in shrub vegetation maps from simulated EnMAP data, Remote Sensing, 7, 10668-10688.

Swayze, G., K. Smith, R. Clark, S. Sutley, R. Pearson, J. Vance, P. Hageman, P. Briggs, A. Meier, M. Singleton, and S. Roth (2000), Using imaging spectroscopy to map acidic mine waste, 34, 47–54.

Swayze, G. A., R. N. Clark, A. F. H. Goetz, K. E. Livo, G. N. Breit, F. A. Kruse, S. J. Sutley, L. W. Snee, H. A. Lowers, J. L. Post, R. E. Stoffregen, and R P. Ashley (2014), Mapping Advanced Argillic Alteration at Cuprite, Nevada, Using Imaging Spectroscopy, Economic Geology 109 (5), 1179–1221.

Takeuchi N. (2002), Optical characteristics of cryoconite (surface dust) on glaciers: the relationship between light absorbency and the property of organic matter contained in the cryoconite, Annals of Glaciology, 34, 409–14.

Tanikawa T., T. Aoki, and F. Nishio (2002), Remote sensing of snow grain size and impurities from airborne multispectral scanner data using a snow bidirectional reflectance distribution function model, Annals of Glaciology 34, 74–80.

Taylor, G. R. (2004), Field and image spectrometry for soil mapping, in 12th Australian Remote Sensing Conference, Fremantle, WA, Australia.

Taylor, G. R., P. Hemphill, D. Currie, T. Broadfoot, and R. L. Dehaan (2001), Mapping dryland salinity with hyperspectral imagery, In: International Geoscience and Remote Sensing Symposium: Scanning the Present and Resolving the Future, vol. 1, pp. 302–304, Piscataway, NJ, USA.

Tenhunen, J., R. Valentini, B. Koestner, R. Zimmermann, and A. Granier (1998), Variation in forest gas exchange at landscape to continental scales, Annales des Sciences Forestieres, 55, 1–11.

Thiemann, S., and H. Kaufmann (2000), Determination of chlorophyll content and trophic state of lakes using field spectrometer and IRS-1C satellite data in the Mecklenburg lake district, Germany, Remote Sensing of Environment, 73 (2), 227–235.

Thiemann, S., and H. Kaufmann (2002), Lake water quality monitoring using hyperspectral airborne data - a semiempirical multisensor and multitemporal approach for the Mecklenburg lake district, Germany, 81 (2-13), 228–237.

Thompson, R., Y. Olsen, R. Mitchell, A. Davis, S. Rowland, A. John, D. McGonigle, and A. Russell (2004), Lost at sea: Where is all the plastic?, Science, 304 (5672), 838.

Thompson, D. R., I. Leifer, H. Bovensmann, M. Eastwood, M. Fladeland, C. Frankenberg, K. Gerilowski, R.O. Green, S. Kratwurst, T. Krings, B. Luna, and A.K. Thorpe (2015), Real-time remote detection and measurement for airborne imaging spectroscopy: a case study with methane. Atmospheric Measurement Techniques 8 (10), 4383-4397.

Thorpe, A. K., C. Frankenberg, and D. A. Roberts (2014), Retrieval techniques for airborne imaging of methane concentrations using high spatial and moderate spectral resolution: application to AVIRIS. Atmospheric Measurement Techniques 7(2), 491-506.

Torres, R., P. Snoeij, D. Geudtner, D. Bibby, M. Davidson, E. Attema, P. Potin, B. Rommen, N. Floury, M. Brown, I. N. Traver, P. Deghaye, B. Duesmann, B. Rosich, N. Miranda, C. Bruno, M. L'Abbate, R. Croci, A. Pietropaolo, M. Huchler, and F. Rostan (2012), GMES Sentinel-1 mission, Remote Sensing of Environment, 120 (0), 9–24.

Tralli, D. M., R. G. Blom, V. Zlotnicki, A. Donnellan, and D. L. Evans (2005), Satellite remote sensing of earthquake, volcano, flood, landslide and coastal inundation hazards, ISPRS Journal of Photogrammetry and Remote Sensing, 59 (4), 185–198.

Turner, D. J., B. Rivard, and L. A. Groat (2014), Visible and Short-Wave Infrared Reflectance Spectroscopy of REE Fluorocarbonates, American Mineralogist, 99 (7), 1335–1346.

Ubilava, D. (2012), El Nino, La Nina, and world coffee price dynamics, Agricultural Economics, 43 (1), 17–2

UN (2012), World urbanization prospects: the 2011 revision, United Nations, New York.

UNCCD (1994), United Nations convention to combat desertification, Tech. rep., United Nations, http://www.unccd.int.

Underwood, E., S. Ustin, and D. Dipietro (2003), Mapping nonnative plants using hyperspectral imagery, Remote Sensing of Environment, 86, 150–161.

UNEP (2009), Marine litter: A global challenge, Tech. rep.

UNEP (2012), Global environment outlook (geo) 5, Tech. rep., United Nations Environment Programme.

Ungar, S.G., J. S. Pearlman, J. A. Mendenhall, and D. Reuter (2003), Overview of the earth observing one (EO-1) mission. IEEE Transactions on Geoscience and Remote Sensing, 41, 1149–1159.

Ustin, S., D. Roberts, J. Gamon, G. Asner, and R. Green (2004), Using imaging spectroscopy to study ecosystem processes and properties, Bioscience, 54 (6), 523–534.

Ustin, S.L., and J. A. Gamon (2010), Remote sensing of plant functional types, New Phytologist, 186, 795-816.

Vafeidis, A., B. Neumann, J. Zimmermann, and R. Nicholls (2011), Analysis of land area and population in the low-elevation coastal zone, Tech. rep.

Vahtmaee, E., T. Kutser, G. Martin, and J. Kotta (2006), Feasibility of hyperspectral remote sensing for mapping benthic macroalgal cover in turbid coastal waters - a Baltic sea case study, Remote Sensing of Environment, 101, 342–351.

Vahtmaee, E., T. Kutser, J. Kotta, and M. Paernoja (2011), Detecting patterns and changes in a complex benthic environment of the Baltic Sea, Journal of Applied Remote Sensing, 5 (1), 053559.

van der Linden, S., and P. Hostert (2009), The influence or urban surface structures on the accuracy of impervious area maps from airborne hyperspectral data, Remote Sensing of Environment, 113, 2298–2305.

van der Linden, S., A. Janz, B. Waske, M. Eiden, and P. Hostert (2007), Classifying segmented hyperspectral data from a heterogeneous urban environment using support vector machines, Journal of Applied Remote Sensing, 1, 013,543.

van der Linden, S., A. Rabe, M. Held, B. Jakimow, P. J. Leitão, A. Okujeni, M. Schwieder, S. Suess, and P. Hostert (2015), The EnMAP-Box—A Toolbox and Application Programming Interface for EnMAP Data Processing, Remote Sensing 7 (9), 11249–11266.

van der Meer, F. (2004), Analysis of Spectral Absorption Features in Hyperspectral Imagery, International Journal of Applied Earth Observation and Geoinformation 5 (1), 55–68.

van der Meer, F. D., H. M. A. van der Werff, F. J. A. Van Ruitenbeek, C. A. Hecker, W. H. Bakker, M. F. Noomen, M. van der Meijde, E. J. M. Carranza, J. B. d. Smeth, and T. Woldai (2012), Multi- and hyperspectral geologic remote sensing: A review, International Journal of Applied Earth Observation and Geoinformation, 14 (1), 112–128.

Vane, G., A. F. H. Goetz, and J. B. Wellman (1983), Airborne imaging spectrometer: A new tool for remote sensing, in International Geoscience and Remote Sensing Symposium, Proceedings IEEE.

Vane, G., R. O. Green, T. G. Chrien, H. T. Enmark, E. G. Hansen, and W. M. Porter (1993), The airborne visible/infrared imaging spectrometer (AVIRIS), Remote Sensing of Environment, 44 (2-13), 127 – 143.

Vapnik, V. (1998), Statistical learning theory, Wiley, New York.

Veraverbeke, S., E. N. Stavros, and S. J. Hook (2014), Assessing fire severity using imaging spectroscopy data from the Airborne Visible/Infrared Imaging Spectrometer (AVIRIS) and comparison with multispectral capabilities, Remote Sensing of Environment, 154, 153-163.

Verhoef, W., and H. Bach (2003), Simulation of hyperspectral and directional radiance images using coupled biophysical and atmospheric radiative transfer models, Remote Sensing of Environment, 87 (1), 23–41.

Verrelst, J., J. Munoz, L. Alonso, J. Delegido, J. P. Rivera, G. Camps-Valls, and J. Moreno (2012), Machine learning regression algorithms for biophysical parameter retrieval: Opportunities for sentinel-2 and -3, Remote Sensing of Environment, 118, 127–139.

Vitousek, P. M. (1997), Human domination of earth’s ecosystems, Science, 277 (5325), 494–499.

Waring, R.H., and S.W. Running (2007), Forest ecosystems. Analysis at multiple scales, Elsevier Academic Press., Amsterdam, Boston, Heidelberg.

Warren, S. G., and W. J. Wiscombe (1980), A model for the spectral albedo of snow. II: Snow containing atmospheric aerosols., Journal of Atmospheric Sciences, 37, 2734–2745.

Waske, B., S. van der Linden, C. Oldenburg, B. Jakimow, A. Rabe, and P. Hostert (2012), ImageRF – a user-oriented implementation for remote sensing image analysis with random forests, Environmental Modelling & Software 2012, 35, 192-193.

Weiss, M., D. Troufleau, F. Baret, H. Chauki, L. Prevot, A. Olioso, N. Bruguier, and N. Brisson (2001), Coupling canopy functioning and radiative transfer models for remote sensing data assimilation, Agricultural and Forest Meteorology, 108 (2), 113–128.

Weiss, M., F. Baret, H. Eerens, and E. Swinnen (2010), Fapar over europe for the past 29 years: A temporally consistent product derived from avhrr and vegetation sensors, in Recent Advances in Quantitative Remote Sensing, edited by J. Sobrino, pp. 428–433, Publicacions de la Universitat de Valencia.

Weng, Q., X. Hu, and D. Lu (2008), Extracting impervious surfaces from medium spatial resolution multispectral and hyperspectral imagery: A comparison, Int. J. Remote Sens., 29, 3209–3232.

Wepener, V., C. van Dyk, L. Bervoets, G. OBrien, A. Covaci, and Y. Cloete (2011), An assessment of the influence of multiple stressors on the Vaal river, South Africa, Physics and Chemistry of the Earth, 36 (14), 949–962.

White, M. A., P. E. Thornton, S. W. Running, and R. R. Nemani (2000), Parameterization and sensitivity analysis of the BIOME-BGC terrestrial ecosystem model: Net primary production controls, Earth Interactions, 4 (3), 1–85.

Williamson, G. B., W. F. Laurance, A. A. Oliveira, P. Delamanica, C. Gascon, T. E. Lovejoy, and L. Pohl (2000), Amazonian tree mortality during the 1997 El Nino drought, Conservation Biology, 14 (5), 1538–1542.

Witten, D.M., R. Tibshirani, and T. Hastie (2009), A penalized matrix decomposition, with applications to sparse principal components and canonical correlation analysis, Biostatistics, 10, 515-534.

Wold, S., M. Sjostrom, and L. Eriksson, (2001), PLS-regression: A basic tool of chemometrics, Chemometrics and Intelligent Laboratory Systems, 58, 109-130.

Wong, M. H., S. C. Wu, W. J. Deng, X. Z. Yu, Q. Luo, A. O. W. Leung, C. S. C. Wong, W. J. Luksemburg, and A. S. Wong (2007), Export of toxic chemicals - A review of the case of uncontrolled electronic-waste recycling, Environmental Pollution, 149 (2), 131–140.

Wu, C., and A. T. Murray (2003), Estimating impervious surface distribution by spectral mixture analysis, Remote Sensing of Environment, 84 (4), 493–505.

Wulder, M.A., J. C. White, A. L. Carroll,and N. C. Coops (2009), Challenges for the operational detection of mountain pine beetle green attack with remote sensing, The Forestry Chronicle, 85, 32-38.

Wulf, H., T. Mulder, M. E. Schaepman, A. Keller, and P. C. Joerg, (2015), Remote sensing of soils, Zürich: University of Zurich, Remote Sensing Laboratories.

Xu, B., and P. Gong (2007), Land-use/Land-cover classification with multispectral and hyperspectral EO-1 data, Photogramm. Eng. Remote Sensing, 73, 955–965.

Xu, W., M. Wooster, and C. Grimmond (2008), Modelling of urban sensible heat flux at multiple spatial scales: A demonstration using airborne hyperspectral imagery of shanghai and a temperature-emissivity separation approach, Remote Sensing of Environment, 112 (9), 3493–3510.

Yang, L. (2000), Integration of a numerical model and remotely sensed data to study urban/rural land surface climate processes, Computers & Geosciences, 26.

Yang, Y. (2009), Remote sensing and geospatial technologies for coastal ecosystem assessment and management, in Lecture Notes in Geoinformation and Cartography, pp. 1–14, Springer Heidelberg.

Zabel, F., B. Putzenlechner, and W. Mauser (2014), Global Agricultural Land Resources – A High Resolution Suitability Evaluation and Its Perspectives until 2100 under Climate Change Conditions, PLOS ONE, 9(9), e107522.

Zarfl, C., D. Fleet, E. Fries, F. Galgani, G. Gerdts, G. Hanke, and M. Matthies (2011), Microplastics in oceans, Marine Pollution Bulletin, 62, 1589–1591.

Zege, E., A. Malinka, I. Katsev, A. Prikhach, G. Heygster, L. Istomina, G. Birnbaum, and P. Schwarz (2015), Algorithm to retrieve the melt pond fraction and the spectral albedo of Arctic summer ice from satellite optical data, Remote Sensing of Environment, 163, 153-164.

Zhang, J. (2010), Multi-source remote sensing data fusion: Status and trends, Int. J. Image Data Fusion, 1, 5–24.

Zhao, X., Z. Xiao, Q. Kang, Q. Li, and L. Fang (2010) Overview of the fourier transform Hyperspectral Imager (HSI) boarded on HJ-1A satellite. Proceedings of the 2010 IEEE International Geoscience and Remote Sensing Symposium (IGARSS), Honolulu, HI, USA, 25–30 July 2010; pp. 4272–4274.

Zhu, J., and T. Hastie (2005), Kernel logistic regression and the import vector machine, Journal of Computational and Graphical Statistics, 14, 185–205.

List of acronyms

A list of abbreviations is provided in Table 4, while an extended glossary of terms and abbreviations is publically available at the EnMAP website at http://www.enmap.org/sites/default/files/pdf/EnMAP_Glossary.pdf.

Table 4: List of abbreviations used in this document.

Acronym	Name
APAR	Absorbed Photosynthetically Active Radiation
API	Application Programming Interface
BRDF	Bidirectional Reflectance Distribution Function
CBD	Convention on Biological Diversity
CNES	Centre National d'Études Spatiales
DEM	Digital elevation model
DLR	German Aerospace Agency
EBV	Essential Biodiversity Variables
EeteS	EnMAP end-to-end scene simulator
EnMAP	Environmental Mapping and Analysis Program
EnSAG	EnMAP Science Advisory Group
fAPAR	Fraction of Absorbed Photosynthetically Active Radiation
GBIF	Global Biodiversity Information Facility
GCOS	Global Climate Observing Systems
GEO	Global Environment Outlook
GEO	Group on Earth Observations
GEOSS	Global Earth Observation System of Systems
GFZ	German Research Centre for Geosciences
GLP	Global Land Project
GOOS	Global Ocean Observing System
GTOS	Global Terrestrial Observing System
GUI	Graphical User Interface
HISUI	Hyperspectral Imager Suite
HRS	Hyperspectral Remote Sensing
HUB	Humboldt-Universität zu Berlin
HZG	Helmholtz-Zentrum Geesthacht
IGBP	International Geosphere-Biosphere Program
IHDP	International Human Dimensions Program
IPBES	Intergovernmental Platform on Biodiversity & Ecosystem Services

Acronym	Name
IPCC	Intergovernmental Panel on Climate Change
IUCN	International Union for Conservation of Nature
JAXA	Japanese Aerospace Exploration Agency
LAI	Leaf Area Index
LCZ	Local Climate Zone
LMA	Leaf Mass per Area
LMU	Ludwig-Maximilians-Universität München
LOICZ	Land Ocean Interaction in the Coastal Zone Program
MERIS	MEdium Resolution Imaging Spectrometer
NIR	Near infrared
PRISMA	PRescursore IperSpettrale della Missione Operative
REDD	UN Collaborative Initiative on Reducing Emissions from Deforestation and Forest Degradation
SAR	Synthetic Aperture Radar
SBA	Societal Benefit Area
SDG	Sustainable Development Goal
SNR	Signal-to-noise ratio
SZA	Solar Zenith Angle
SWIR	Shortwave-infrared
UB	University of Bonn
UT	University of Trier
VIS	Visible
V-I-S	Vegetation – Impervious surface - Soil
VZA	Viewing Zenith Angle
WCRP	World Climate Research Program

Acknowledgements

We are thankful to Ashley Bracken, Theodor Becker and Kathrin Ward for their thoughtful reviews of the document. EnMAP is funded by the German Federal Ministry for Economic Affairs and Energy on the basis of a decision by the German Bundestag and contributions from DLR, GFZ and OHB System AG.